REPUBLIC OF TURKEY
ACIBADEM MEHMET ALI AYDINLAR UNIVERSITY
INSTITUTE OF SCIENCE

Assessment of Gait Adaptation Following Surgery in Pediatric Patients with Split Cord Malformation

ENİS ŞABAN

MASTER THESIS

DEPARTMENT OF MEDICAL ENGINEERING

SUPERVISOR
Asst. Prof. Hande Argunsah

ISTANBUL – 2023

LIST OF FIGURES

LIST OF PHOTOS

LIST OF TABLES

LIST OF SYMBOLS

°/s	Angular Velocity
%	Percentage
°	Degree
n	Number
cm	Centimeter
m	Meter
s	Second
N	Force
P	Pressure
J	Work
Nm	Energy
W	Power
m/s	Speed
m/s^2	Acceleration
Hz	Hertz
kg	Kilogram
Ag–AgCl	Silver-silver chloride
Σ	Sum
a	Alfa
ω	Omega
T1 weighted	Sequences of the Magnetic resonance imaging
T2 weighted	Sequences of the Magnetic resonance imaging
R	Right
L	Left
M	Male
F	Female
+	Positive
1^{st}	First
5^{th}	Fifth

LIST OF ABBREVIATIONS

2D	Two-dimensional
3D	Three-dimensional
COG	Center of gravity
COM	Center of mass
COP	Center of pressure
CT	Computerized tomography
GMFM	Gross motor function measure
GMPM	Gross motor performance measure
GRF	Ground reaction force
GRFV	Ground reaction force vector
DF	Dorsiflexion
EEI	Energy expenditure index
EMG	Electromyography
HD	High definition
IC	Initial Contact
ISW	Initial Swing
LMM	Lipomeningomyelocele
LR	Loading Response
L5	5th lomber vertebra level
L2,3,4	Lumbosacral nerve roots
M.	Muscle
MM	Meningomyelocele

MST	Mid-stance
MSW	Mid-swing
MRI	Magnetic resonance imaging
N.	Nerve
PCC	Pearson correlation coefficient
PF	Plantar flexion
PSW	Pre-swing
ROM	Range of Motion
RMSE	Root mean square error
S1,2,3	Sacral nerve roots
SCM	Split Cord Malformation
SD	Standard deviation
TST	Terminal stance
TSW	Terminal swing
US	Ultrasonography

ACKNOWLEDGEMENT

I would like to express my gratitude to those who contributed to the completion of this dissertation.

Firstly, I would like to thank my supervisor, Asst.Prof. Hande ARGUNŞAH, for her academic guidance and constructive feedback on my work. She was also kind enough to give me ongoing support and show me a welcoming attitude since the beginning of my dissertation study. Her supportive attitude increased my confidence and motivation, which helped me keep working hard at each step of the process.

I would like to thank my committee members, Prof.Dr. M. Memet ÖZEK, Asst. Prof. Hande ARGUNŞAH, Assoc. Prof. Zeynep HOŞBAY and Asst. Prof. Elçim Elgün KIRIMLI for their useful critiques and suggestions that enabled me to improve my perspective on the topic and helped me in shaping this dissertation.

I also want to thank to my collegues and dearest friends Fatih EROL and Gökçen EROL for their valuable support and comments on my work and encouraging approach when I felt confused and lost.

Special thanks should be given to the participants who volunteered and took an active role in all parts of the research. Their collaboration helped me maintain my motivation and experience a smooth research process.

I also want to express my wholehearted thanks to my professor and my mentor, Prof.Dr. M. Memet ÖZEK, for his valuable support and academic advice throughout the process. He believed in the value of my work and always supported me by providing the necessary resources to complete the dissertation. He helped me improve my vision and academic skills by sharing her invaluable knowledge and experience with me throughout the process. Without him, this dissertation would not have been completed.

I also would like to thank my co-workers, in especial Gizem GÜRZOĞLU and Özlem ARAL from Altunizade Acıbadem Hospital, Pediatric Rehabilitation Unit. Their comments and suggestions on the topic and on my work helped me a lot.

Last, but by no means least I thank my family for their continuous support and patience in every step of my doctoral study. I thank my mothers, Ruzica and Samiye; my fathers, Abduraman and Kemal; my sister Enisa, my brother-in-law Cem, my nephew Mert who have supported me during all time.

Special thanks should be given to my life partner, Canan ŞABAN, for helping me create time and space for my study during the busiest times; our angels, Kerem, Merve, and Mine, for their close interest in my study and motivational talks to remind me that I have a dissertation to finish.

Thank you all.

SUMMARY

Split cord malformation (SCM) is a midline abnormality of the spine that may arise during embryological development. Once the diagnosis of SCM is established, careful planning of surgery with regular follow-up assessments and scheduled physical therapy sessions are essential for improved outcomes. Using 3D Gait Analysis Technology enables objective follow-up of the improvements in these patients. This study aimed to assess the long-term gait adaptation of SCM patients after surgical intervention. Lower extremity kinetic and kinematic parameters were collected from 41 SCM patients between 2 and 18 years (mean=7.9 ±4.5) one year following the surgery. The follow-up data were collected from 15 SCM patients 2-3 years following the surgery. The control group is constituted of 28 age-matched typically developed children. Our results showed significant alterations in joint movements, particularly in the hip and ankle joints. The SCM group was characterized by higher cadence, shorter stride time, higher opposite foot off percentage, lower step time, significantly higher double support percentage, shorter step length, and slightly lower walking speed compared to the control group. The follow-up data showed that the compulsory adaptation in the pelvic joint determined in the initial motion analysis continued similarly, and there was no improvement in any of the lower extremity joints in this regard. The changes in hip and ankle joint biomechanics reflect a compensatory process in which the stress owing to body weight is transferred to the pelvis joint to restore the compromised balance during ambulation. Early and consistent physical therapy is fundamental to improving muscle strength, flexibility, coordination, and balance in SCM patients. Orthotic devices, such as insoles or orthopedic shoes, may be recommended to provide stability and support during walking.

Keywords: 3-Dimensional Gait Analysis, Gait Alteration, Physical Therapy, Split Cord Malformation

ÖZET

Ayrık Omurilik Malformasyonu (AOM), embriyolojik gelişim sırasında ortaya çıkabilecek omurganın orta hat anomalisidir. AOM tanısı nedeniyle opere olan hastaların sıra düzenli takip değerlendirmeleri ile beraber fizik tedavi programlarının planlanması gerekir. Üç Boyutlu Yürüme Analizi Teknolojisini kullanmak, bu hastalardaki gelişmelerin objektif olarak takip edilmesini sağlar. Bu çalışmada, cerrahi müdahale sonrası AOM hastalarının uzun süreli yürüyüş adaptasyonlarını değerlendirmek amaçlandı. Alt ekstremite kinetik ve kinematik parametreleri, ameliyattan bir yıl sonra 2 ila 18 yaş arasındaki (ortalama=7.9 ±4.5) toplam 41 AOM hastasından toplandı. Takip verileri, ameliyattan 2-3 yıl sonra 15 AOM hastasından elde edildi. Kontrol grubu ise, aynı yaştaki normal gelişim gösteren 28 çocuktan oluşturulmuştur. Sonuçlarımız eklem hareketlerinde, özellikle kalça ve ayak bileği eklemlerinde önemli değişiklikler gösterdi. AOM grubu, kontrol grubuna kıyasla daha yüksek kadans, daha kısa yürüme siklusu zamanı, daha yüksek karşıt ayak basma yüzdesi, daha düşük adım zamanı, önemli ölçüde daha yüksek çift destek yüzdesi, daha kısa adım uzunluğu ve daha düşük yürüme hızı ile karakterize edildi. Takip verileri, ilk yürüme analizinde belirlenen pelvisteki zorunlu adaptasyonun benzer şekilde devam ettiği ve bu konuda alt ekstremite eklem hareket açıklıklarında değişiklik olmadığı gözlendi. Kalça ve ayak bileği eklemi biyomekaniğindeki değişiklikler, vücut ağırlığından kaynaklanan stresin, ambulasyon sırasında dengeyi yeniden sağlamak için pelvis eklemine aktarıldığı süreci yansıtır. Düzenli fizik tedavi, AOM hastalarında kas kuvveti, esneklik, koordinasyon ve dengeyi geliştirmek için esastır. Yürüme sırasında stabilite ve destek sağlamak için tabanlık veya ortopedik ayakkabı gibi ortez cihazları önerilebilir.

Anahtar Kelimeler: 3 Boyutlu Yürüyüş Analizi, Ayrık Omurilik Malformasyonu, Fizik Tedavi, Yürüme Adaptasyonu

1. BACKGROUND AND THE AIM OF THE STUDY

Split cord malformation (SCM) is a midline abnormality of the spine that may arise during embryological development. The term “split cord malformation” was coined by Pang et al. in 1992 as an umbrella term to describe all diplomyelia malformations [1, 2]. SCM represents 3.8% to 5% of all developmental spinal anomalies, with a reported prevalence rate of 1/5000 [3]. Although dermatological symptoms are a key for early diagnosis [4], leg pain, gait disorder, spasticity, motor and sensory loss in the lower extremity, and foot deformities also commonly occur in patients with SCM [5]. The movement disorders vary according to the level of the lesion, resulting in different gait patterns. Lesions located in the thoracic or upper lumbar region may be associated with weakness in quadriceps muscles, while those located in the lower lumbar area may lead to weakness in the gluteus medius and gluteus maximus with preservation of quadriceps and hamstring muscles. Upper sacral lesions cause weakness in the gastrocnemius and soleus, and those in the lower sacral region spare these muscles [6,7]. Once the diagnosis is established, careful surgery planning with regular follow-up assessments is essential for improved outcomes [8].

SCM can lead to sensory and motor impairments in the lower extremities due to the disruption of nerve signals within the spinal cord. The divided spinal cord can result in asymmetrical innervation and impaired coordination of leg muscles, affecting the normal walking pattern. According to the level of spinal cord division and the affected nerve roots, muscle weakness, and imbalances may occur. This can lead to difficulty maintaining proper muscle tone and control during walking, resulting in an abnormal gait pattern. SCM can result in sensory deficits, such as loss of sensation or altered sensation in the lower extremities. Sensory feedback plays a crucial role in maintaining balance and coordinating movements during walking. The impaired sensation can affect proprioception and disrupt the normal gait pattern. Hence gait assessment of patients with SCM is essential for evaluating the treatment outcome, identifying the functional limitations, and determining the best therapeutic interventions through facilitating the preoperative diagnostic workup and allowing pre- and post-operative comparisons of the status of the locomotor system [8, 9].

This thesis aimed to delineate the long-term gait alterations of SCM patients after surgical intervention. The comprehensive analysis also included 5 group comparisons 1) thicker-weaker hemi cord; 2) below- above L5 level; 3) below-above seven years old; 4) tethered cord- no tethered cord; 5) Type I- Type II SCM.

2. INTRODUCTION

2.1. Definition

Split Cord Malformation (SCM) is a developmental midline abnormality of the spine during embryological development. This congenital anomaly is characterized by a spinal cord consisting of two separate halves within a single or double dural sheath. It occurs in childhood and is a rare form of Spina Bifida Occulta. The term SCM was first used in the 17th century. The term diastematomyelia (diastema= split, myelos= spinal cord) was used by Ollivier and Hertwig in 1837. Bruce proposed the term diplomyeli (Diplo= double, myelos= spinal cord) in 1906. In 1992, Pang et al. ended to the confusion of terms and gathered all double spinal cord malformations under the name SCM. They defined two types of SCM, types 1 and 2. In type 1 SCM, there are two separate spinal cords, each surrounded by its own dural sheath, with a rigid septum made of bone or cartilage between them. The septum is usually located behind the vertebral body. Type 1 SCM describes diastematomyelia with the old nomenclature. In type 2 SCM, the spinal cord, which is divided into two, is surrounded by a single dural sheath, and there is no bone or cartilage septum, and there are fibrous bands between them. This type of SCM defines diplomacy by the old nomenclature. Kumar et al. described the complex type of SCM in 2002. The anomaly seen in this type is a pathology accompanying other spinal dysraphisms such as meningomyelocele (MM) and lipomeningoyelocele (LMM) [1].

2.2. Embryological Development

The blastoderm, formed in the second week during the embryological development of humans, consists of 2 layers. There is an epiblast layer close to the amniotic sac and a hypoblast layer close to the yolk sac. Below the epiblasts is the basement membrane, except in the primitive cleft. In the primitive cleft in the tail of the Hensen nodule, epiblast cells in the midline migrate downward and below the basement membrane and to the sides to form endoderm and mesoderm. Ectoderm is formed by the remaining epiblast cells. This 3-layered appearance is called

gastrulation. Cells in the Hensen nodule anterior to the primitive cleft will then form the notochord. These cells in the middle of the nodule form the notochordial projection between the ectoderm and the endoderm. Hensen's nodules move downward during gastrulation and lie opposite the coccyx. The amniotic cavity and the lumen in the middle of the notochordial prominence are connected by the primitive pit. In the third week, the notochordial process and the underlying endoderm unite to form the neuroentic canal. Through this channel, a connection is made between the yolk sac and the amniotic sac. The canal separates from the endoderm after approximately 48 hours and forms the notochord. Bremer et al. stated that if the canal is permanent, diastematomyelia develops [1,10].

The remaining epiblast cells form the superficial ectoderm and neural tube. Neuroepithelial development from the ectoderm is not yet fully understood. While the notochord and the surrounding mesoderm are thought to have a role in the development of the neuroepithelium, recent studies have shown that the endoderm also plays an important role [1,10].

According to the unified theory presented by Pang et al., SCM occurs due to an ontogenetic error in the closure of the primitive neuroentic channel (Figure 1). Continuous contact between ectoderm and endoderm is maintained with the accessory neuroentic canal, which passes through the embryonic disc in the midline and connects the yolk sac and the amniotic sac. The accessory neuroentic channel and the notochord, and the overlying neural plate divide into two in this region. In all malformations involving a double spinal cord, this accessory canal formation is the first stage. In the lower part of the canal, the endoderm and surrounding mesoderm form the endo mesenchymal tract. Before neurulation is complete, this tract divides the notochord and the neural plate into two. Both halves complete neurulation separately, forming two spinal cords. Primitive meninges with a loose matrix and a few cells form the dura mater. If the primitive meninges mix with endo mesenchymal tract cells, a dural sheath develops between the two hemispheres. Since the cells of this sheath are sclerogenic,

they form the bone septum. In this way, the dural sheaths surrounding the two hemispheres of the spinal cord with a bony septum between them are formed. This condition is named Type 1 SCM. If the endomesenchymal tract and primitive meninges do not mix, both hemispheres are found in a single dural sheath. Tract cells form a soft septum on the inner surface of the semi-spinal cords. In this way, when both hemispheres are in a single dural sheath and are connected by a fibrous septum, it is called Type 2 SCM. The reason behind the spinal cord is dividing into two asymmetric hemicords may be the accessory neurenteric canal which is slightly eccentric in the axial plane. In this case, the notochord divides asymmetrically. The hemicord that develops from the wider neural plate becomes inevitably thicker than the other one pushing the endomesenchymal tract aside. This may be related to the spur's frequently having an oblique course on the axial plane in the case of asymmetrical hemicords [1,10].

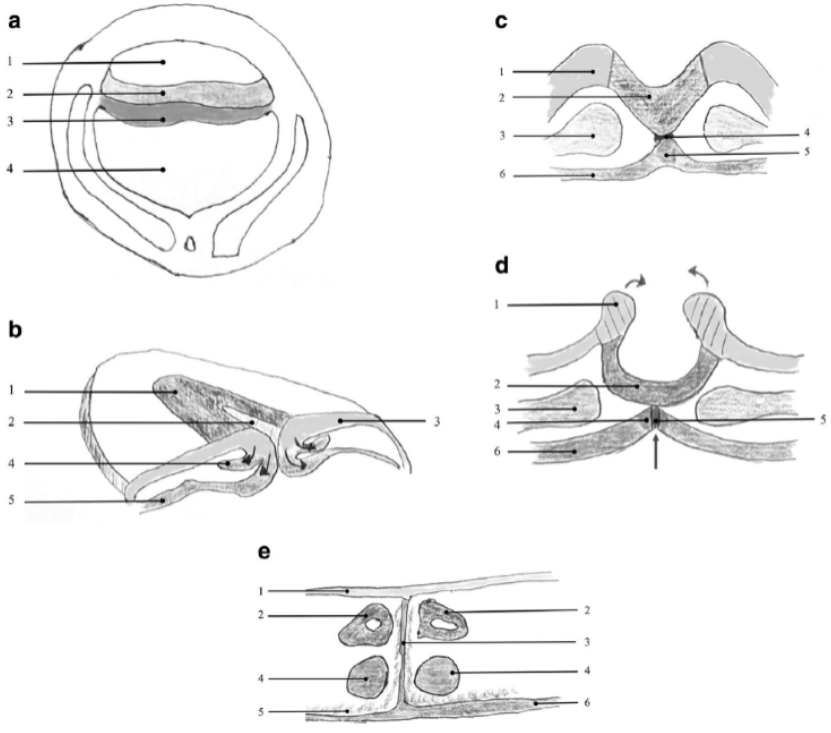

Figure 1. Embryological theory of SCM according to Pang theory.
a 1 amnionic sac, 2 epiblast, 3hypoblast, and 4 yolk sac; b 1 neural plate, 2 primitive groove, 3 ectoderm, 4 mesoderm, and 5 endoderm; c 1 ectoderm, 2 neural plate, 3 somite, 4 ecto-endoderm adhesion, 5 future notochord, 6 endoderm; d 1 neural crest, 2 neural plate, 3 somite, 4 hemi notochord, 5 accessory neurenteric canal, 6 endoderm; black arrows shows the neural folding and brown arrow show the invagination of the accessory endoderm/neurenteric canal); e 1 cutaneous ectoderm, 2 hemi neural tubes, 3 endomesenchymal tract, 4 hemi notochords, 5 mesenchyme, 6 endoderm (11)

2.3. Clinical Manifestation

SCM represents 3.8% to 5% of all developmental spinal anomalies. Studies have shown that the prevalence is 5000/1. In terms of gender, it is three times more common in females. It is most often diagnosed in the age group of 4-7 years, and second most often in the age group of 12-16. Additionally, it can be detected in the adult group. SCM is mostly located in the lumbar region, followed by the thoracic region. Rarely SCM is located in the cervical and sacral regions. Several cases have been defined with several clefts, each consisting of a septum. According to Naidich, two spurs in two splitted clefts are manifested in 5- 6% of cases. According to French, the spur or the septum is attached to the anterior and posterior parts of the vertebrae in 68% of cases, only to the posterior parts in 11%, and only to the anterior parts in 24%. It is often associated with Klippel-Feil Syndrome when seen in the cervical region [10].

Skin symptoms are the most critical finding for early diagnosis. Hair growth (hypertrichosis), especially in the waist and back areas, is the most common skin symptom (Picture 1a). The frequency of coexistence of hypertrichosis with SCM is higher than other skin manifestations. Other symptoms include abnormal vascular structures (capillary hemangioma), skin dimples, lipoma dermal sinus, and skin discoloration. Bone deformities may accompany SCM; scoliosis, block vertebra, butterfly vertebra, narrow disc space, and hemivertebra anomalies are seen in most cases [10].

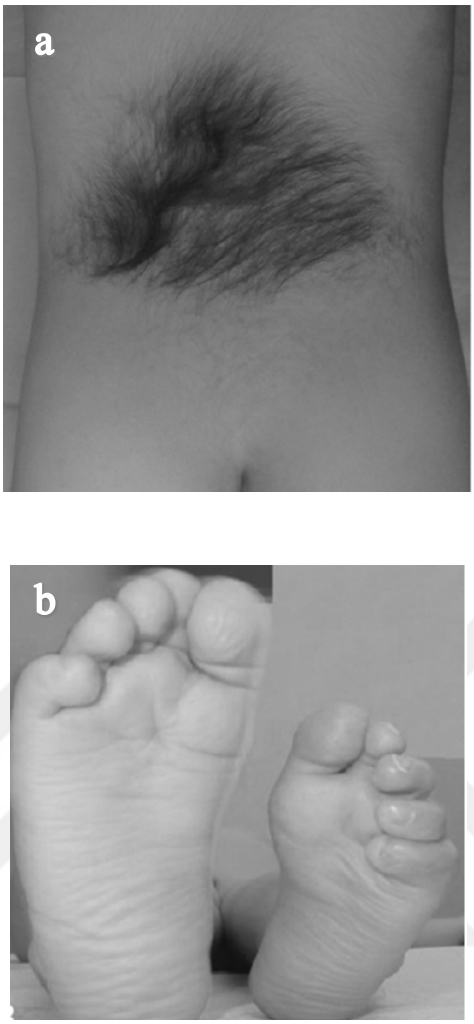

Picture 1. a Hypertrichosis clinical mark in lomber area**. b** Foot length asymmetry [70].

Scoliosis is usually seen due to stretching of the spinal cord in SCM. Scoliosis can be seen in approximately half of the cases, and its frequency is higher with Type 1. SCM has also been detected in patients with congenital scoliosis. Urinary and stool incontinence problems may occur. SCM may accompany meningocele, meningomyelocele and lipomeningomyelocele [10].

Neurological findings vary according to age and other accompanying spinal malformations. Although neurological findings are uncommon in newborns, as age progresses, the findings occur due to stretching of the spinal cord. While pain is prominent in adults, it is less common in children. Neurological deficits due to physical activity and trauma have been reported in the literature in some asymptomatic cases [10]. Leg pain, gait disturbance, spasticity, motor and sensory loss in the lower

extremities, and foot deformities (Picture 1b) are common in SCM. If a size difference is detected between the feet, it should be remembered that the small foot and the thin semi-spinal cord are together and appear on the same side (Picture 1b) [10].

Movement disorders may vary according to the level of the lesion in SCM. As a result, they may exhibit different walking patterns. Weakness in the quadriceps muscles may be seen in lesions located in the thoracic and upper lumbar regions. In lesions in the lower lumbar region, there is weakness in the Gluteus Medius and Gluteus Maximus muscles, while the Quadriceps and Hamstring muscles continue their functions. While weakness is detected in the gastrocnemius and soleus muscles in lesions in the upper sacral region, these muscles preserve their functions in lesions in the lower sacral region (10). Weakness of the muscles around the hip negatively affects the hip joint. Although walking speeds are not affected, an imbalance in the oscillating movements of the pelvis and compensatory spinal anomalies may occur due to muscle weakness. An imbalance between knee flexion and extension movements and knee valgum deformity can affect knee joint movements. Contracture in the knee flexion muscles is more common in lesions of the thoracic region. Weakness of the quadriceps muscle and spasticity in the Gastrocnemius and Soleus muscles may predispose to knee flexion contracture. The increase in knee flexion angle during walking causes more effort and oxygen consumption; as a result, the quality of walking deteriorates. Valgum deformity of the knee also causes pain in this region. Affected hip joint rotation movements, tibial torsion, trunk, and pelvis movements may predispose to the formation of valgum deformity in the knee. While external tibial torsion usually develops secondary to muscle dysfunction, internal tibial torsion is usually associated with clubfoot deformity. Foot deformities are seen in almost all SCM patients. Equine deformity in the foot is more common in lesions of the thoracic and upper lumbar regions. Foot calcaneovagus deformity may occur due to lumbar region lesions and weakness of ankle plantar flexor muscles. The dominance of the ankle evertor muscles and the involvement of the anterior and posterior tibial muscles may predispose to this. The weakness of the Soleus muscle in lumbar region lesions affects the movement of the fibula bone during walking. As a result, shortness of the fibula bone may occur. Thus, the growth rate of the outer and inner regions of the tibial

bone is affected. In this situation, the talus bone is inclined towards the valgus. This deformity may cause skin areas to be affected and ulcerations in the future. Cavus deformities can be seen in lower lumbar and sacral region lesions. Here, the primary deformity is achieved, and varus occurs because of the imbalance between the functions of the Tibialis Posterior and Peroneal muscles. The weakness of the intrinsic muscles also prepares the ground for this situation. Since bone anomalies are common in SCM patients, direct vertebral radiographs can show many findings. Segmentation and formation disorders can be detected in bone, block vertebrae, bifid lamina, bone speculum, scoliosis, kyphosis, and kyphoscoliosis. In addition to direct radiographs, scoliosis radiographs must be added [10].

2.4. Radiological Evaluation

Examination with Computerized Tomography (CT) or 3D reconstruction CT is beneficial in revealing the type and number of vertebral anomalies. They can provide useful information, especially in Type 1 SCM. Bone anomalies may accompany approximately 85% of SCM patients. Bifid vertebrae, bifid lamina, butterfly vertebrae, and hemivertebrae are the most common. While CT-myelography was used in the diagnosis before, magnetic resonance imaging (MRI) has taken its place with the developing technology. The diagnosis of SCMs has been facilitated by the MRI method and has resulted in an increase in the diagnosis of this disease in recent years. MRI has been the best method for both prenatal and postnatal diagnosis (Picture 2). It can show the level of the discrete part and its subject, accompanying pathology, anomalies, phylum lesions, and dermal sinus tracts. MRI can show whether the atrophic and short lower extremities and the thinner half-spinal cord are on the same side.

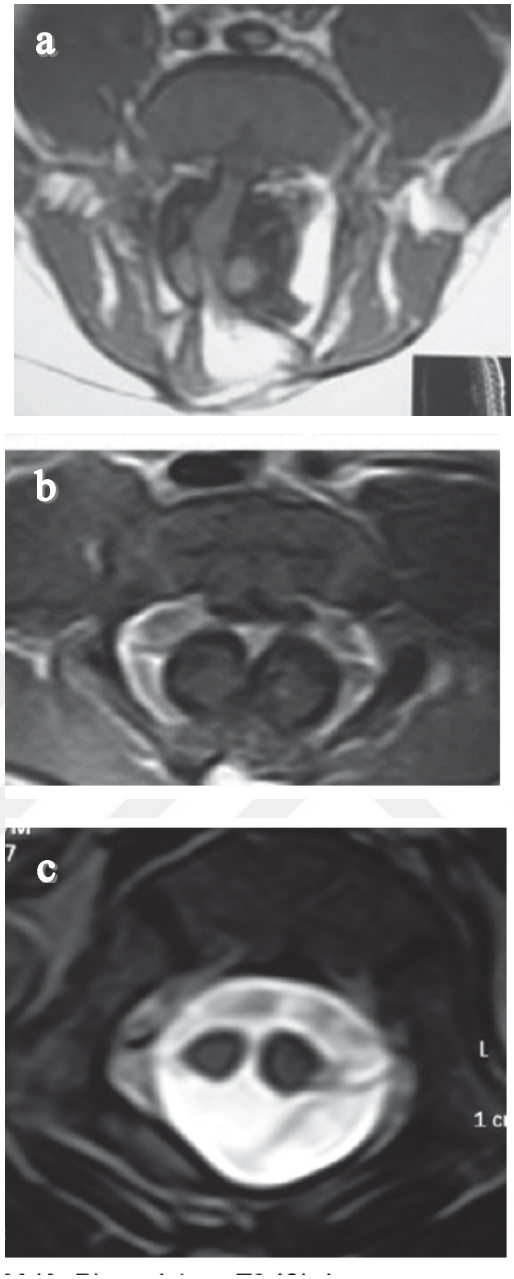

Picture 2. a T1-weighted axial MRI demonstrating type 1 split cord malformation with an asymmetric hemi medullas. **b** T1-weighted axial MRI demonstrating type 1 split cord malformation with a bony spur. **c** T2-weighted axial MRI demonstrating type 2 split cord malformation [70].

While phylum lesions are better shown on T1-weighted MRI sections, how many dural sacs are present in T2-weighted MRI sections is more helpful in distinguishing Type 1 and Type 2 SCM and syringomyelia. In approximately 50% of all cases, syringomyelia is detected proximal to the SCM (10). Pang et al. found additional

anomalies that would stretch the spinal cord in SCM lesions in the thoracic or lumbar region. Among them, the most common anomaly is short thick filum terminale. Therefore, the entire spinal region should be evaluated in detail while investigating SCM. The hydromyelic cavity often starts from above and progresses to the SCM, sometimes descending below [10].

Neurological and urodynamic tests and ultrasonography (US) should be performed before the operation if possible. Especially neurological and urodynamic tests do not help diagnose SCM; they gain importance in determining the patient's objective status after diagnosis and in subsequent follow-ups. The rapid deterioration of neurological tests in the late postoperative period should bring to mind tethered cord syndrome or syringomyelia [10].

Radiological imaging and urodynamic tests are valuable in the postoperative follow-up of the patient.

2.5. Treatment

Operation indication is acquired for patients presenting a quick degeneration of urological, neurological, or orthopedic function when they were previously bereft of symptoms. The surgery outcome in these patients is particularly satisfactory, with a rapid return of the function to the premorbid state. In cases of chronic neurological deficit characterized by an orthopedic syndrome with a lack of reflexes, long-standing sensory deficits, foot deformation, and leg atrophy, surgery aims to prevent further severe deterioration [10]. The patients with SCM have been operated on without monitoring, and it is thus hard to approximate if the results were better in the hands of surgeons who used this equipment. In a current series of combined SCM and hemivertebra documented by an orthopedic, neurologic, and surgical team, the use of spinal cord monitoring was recommended only during spinal surgery.

2.6. Basic Anatomical Positions

The coronal (frontal) plane is the vertical plane that divides the body or body segment into anterior (ventral) and posterior (dorsal) parts. The sagittal plane is a vertical plane separating the body or body segment into right and left sides. The transverse plane is horizontal and divides the body or body segment into superior and inferior parts (Figure 2).

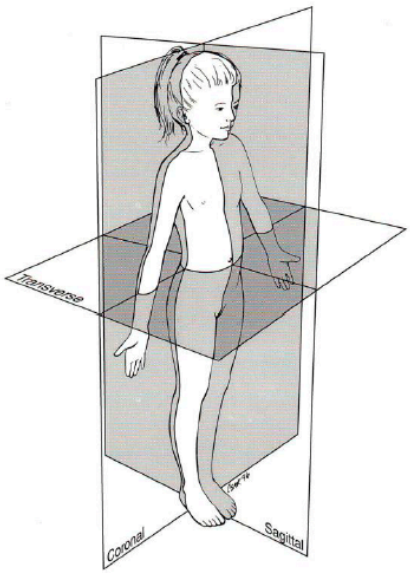

Figure 2. Three Anatomical planes [12]

Anterior (ventral) is the orientation that points toward the front of the body or body segment. Posterior (dorsal) is the orientation that points toward the back of the body or body segment. The orientation of the superior means towards the head. Also, it directs to the upper part of a structure. The Inferior (caudal) orientation means out from the head towards the toes. It also reveals the lowest part of a structure. The orientation of the medial is pointing towards the midsagittal plane of the body or midline of a structure. The orientation of lateral is the direction that points away from the mid-sagittal plane of the body or midline of a structure. The Proximal is the orientation closer to the connection of an extremity or limb to the trunk. The orientation of the distal is a distance away from the attachment of a limb or extremity [12].

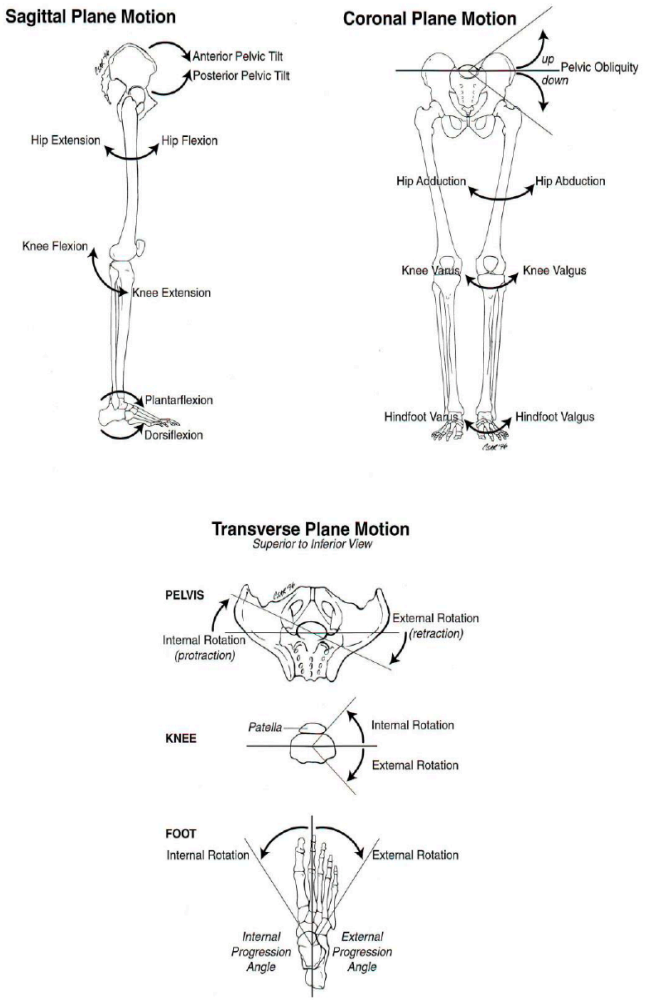

Figure 3. Anatomical planes of hip, knee, ankle joints and their types of motion [12]

In the three anatomical planes, motion analysis enables the accurate description of the movements of the body parts (Figure 3). The motion of the sagittal plane is often described by the extension and flexion of the terms. The extension is the action that increases the internal angle, whereas flexion is the action that decreases the internal angle formed between two articulating bones. Dorsiflexion (DF) and plantarflexion (PF) are terms associated with ankle and foot motion. DF is the excursion of the foot toward the anterior tibia. PF is defined as the excursion of the foot away from the anterior tibia. Adduction, abduction, varus, valgus, eversion, and inversion are associated with coronal plane motion. Adduction is the motion of bringing the body

part back towards the midline of the body. Abduction is the act of moving a body part away from the midline of the body in the coronal plane. Varus is described as the medial angulation posture of the distal segment of a joint, whereas valgus is described as the lateral angulation posture of the distal segment of a joint. Eversion and inversion are terms linked to foot and ankle motion in the coronal plane. Eversion of the foot is the opposite motion, whereas inversion of the foot refers to the sole turning towards the midsagittal plane of the body.

The motion in the transverse plane is generally limited to joint rotations and foot progression angles. It is defined in terms of internal and external directions. Practicing the right-hand rule for right-side joint rotations, if the fingers are curled in the direction of rotation, then internal rotation causes the thumb to point proximally. On the other hand, external rotation is the opposite of gesticulation, causing the thumb to indicate distally. The left-hand rule is used for left-side joint rotations [12].

2.7. Anatomy of the Muscles of the Lower Extremity

2.7.1. Muscles of the Hip Region

2.7.1.1. M. Iliopsoas

This muscle consists of 2 separate parts: M. Iliacus and M. Psoas Major (Figure 4). These muscles tendon inserts on the trochanter minor of the femur, but the origins are different. M. Iliacus originates from iliac wing and spina iliaca anterior inferior. M. Psoas Major originates from the last thoracic and transverse processes of the entire lumbar vertebra. The strongest flexor muscle of the thigh is the M. Iliacus. It also externally rotates the thigh. M. Psoas Major flexes and externally rotates the thigh. In addition, when the thigh is fixed, it bends the lumbar vertebrae forward if it contracts bilaterally, and laterally and forward if it contracts unilaterally. M. Iliopsoas plays an essential role in stabilizing the pelvis. It also raises the trunk when moving from the supine position to the sitting position. It works as an antagonist of the M. Gluteus

Maximus. Innervation of this muscle is provided by branches from the plexus lumbalis [13] (Table 2).

2.7.1.2. M. Psoas Minor

It is a cylindrical muscle anterior to the M. Psoas Major (Figure 4). It originates from the discus of the last thoracic and all lumbar vertebra, and insertion ends at the pecten ossis pubis, eminentia iliopubica, and laterally at the fascia iliaca. Innervation is provided by the plexus lumbalis. Functionally, this muscle leans the trunk forward [14] (Table 2).

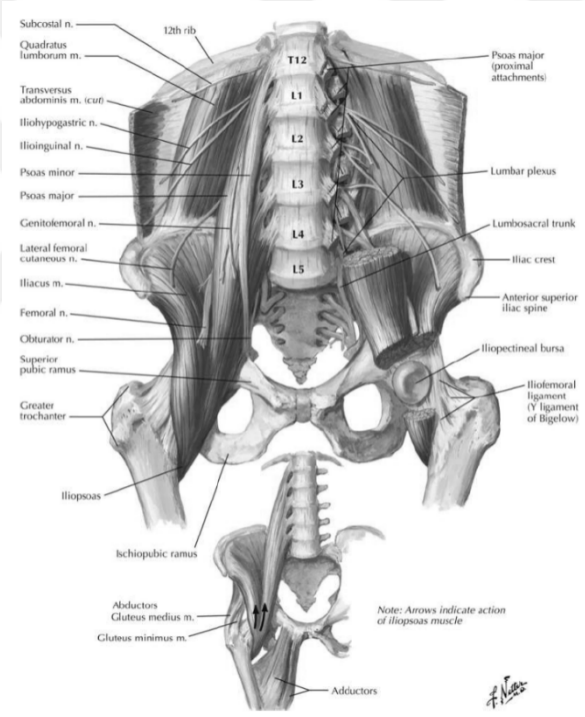

Figure 4. Psoas and Iliacus muscle (13)

2.7.1.3. M. Gluteus Maximus

It is a broad and 4-sided muscle and is the most superficial muscle of this region (Figure 5). It is a postural muscle like M. Iliopsoas. It originates from the ligameuntum sacrotuberale and the fascia glutes covering the muscle and inserts on the tractus

iliotibialis and tuberositas glutea. It is the strongest extensor muscle of the thigh and is the antagonist of the M. Iliopsoas muscle. External rotation, abduction (with the upper half), and adduction (with the lower half) of the thigh are the functions of this muscle. It also aids in leg extension as it joins the tractus iliotibialis. Innervation is provided by N. Gluteus Inferior [14] (Table 1).

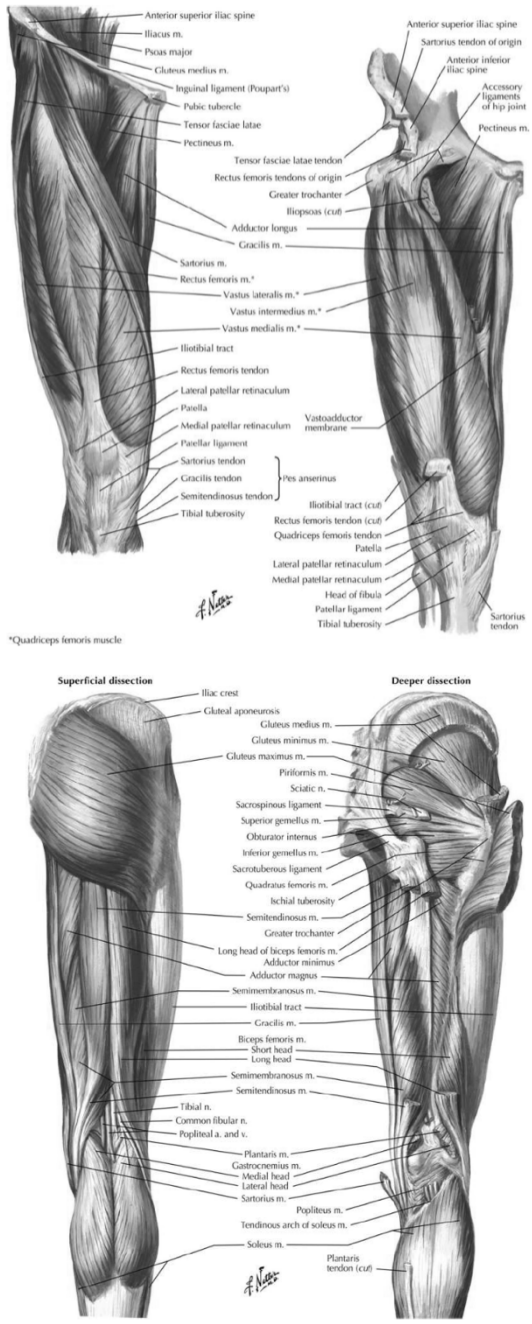

Figure 5. Muscles of anterior and posterior compartment of the thigh [13]

2.7.1.4. M. Gluteus Medius

It originates from the area between the linea glutea anterior, the crista iliaca and the linea glutea posterior, and the overlying fascia glutea. It inserts laterally into the trochanter major of the femur (Figure 5). It is the strongest adductor muscle of the thigh and executes internal rotation with the anterior part fibers. While walking, it pulls the pelvis towards the side of the foot on the ground, thus pulling the gravity center to the side of the foot. Since this function cannot be performed in the lesion, the pelvis on the side of the swinging leg falls. This is called Trendelenburg (+). Innervation is provided by N. Gluteus Superior [14] (Table 1).

2.7.1.5. M. Gluteus Minimus

It is the smallest gluteal muscle covered by M. Gluteus Medius (Figure 5). This muscle originates from the area between the anterior and inferior glutea. It extends posteriorly to the incisura ischiadica major and inserts on the anterior margin of the trochanter major of the femur. Abduction and internal rotation of the thigh are the main functions of the muscle. Innervation is provided by N. Gluteus Superior [14] (Table 1).

2.7.1.6. M. Tensor Fascia Latae

It is a flat, small muscle (Figure 5). It originates from the anterior part of the crista iliaca and the anterior superior of the spina iliaca. Between the two leaves of the tractus iliotibialis, it inserts on the fascia lata where the upper and middle 1/3 of the thigh meet. It executes flexion, internal rotation, and abduction of the thigh. In addition, it aids in leg extension and external rotation through the tractus iliotibialis. It supports the knee joint and stabilizes the pelvis. This muscle works with M. Gluteus Medius and M. Gluteus Minimus while walking. Innervation is provided by N. Gluteus Superior [14] (Table 1).

2.7.1.7. M. Piriformis

It is a flat, pyramid-shaped muscle (Figure 5). It originates from the anterior surface of the sacrum and the posterior inferior of the spina iliaca. It inserts on the upper border of the trochanter major. Functionally, it abducts the femur during flexion of the hip and rotates the femur during the hip extension. Innervation is provided by N. Musculi Piriformis (branch of plexus sacralis) [14] (Table 1).

2.7.1.8. M. Obturatorius Internus

This muscle originates from the medial surface of the membrana obturatoria and surrounding bone and inserts on the inner surface of the trochanter major (Figure 5). Functionally, it externally rotates the femur when the hip is abducted and extends it when it is flexed. Innervation is provided by N. Musculi Obturatorii Interni (branch of plexus sacralis) [14] (Table 1).

2.7.1.9. M. Gemellus Superior

It originates from the outer surface of the spina ischiadica, fused with the upper edge of the M. Obturatorius Internus, and insertion ends on the inner surface of the femur trochanter major (Figure 5). It abducts and externally rotates the thigh from the flexed hip. Also, in the acetabulum, it stabilizes the head of the femur. Its innervation is provided by branches from the plexus sacralis [14] (Table 1).

2.7.1.10. M. Gemellus Inferior

It originates from the tuber ischiadicum, fuses with the lower border of the M. Obturatorius Internus, and inserts on the inner surface of the femur trochanter major (Figure 5). Functionally, it externally rotates the weakly extended thigh and abducts the flexed thigh. Its innervation is provided by branches from the plexus sacralis [14] (Table 1).

2.7.1.11. M. Obturatorius Externus

It is a flat and triangular muscle (Figure 5). It originates from the medial 2/3 of the outer surface of the membrana obturatoria and the bone structure and inserts on the fossa trochanterica. This muscle is covered by adductor muscles. It externally rotates the thigh and supports the femoral head from below. This muscle is the only external rotator muscle of the thigh innervated by the N. Obturatorius [14] (Table 1).

2.7.1.12. M. Quadratus Femoris

It is a flat, thick, and 4-cornered muscle (Figure 5). It originates on the outer surface of the tuber ischiadicum and inserts on the upper part of the crista intertrochanterica. It is the strongest external rotator muscle of the thigh. Innervation is provided by N. Musculi Quadrati Femoris (branch of plexus sacralis) [14] (Table 1).

Table 1. Gluteal region muscles

Muscle	Origin	Insertion	Nerve Supply	Nerve Root	Action
Gluteus maximus	Outer surface of ilium, sacrum, coccyx, sacrotuberous ligament	Iliotibial tract and gluteal tuberosity of femur	Inferior gluteal nerve	L5, S1,2	Extends and laterally rotates hip joint; through iliotibial tract, it extends knee joint
Gluteus medius	Outer surface of ilium	Lateral surface of greater trochanter of femur	Superior gluteal nerve	L5, S1	Abducts thigh at hip joint; tilts pelvis when walking to permit opposite leg to clear ground
Gluteus minimus	Outer surface of ilium	Anterior surface of greater trochanter of femur	Superior gluteal nerve	L5, S1	Abducts thigh at hip joint; tilts pelvis when walking to permit opposite leg to clear ground
Tensor fasciae latae	Iliac crest	Iliotibial tract	Superior gluteal nerve	L4,5	Assists gluteus maximus in extending the knee joint
Piriformis	Anterior surface of sacrum	Upper border of greater trochanter of femur	First and second sacral nerves	L5, S1	Lateral rotator of thigh at hip joint
Obturator internus	Inner surface of obturator membrane	Upper border of greater trochanter of femur	Sacral plexus	L5, S1	Lateral rotator of thigh at hip joint
Gemellus supenor	Spine of ischium	Upper border of greater trochanter of femur	Sacral plexus	L5, S1	Lateral rotator of thigh at hip joint
Gemellus inferior	Ischial tuberosity	Upper border of greater trochanter of femur	Sacral plexus	L5, S1	Lateral rotator of thigh at hip joint
Quadratus femoris	Lateral border of ischial tuberosity	Quadrate tubercle of femur	Sacral plexus	L5, S1	Lateral rotator of thigh at hip joint

2.7.2. Muscles of the Thigh Region

2.7.2.1. M. Sartorius

This muscle is the longest muscle in the body (Figure 5), also known as the tailor's muscle. It originates from spina iliaca anterior superior. As it descends from top to bottom, it crosses the front of the thigh from outside to inside and inserts on the pes anserinus inside the tibia. It is a biarticular muscle that moves both the thigh and the leg.

Functionally, it flexes, abducts, and externally rotates the thigh. It also flexes the leg at the knee joint and internally rotates the flexed leg. Innervation is provided by N. Femoralis [14].

2.7.2.2. M. Quadriceps Femoris

It is the largest muscle in the body (Figure 5). Additionally, it is the strongest extensor of the leg and the postural muscle. The M. Quadriceps Femoris muscle functions in climbing, running, jumping, climbing stairs, and getting up from a sitting position. [14]. Innervation is provided by N. Femoralis. It consists of four parts:

M. Rectus Femoris: It is a spindle-shaped muscle whose fibers resemble bird feathers. The muscle has two parts. The straight head originates from the anterior inferior of the spina iliaca, reflected head originates from the upper part of the acetabulum. Its two heads insert into the base of the patella. Functionally, it extends the leg at the knee joint and flexes the thigh at the hip joint [14].

M. Vastus Lateralis: It is the biggest part of the quadriceps muscle. It originates from linea aspera labium laterale, linea intertrochanterica and trochanter major. This muscle inserts on the outer half of the basis patella and the tendon of the M. Quadriceps

Femoris. Its medial edge is fused with M. Vastus Intermedius. Functionally, it extends the leg at the knee joint [14].

M. Vastus Intermedius: It is deep within the M. Rectus Femoris. It originates below the anterior lateral aspect of the femur and the linea intertrochanterica and inserts on the outer part of the patella and the tendon of the M. Quadriceps Femoris. Functionally, it extends the leg at the knee joint [14].

M. Vastus Medialis: This muscle lies down on the inner thigh, between the lower parts of M. Sartorius and M. Rectus Femoris. It originates from linea aspera labium laterale, linea intertrochanterica and trochanter major. It inserts on the outer half of the basis patella and the tendon of the M.Quadriceps Femoris. Its lateral margin is fused with M. Vastus Intermedius. This muscle also prevents the patella from sliding laterally, thereby, it is stabilizing the patella. Functionally, it extends the leg at the knee joint [14].

Table 2 shows the summary of the anterior compartment muscles of the hip and thigh.

Table 2. Muscles of the anterior compartment of the thigh (15)

Muscle	Origin	Insertion	Nerve Supply	Nerve Root	Action
Sartorius	Anterosuperior iliac spine	Upper medial surface of shaft of tibia	Femoral nerve	L2,3	Flexes, laterally rotates, abducts thigh at hip joint; flexes and medially rotates leg at knee joint
Iliacus	Iliac fossa of hip bone	With psoas into lesser trochanter of femur	Femoral nerve	L2,3	Flexes thigh on the trunk; when the thigh is fixed, it flexes the trunk on the thigh as in sitting up from lying down
Psoas	Transverse processes, bodies, and intervertebral discs of the 12th thoracic and five lumbar vertebrae	With iliacus into lesser trochanter of femur	Lumbar plexus	L1,2,3	Flexes thigh on trunk; if thigh is fixed, it flexes the trunk on the thigh as in sitting up from lying down
Pectineus	Superior ramus of pubis	Upper end of linea aspera of shaft of femur	Femoral nerve (sometimes obturator nerve)	L2,3	Flexes and adducts thigh at hip joint
Quadriceps Femoris					
Rectus femoris	Straight head: anteroinferior iliac spine Reflected head: ilium above acetabulum	Quadriceps tendon into patella, then via ligamentum patellae into tubercle of tibia	Femoral nerve	L2,3,4	Extension of leg at knee joint; flexes thigh at hip joint
Vastus lateralis	Upper end and shaft of femur	Quadriceps tendon into patella, then via ligamentum patellae into tubercle of tibia	Femoral nerve	L2,3,4	Extension of leg at knee joint
Vastus medialis	Upper end and shaft of femur	Quadriceps tendon into patella, then via ligamentum patellae into tubercle of tibia	Femoral nerve	L2,3,4	Extension Of leg at knee joint; stabilizes patella
Vastus intermedius	Anterior and lateral surfaces of shaft of femur	Quadriceps tendon into patella, then via ligamentum patellae into tubercle of tibia	Femoral nerve	L2,3,4	Extension of leg at knee joint; articularis genus retracts synovial membrane

2.7.2.3. M. Articularis Genus

It is a small muscle, sometimes in the form of a continuation of fibers of M. Vastus Intermedius (Figure 5). It originates from the distal anterior aspect of the femur and inserts on the upper edge of the knee joint capsule. Functionally, it stretches the joint capsule. Innervation is provided by N. Femoralis [14].

2.7.2.4. M. Gracilis

It lies down the medial to the thigh and is the most superficial of the adductor group muscles (Figure 5). It is wide at the top and narrows as it goes down. This muscle originates from the upper half of the ischium pubis arm and the lower half of the symphysis pubica. It inserts on the upper part of the inner surface of the tibia and forms the Pes Anserinus. It is the weakest of the adductor group muscles. It flexes the leg, adducts the thigh, and internally rotates the leg when flexed (Table 3). It is innervated by N. Obturatorius [14].

2.7.2.5. M. Pectineus

It is a flat muscle located on the upper-inner border of the thigh (Figure 5). It originates from the pecten ossis pubis and is inserted into the linea pectinea of the femur. Functionally it adducts, flexes, and internally rotates the thigh. Innervation is cared for by N. Femoralis (sometimes innervated by N. Obturatorius) [14] (Table 3).

2.7.2.6. M. Adductor Longus

It originates from the ramus superior ossis pubis and inserts on the middle 1/3 of the medial labium of the linea aspera (Figure 5). Functionally, it adducts the thigh. Its innervation is cared for by N. Obturatorius [14] (Table 3).

2.7.2.7. M. Adductor Brevis

It lies below the M. Adductor Longus and has a triangular shape (Figure 5). The muscle originates from the inferior ossis pubis and inserts on the upper 1/3 of the linea aspera labium mediale. Functionally, it adducts the thigh. Innervation is cared for by N. Obturatorius [14].

2.7.2.8. M. Adductor Magnus

It is the largest and strongest adductor group muscle (Figure 5). The muscle has a triangular shape and is located on both the inner and back of the thigh. It consists of two parts: the adductor and the hamstring parts. It originates from ramus inferior ossis pubis, ramus ossis ischia and tuber ischiadicum. The muscle inserts on the labium mediale and femur epicondylis medialis. A small superficial part of the muscle is called M. Adductor Minimus. Adduction and extension of the thigh are the functions of the muscle. Innervation is provided by N. Obturatorius (adductor part) and N. Tibialis (hamstring part) [14] (Table 3).

Table 3. Muscles of the medial compartment of the thigh [15]

Muscle	Origin	Insertion	Nerve Supply	Nerve Root	Action
Gracilis	Inferior ramus of pubis, ramus of ischium	Upper part of shaft of tibia on medial surface	Obturator nerve	L2,3	Adducts thigh at hip joint; flexes leg at knee joint
Adductor longus	Body of pubis, medial to pubic tubercle	Posterior surface of shaft of femur (linea aspera)	Obturator nerve	L2,3,4	Adducts thigh at hip joint and assists in medial rotation
Adductor brevis	Inferior ramus of pubis	Posterior surface of shaft of femur (linea aspera)	Obturator nerve	L2,3,4	Adducts thigh at hip joint
Adductor magnus	Inferior ramus of pubis, ramus of ischium, ischiai tuberosity	Posterior surface of shaft of femur, adductor tubercle of femur	Adductor portion: obturator nerve Hamstring portion: sciatic nerve	L2,3,4	Adducts thigh at hip joint and assists in medial rotation; hamstring portion extends thigh at hip joint
Obturator externus	Outer surface of obturator membrane and pubic and ischial rami	Medial surface of greater trochanter	Obturator nerve	L3,4	Laterally rotates thigh at hip joint

2.7.2.9. M. Biceps Femoris

It lies down on the outer back of the thigh (Figure 5). It has two heads, Caput Longum and Caput Breve. Caput Longum originates from the tuber ischiadicum, fused with the M. semitendinosus tendon. Caput Breve originates from the linea aspera labium laterale. It inserts on the caput fibulare. Both heads flex the leg and externally rotate the flexed leg. Additionally, it aids in the extension of the trunk. Moreover, the Caput Longum part extends, adducts, and externally rotates the thigh. Innervation of the Caput Longum part is provided by N. Tibialis. Caput Breve part is innervated by N. Fibularis (Peroneus) Communis [14] (Table 4).

2.7.2.10. M. Semitendinosus

The muscle lies down superficial to M. Semimebranosus (Figure 5). It originates from tuber ischiadicum and inserts below the tibia's medial condyle, joining the Pes Anserinus. Flexion of the leg, internal rotation of the flexed leg, and extension of the thigh are the functions of the muscle. Innervation is provided by N. Tibialis [14] (Table 4).

2.7.2.11. M. Semimembranosus

It originates from the tuber ischiadicum and inserts behind the medial condyle of the tibia (Figure 5). Flexion of the leg, internal rotation of the flexed leg, and extension of the thigh are the functions of the muscle. Innervation is provided by N. Tibialis [14] (Table 4).

Table 4. Muscles of the posterior compartment of the thigh (15)

Muscle	Origin	Insertion	Nerve Supply	Nerve Root	Action
Biceps femoris	Long head: ischial tuberosity	Head of fibula	Long head: tibial portion of sciatic nerve	L5; S1,2	Flexes and laterally rotates leg at knee joint; long head also extends thigh at hip joint
	Short head: linea aspera, lateral supracondylar ridge of shaft of femur		Short head: common fibular portion of sciatic nerve		
Semitendinosus	Ischial tuberosity	Upper part of medial surface of shaft of tibia	Tibial portion of sciatic nerve	L5; S1,2	Flexes and medially rotates leg at knee joint; extends thigh at hip joint
Semi membranosus	Ischial tuberosity	Medial condyle of tibia	Tibial portion of sciatic nerve	L5; S1,2	Flexes and medially rotates leg at knee joint; extends thigh at hip joint
Adductor magnus (hamstring portion)	Ischial tuberosity	Adductor tubercle of femur	Tibial portion of sciatic nerve	L2,3,4	Extends thigh at hip joint

2.7.3. Muscles of the Leg Region

2.7.3.1. M. Tibialis Anterior

It originates from the lateral condyle of the tibia and 2/3 of its outer surface and the fascia cruris (Figure 6). Muscle inserts on the inside and underside of the first cuneiform bone and at the base of the first metatarsal bone on the inside of the foot. Foot DF and inversion are the functions of the muscle. It is the strongest dorsiflexor muscle of the foot. It also plays a role in the protection of the foot arch. Innervation is provided by N. Fibularis (Peroneus) Profundus [14] (Table 5).

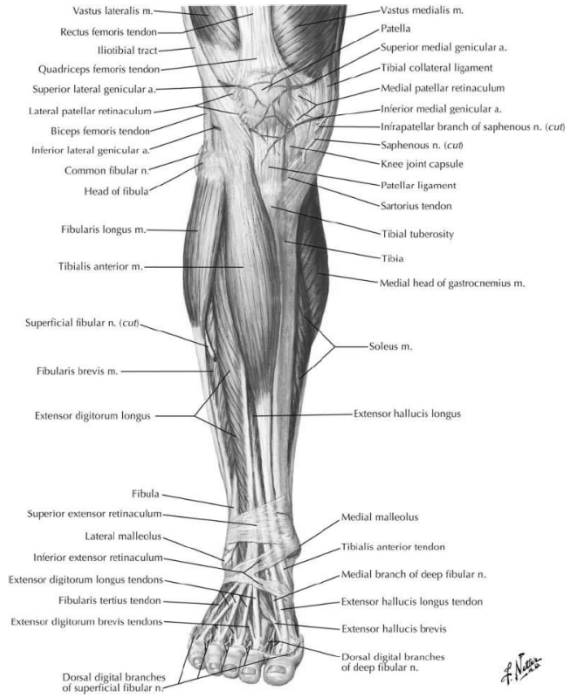

Figure 6. Muscles of anterior compartment of the leg [13]

2.7.3.2. M. Extensor Hallucis Longus

It lies underneath M. Extensor Digitorum Longus and M. Tibialis Anterior (Figure 6). It originates from the middle of the interossea cruris and the fibula and inserts on the dorsal aspect of the last phalanx of the thumb. Functionally, it extends the thumb. Additionally, it dorsiflexes and inverts the foot. Innervation is provided by N. Fibularis (Peroneus) Profundus [14] (Table 5).

2.7.3.3. M. Extensor Digitorum Longus

It originates from the medial condyle of the tibia, the upper 3/4 of the anterior surface of the fibula, the membrane interossea cruris, and the fascia cruris (Figure 6). Muscle inserts on the dorsal aponeurosis of the medial and distal phalanges of the fingers. Functionally, it extends the other four fingers except for the thumb.

Additionally, it dorsiflexes and everts the foot. Innervation is provided by N. Fibularis (Peroneus) Profundus [14] (Table 5).

2.7.3.4. M. Fibularis (Peroneus) Tertius

Muscle consists of fibers separated from M. Extensor Digitorum Longus (Figure 6). Therefore, it can be considered the fifth tendon of this muscle. It originates from the distal 1/3 of the anterior surface of the fibula and the lower half of the membrane interossei. It inserts on the fifth metatarsal and adheres to the upper surface of the bone. Functionally, it dorsiflexes and everts of the foot. Innervation is provided by N. Fibularis (Peroneus) Profundus [14] (Table 5).

Table 5. Muscles of the anterior compartment of the leg (15)

Muscle	Origin	Insertion	Nerve Supply	Nerve Root	Action
Tibialis anterior	Lateral surface of shaft of tibia and interosseous membrane	Medial cuneiform and base of first metatarsal bone	Deep fibular nerve	L4, 5	Extends foot at ankle joint; inverts foot at subtalar and transverse tarsal joints; holds up medial longitudinal arch of foot
Extensor hallucis longus	Anterior surface of shaft of fibula	Base Of distal phalanx of great toe	Deep fibular nerve	L5; S1	Extends big toe; extends foot at ankle joint; inverts foot at subtalar and transverse tarsal joints
Extensor digitorum longus	Anterior surface of shaft of fibula	Extensor expansion of lateral four toes	Deep fibular nerve	L5; S1	Extends toes; extends foot at ankle joint
Fibularis tertius	Anterior surface of shaft of fibula	Base Of fifth metatarsal bone	Deep fibular nerve	L5; S1	Extends foot at ankle joint; everts foot at subtalar and transverse tarsal joints

2.7.3.5. M. Fibularis (Peroneus) Longus

The muscle originates from the fibula and the upper 2/3 of the outer surface of the fibula, the fascia cruris, and the septum intermusculare cruris anterius and posterius (Figure 7). It extends medially on the sole and inserts on the first metatarsal and cuneiform bones. Muscle actively supports the arch of the foot together with the tendon of the M. Tibialis Anterior. Functionally, it plantar flexes and everts the foot. Moreover, it prevents the foot arch from collapsing. Innervation of the muscle is provided by N Fibularis (Peroneus) Superficialis [14] (Table 6).

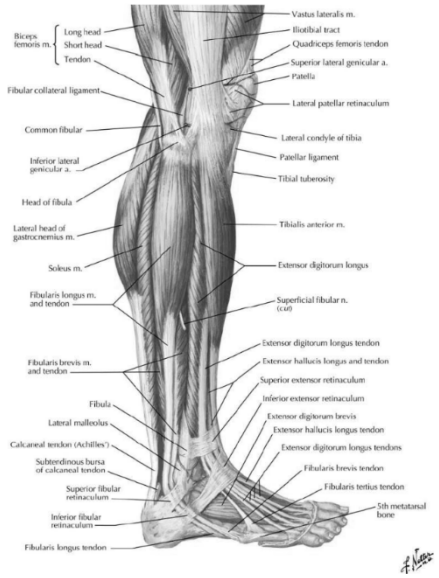

Figure 7. Muscles of lateral compartment of the leg [13]

2.7.3.6. M. Fibularis (Peroneus) Brevis

It originates from the lower 2/3 of the outer surface of the fibula and the septum intermusculare cruris anterius and posterius. The muscle inserts on the tubercle of the fifth metatarsal bone (Figure 7). Functionally, it plantar flexes and everts the foot. Innervation is provided by N. Fibularis (Peroneus) Superficialis [14] (Table 6).

Table 6. Muscles of the lateral compartment of the leg [15]

Muscle	Origin	Insertion	Nerve Supply	Nerve Root	Action
Fibularis longus	Lateral surface of shaft of fibula	Base of first metatarsal and the medial cuneiform	Superficial fibular nerve	L5; S1, 2	Plantar flexes foot at ankle joint; everts foot at subtalar and transverse tarsal joints; supports lateral longitudinal and transverse arches of foot
Fibularis brevis	Lateral surface of shaft of fibula	Base of fifth metatarsal bone	Superficial fibular nerve	L5; S1, 2	Plantar flexes foot at ankle joint; everts foot at subtalar and transverse tarsal joint; supports lateral longitudinal arch of foot

2.7.3.7. M. Triceps Surae

It is formed by two muscles: M. gastrocnemius and M. soleus (Figure 8).

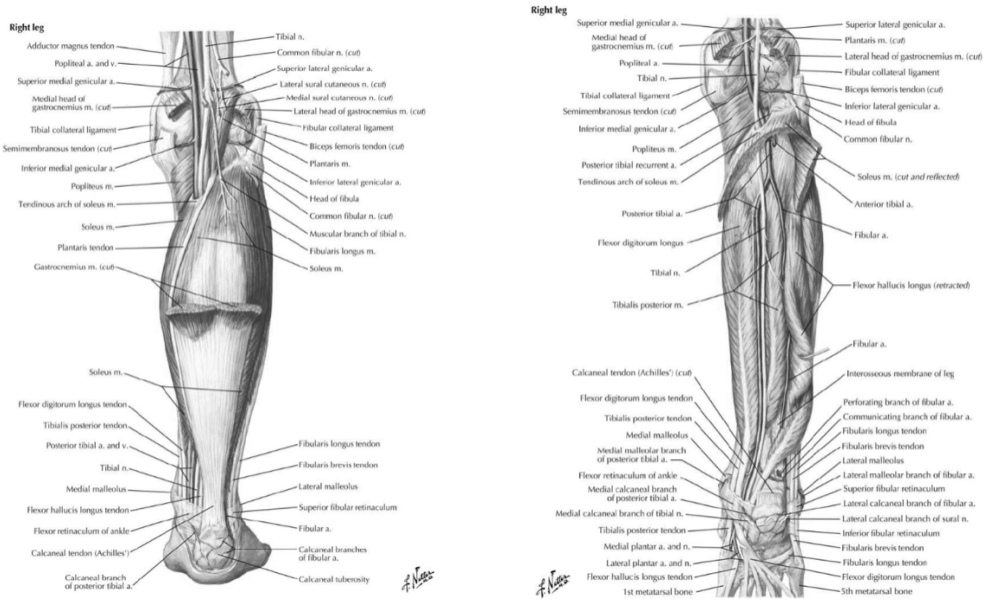

Figure 8. Muscles of posterior compartment of the leg [13]

M. Gastrocnemius: It creates the bulge on the back of the leg (Figure 8). It has two heads, caput laterale and caput mediale. The muscle originates from the caput mediale from the femur epicondylus medialis and the caput laterale from the femur epicondylus lateralis. Together with M. Soleus, it forms the tendon calcaneus (Achilles tendon), and tendon inserts on the posterior lower part of the calcaneus, called the tuber calcanei. Since it is a biarticular muscle, it functions as a PF muscle of the foot and a flexor muscle of the leg at the knee joint. It is the strongest plantar flexor muscle. Innervation is provided by N. Tibialis [14] (Table 7).

M. Soleus: The muscle originates from linea musculi solei, the upper 1/3 of the body of the fibula, and the arcus tendineus musculi solei between the tibia and fibula (Figure 8). It inserts on the tendon calcaneus (Achilles tendon). Functionally, it plantar flexes and inverts the foot. Innervation is provided by N. Tibialis [14] (Table 7).

2.7.3.8. M. Plantaris

It is a small muscle that originates from the lowest part of the labium laterale linea aspera and Lig. Popliteum Obliquum (Figure 8). The muscle inserts on the medial edge of the calcaneus. Functionally, it plantar flexes the foot and flexes the leg at the knee joint. Innervation is provided by N. Tibialis [14] (Table 7).

2.7.3.9. M. Popliteus

It is a thin and flat muscle. The muscle originates from the condylis lateralis of the femur and Lig. Popliteum (Figure 8). Some fibers are additionally attached to the meniscus lateralis. It inserts on the upper part of the linea musculi solei on the posterior surface of the tibia. Functionally, it flexes the leg at the knee joint and internally rotates the leg when flexed. The joint lock of the knee joint is controlled by M. Popliteus. Innervation is provided by N. Tibialis [14] (Table 7).

2.7.3.10. M. Flexor Hallucis Longus

It is the largest and strongest of the deep group muscles (Figure 8). It originates from the lower 2/3 of the posterior surface of the fibula and the lower part of the membrane interossea and inserts on the last phalanx of the thumb. As this muscle passes through the sole, it crosses the tendon of the M. Flexor Digitorum Longus from above. Therefore, the contraction of one affects the other muscle. Functionally, it flexes the thumb, and plantar flexes and inverts the foot. It also supports the foot arch. Innervation is provided by N. Tibialis [14] (Table 7).

2.7.3.11. M. Flexor Digitorum Longus

It originates from the posterior aspect of the tibia and inserts on the 2nd-5th bases of distal phalanges. Functionally, it flexes the distal phalanges of the four fingers except for the thumb. Additionally, it plantar flexes and inverts. Moreover, muscle protects the arch of the foot. Innervation is provided by N. Tibialis [14] (Table 7).

2.7.3.12. M. Tibialis Posterior

It is the deepest muscle of the posterior group muscle of the leg (Figure 8). It is located between M. Flexor Hallucis Longus and M. Flexor Digitorum Longus. It originates from the posterior surface of the tibia, the upper part of the posterior surface of the fibula, and the membrane interossea. The muscle inserts on tuberositas ossis navicularis and other neighboring bones. Some fibers insert on the tip of the sustentaculum tali, three cuneiform bones, cuboid emery, and 2nd-4th. Tendon insertion ends in the metatarsal bones. Together with M. Tibialis Anterior, it is the main inverter muscle of the foot. It also plantar flexes the foot. Moreover, together with M. Tibialis Anterior, M. Flexor Hallucis Longus, and M. Fibularis (Peroneus) Longus, it protects the foot arch. Innervation is provided by N. Tibialis [14] (Table 7).

Table 7. Muscles of the posterior compartment of the leg [15]

Muscle	Origin	Insertion	Nerve Supply	Nerve Root	Action
Superficial Group					
Gastrocnemius	Lateral head from lateral condyle of femur and medial head from above medial condyle	Via tendo calcaneus into posterior surface of calcaneum	Tibial nerve	S1, 2	Plantar flexes foot at ankle joint; flexes knee joint
Plantaris	Lateral supracondylar ridge of femur	Posterior surface of calcaneum	Tibial nerve	S1, 2	Plantar flexes foot at ankle joint; flexes knee joint
Soleus	Shafts of tibia and fibula	Via tendo calcaneus into posterior surface of calcaneum	Tibial nerve	S1, 2	Together with gastrocnemius and plantaris is powerful plantar flexor of ankle joint; provides main propulsive force in walking and running
Deep Group					
Popliteus	Lateral surface of lateral condyle of femur	Posterior surface of shaft of tibia above soleal line	Tibial nerve	L4, 5; S1	Flexes leg at knee joint; unlocks knee joint by lateral rotation of femur on tibia and slackens ligaments of joint
Flexor digitorum longus	Posterior surface of shaft of tibia	Bases of distal phalanges of lateral four toes	Tibial nerve	S2, 3	Flexes distal phalanges of lateral four toes; plantar flexes foot at ankle joint; supports medial and lateral longitudinal arches of foot
Flexor hallucis longus	Posterior surface of shaft of fibula	Base of distal phalanx of big toe	Tibial nerve	S2, 3	Flexes distal phalanx of big toe; plantar flexes foot at ankle joint; supports medial longitudinal arch of foot
Tibialis posterior	Posterior surface of shafts of tibia and fibula and interosseous membrane	Tuberosity of navicular bone and other neighboring bones	Tibial nerve	L4, 5	Plantar flexes foot at ankle joint; inverts foot at subtalar and transverse tarsal joints; supports medial longitudinal arch of foot

2.7.4. Muscles of the Foot Region

Figure 9 shows the Interosseous Muscles of Foot.

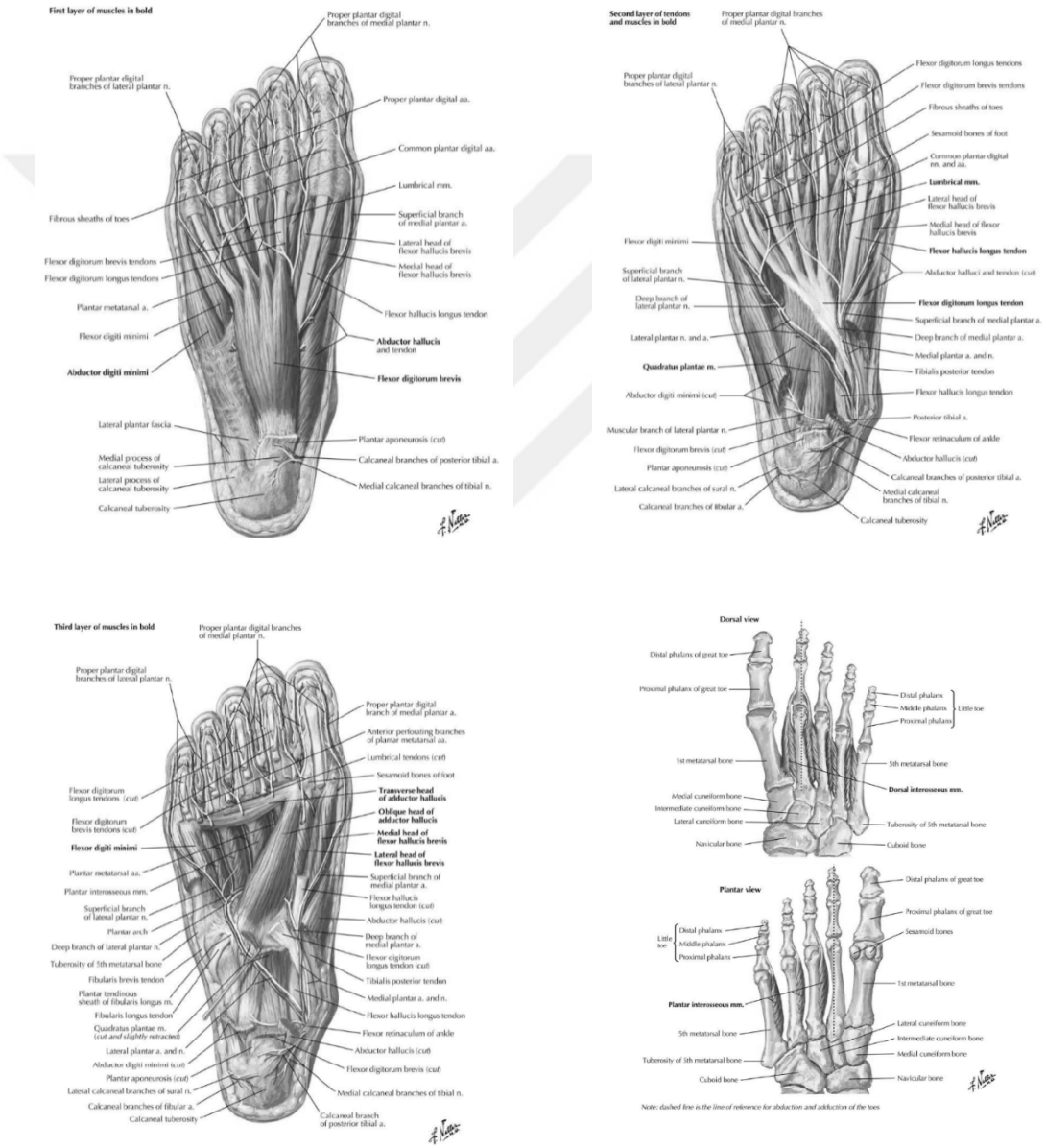

Figure 9. Interosseous muscles of foot [13]

2.7.4.1. M. Abductor Hallucis

The bulge it makes is called eminentia plantaris medialis. It originates from the processus medialis and aponeurosis plantaris of the calcaneus and inserts on the first phalanx of the thumb (Figure 9). Abduction of the thumb is the function of the muscle. Innervation is provided by N. Plantaris Medialis [14] (Table 8).

2.7.4.2. M. Flexor Digitorum Brevis

It originates from the middle of the processus medialis tuber calcanei and aponeurosis plantaris. The muscle inserts on the lateral parts of the middle of the 2.-4. phalanx (Figure 9). Functionally, it flexes the 2.-5. fingers except for the thumb. Innervation is provided by N. Plantaris Medialis [14] (Table 8).

2.7.4.3. M. Abductor Digiti Minimi

It lies down along the lateral edge of the foot (Figure 9). Muscle originates from processus lateralis and medialis tuber calcanei and aponeurosis calcanei. It inserts on the first phalanx of the fifth finger. The bulge it makes is called eminentia plantaris lateralis. Functionally, it abducts the fifth finger. Innervation is provided by N. Plantaris Lateralis [14] (Table 8).

2.7.4.4. M. Quadratus Plantae

It originates from the plantare longum and inserts laterally on the tendon of the M. Flexor Digitorum Longus (Figure 9). It flexes the 2.-5. fingers except for the thumb. Innervation is provided by N. Plantaris Lateralis [14] (Table 8).

2.7.4.5. M. Lumbricales

It consists of four worm-shaped muscles (Figure 9). They originate from the tendons of M. Flexor Digitorum Longus and inserts on 2.-5. proximal phalanges and dorsal aponeuroses of the fingers. Functionally, it flexes the phalanges of the 2.-5. fingers, excluding the thumb, and extends the proximal and distal phalanges. Innervation of the first lumbrical muscle is provided by N. Plantaris Medialis, and the innervation of the other three lumbrical muscles is provided by N. Plantaris Lateralis [14] (Table 8).

2.7.4.6. M. Flexor Hallucis Brevis

It originates from the os cuboideum, os cuneforme laterale, and partly from the tendon of the M. Tibialis Posterior. The muscle inserts on either side of the first phalanx of the thumb (Figure 9). Functionally, it flexes the first phalanx of the thumb. Innervation is provided by N. Plantaris Medialis [14] (Table 8).

2.7.4.7. M. Adductor Hallucis

It consists of two parts: Caput Obliquum and Caput Transversum (Figure 9). Caput Obliquum originates from the base of the 2.-4. metatarsal bones and the tendon of the M. Fibularis (Peroneus) Longus. This part inserts laterally on the first phalanx of the thumb. Caput Transversum originates from the 2.-4. metatarsophalangea and inserts laterally on the first phalanx of the thumb. Functionally, it adducts the thumb. Innervation is terminated by N. Plantaris Lateralis [14] (Table 8).

2.7.4.8. M. Flexor Digiti Minimi Brevis

It originates from the base of the fifth metatarsal bone and the fibrous sheath of the M. Fibularis (Peroneus) Longus. The muscle inserts laterally on the first phalanx

of the fifth finger (Figure 9). Functionally, it flexes the fifth finger's first phalanx. Innervation is provided by N. Plantaris Lateralis [14] (Table 8).

2.7.4.9. M. Interossei Dorsales

They are the deepest muscles of the soles of the feet and are 4 in number (Figure 9). They originate from the metatarsal bones, between which it is located. The first interosseos muscle inserts on the medial side of the second finger, while the second inserts on the lateral side of the second finger. The third and fourth interosseos muscles insert laterally on the fingers they belong to. Functionally, they are responsible for the abduction of the fingers. Innervation is provided by N. Plantaris Lateralis [14].

2.7.4.10. M. Interossei Plantares

They are the deepest muscles of the sole of the feet and are three in number (Figure 9). They are located on the plantar side of the 3.-5. metatarsal bones. They originate from the medial sides of the metatarsal bones and insert on the medial sides of the bases of the first phalanges of the same fingers and their dorsal aponeurosis. Functionally, they adduct the 3.-5. fingers. Innervation is provided by N. Plantaris Lateralis [14].

Table 8. Muscles of the Foot [15]

Muscle	Origin	Insertion	Nerve Supply	Nerve Root	Action
First Layer					
Abductor hallucis	Medial tuberosity of calcaneum and flexor retinaculum	Base of proximal phalanx of big toe	Medial plantar e	S2, 3	Flexes and abducts big toe; braces medial longitudinal arch
Flexor digitorum brevis	Medial tubercle of calcaneum	Four tendons to four lateral toes—inserted into borders of middle phalanx; tendons perforated by those of flexor digitorum longus	Medial plantar nerve	S2, 3	Flexes lateral four toes; braces medial and lateral longitudinal arches
Abductor digiti minimi	Medial and lateral tubercles of calcaneum	Base of proximal phalanx of fifth toe	Lateral plantar nerve	S2, 3	Flexes and abducts fifth toe; braces lateral longitudinal arch
Second Layer					
Quadratus plantae	Medial and lateral sides of calcaneum	Tendon Of flexor digitorum longus	Lateral plantar nerve	S2, 3	Assists flexor digitorum longus in flexing lateral four toes
Lumbricals (4)	Tendons Of flexor digitorum longus	Dorsal extensor expansion; bases of proximal phalanges of lateral four toes	First lumbrical: medial plantar nerve; remainder: lateral plantar nerve		Extends toes at interphalangeal joints
Flexor digitorum longus tendon					
Flexor hallucis longus tendon					
Third Layer					
Flexor hallucis brevis	Cuboid, lateral cuneiform, tibialis posterior insertion	Medial tendon into medial side of base of proximal phalanx of big toe; lateral tendon into lateral side of base of proximal phalanx of big toe	Medial plantar nerve	S2, 3	Flexes metatarsophalangeal joint of big toe; supports medial longitudinal arch
Adductor hallucis	Oblique head bases of second, third, and fourth metatarsal bones; transverse head from plantar ligaments	Lateral side of base of proximal phalanx of big toe	Deep branch lateral plantar nerve	S2, 3	Flexes metatarsophalangeal joint of big toe; holds together metatarsal bones
Flexor digiti minimi brevis	Base of fifth metatarsal bone	Lateral side of base of proximal phalanx of little toe	Lateral plantar nerve	S2, 3	Flexes metatarsophalangeal joint of little toe

2.8. GAIT ANALYSIS

The objective findings of Gait Analysis, its importance in preoperative diagnosis, its use in postoperative follow-up, and the possibility of comparing the patient's locomotor system clinic preoperative and postoperative have led to increasing importance in SCM.

The cycle of coordinated and repetitive movements of the arms and legs to advance the trunk is called walking. A healthy central and peripheral nervous system, coordinated locomotor, proprioceptive and cardiovascular systems are needed for this function to be realized harmoniously. Thus, it is possible to adapt to changing environmental conditions while on the move. When the evaluation of all these systems is taken into consideration, it emerges that gait patterns should be evaluated individually instead of gathering them under a general roof.

One of the essential elements of walking is the anatomy of the locomotor system. It is important to know the anatomy and functions of the lower extremity muscles during the evaluation [17]. The main task of the lower extremity muscles is to carry and support body weight, provide balance, and perform movements such as walking and running. The Gait Cycle consists of 2 main parts: Stance Phases and Swing Phases (Figures 10, 11). During the contact of the leg with the ground, the Stance Phases are formed, and the Swing Phases are formed during the time it takes to get up and move forward. The activity of the lower extremity muscles differentiates during gait cycles (Figure 12).

The Stance phase consists of 5 sub-phases, and the Swing phase consists of 3 sub-phases. All phases are represented as a percentage of the whole gait cycle.

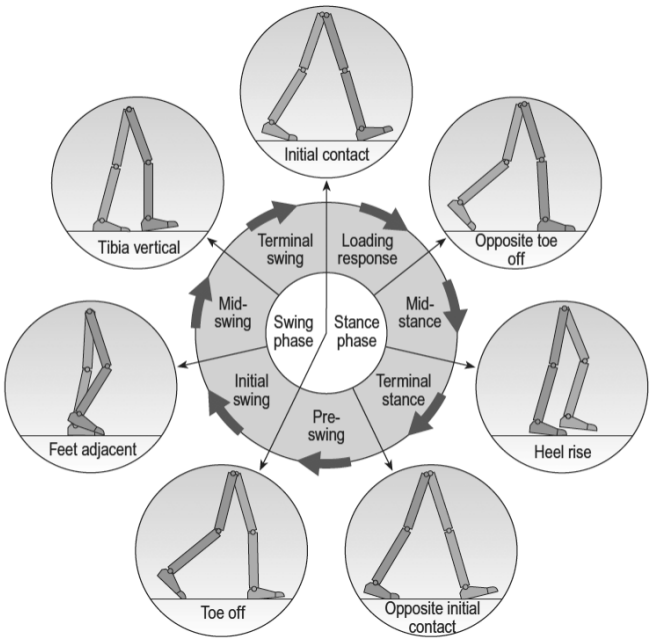

Figure 10. Gait Cycles [18]

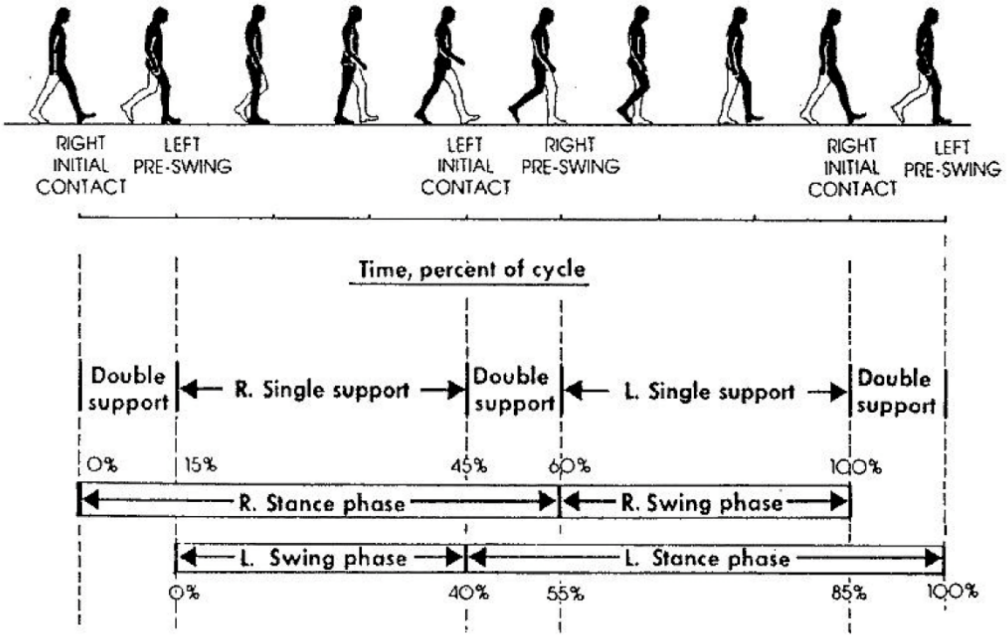

Figure 11. Time as a percentage of cycle during gait [19]

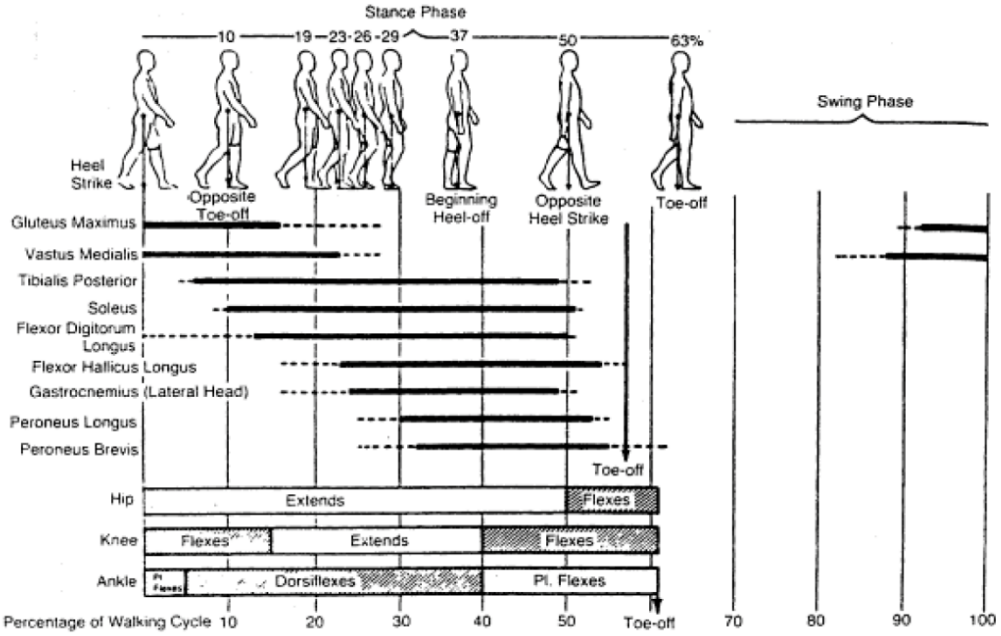

Figure 12. Muscle activity during gait [19]

2.8.1. Stance Phases

Body weight is moved from heel to toe, and the center of gravity is the same. It continues between 0-62% of the gait cycle. Stance phase consists of five sub-phases.

2.8.1.1. Initial Contact Phase (IC)

It is the first phase of the stance phase (Figure 15). In this phase, the heel contacts the ground. It is between 0-2% of the gait cycle. The hip is at 30° of flexion, the knee is extended, and the ankle is in a neutral position so that the heel touches the ground first. Thus, the stride length is increased. The trunk stays behind the foot, and the center of gravity (COG) is at its lowest level. The displacement of the COG is fast. The ground reaction force vector (GRFV) is in front of the hip, creating a force that forces the hip to flex. In this case, M. Gluteus Maximus and Hamstring group muscles contract in order to maintain balance. GRF also creates extensor moment in the knee

joint, and hamstring group muscles contract to maintain balance. Dorsiflexor muscles are active to maintain the ankle in a neutral position [17].

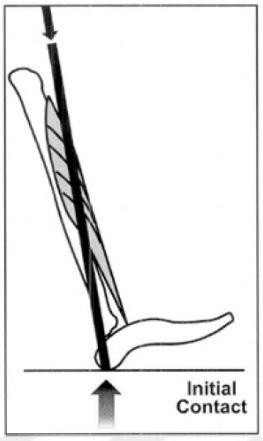

Figure 13. Initial Contact phase [20]

2.8.1.2. Loading Response Phase (LR)

It is the phase after the Initial Contact Phase (Figure 14). The other side's foot is off the ground, and the weight transfer continues until it is lifted. It is between 2-10% of the gait cycle. The hip joint begins to move from flexion to an extension position, with the knee at approximately 20° of flexion and the ankle joint at 10° of PF. COG begins to rise. GRF creates a flexion moment in the hip and knee joint and a PF moment in the ankle joint. M. Gluteus Maximus in the hip, M. Quadriceps Femoris in the knee, and dorsiflexor muscles in the ankle are active to balance against the moments. This phase is completed when the foot is entirely on the ground [17].

Figure 14. Loading Response phase [20]

2.8.1.3. Mid-Stance Phase (MST)

It is between 10-30% of the gait cycle. It starts with the foot flat on the ground and ends with the heel rise of the foot off the ground (Figure 15). The hip and knee joints are in extension, and the ankle is in DF. COG reaches the high, outermost level and is advanced forward. As GRF passes through the middle, the activity of the hip muscles is minimal. Since GRF passes behind the knee, the M. Quadriceps Femoris muscle tries to maintain balance by contracting. The M. Triceps Surae group muscles contract simultaneously as the GRF passes in front of the ankle. The dropping motion of the pelvis is controlled by the contraction of the hip abductor muscles [17].

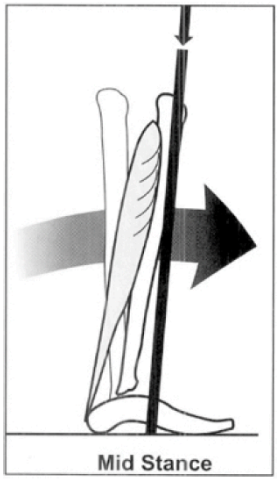

Figure 15. Mid Stance phase [20]

2.8.1.4. Terminal Stance Phase (TST)

It is between 30-50% of the gait cycle when the heel rises off the ground (Figure 16). COM gets in front of the COG support center. GRF is behind the hip, and M. Iliopsoas contracts. At the same time, the GRF passes in front of the knee and ankle. M. Gastrocnemius and M. Triceps Surae muscles work. The hip abductor muscles are activated until the opposite foot contacts the ground [17].

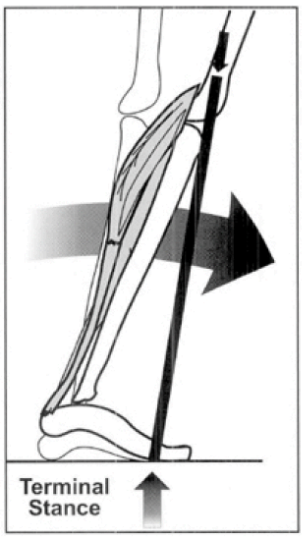

Figure 16. Terminal Stance phase [20]

2.8.1.5. Pre-Swing Phase (PSW)

It is between 50-60% of the gait cycle. It starts when the heel of the opposite foot contacts the ground (Figure 17). It ends with the fingers snapped off the ground. The target movement is to prepare the leg for swing. Hip extension is increased. GRFV passes behind the knee. The flexion angle of the ankle joint and the PF angle of the ankle joint also increased. M. Iliopsoas, M. Rectus Femoris, Adductor muscles, and M. Triceps Surae remain contracted. Knee flexion is passive. M. The Rectus Femoris muscle restricts extension in the knee joint and assists in flexing the hip joint [17].

Figure 17. Pre-Swing phase [20]

2.8.2. Swing Phases

The same side initiates with the foot off the ground and terminates with the foot touching the ground. It continues between 62-100% of the gait cycle. The swing phase consists of three sub-phases.

2.8.2.1. Initial Swing Phase (ISW)

It is between 60-73% of the gait cycle. The foot is off the ground and moving forward until it reaches the level of the other leg (Figure 18). Flexion increases in the hip and knee, and DF occurs in the ankle. However, flexion in the knee joint occurs passively [17].

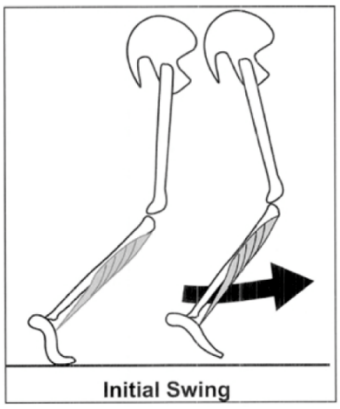

Figure 18. Initial Swing phase [20]

2.8.2.2. Mid-Swing Phase (MSW)

It is between 73-87% of the gait cycle. In mid-swing, the leg comes next to the opposite leg and passes in front of it (Figure 19). It is the period when the foot is highest above the ground. The aim is to move the leg forward without the foot touching the ground. The degree of flexion in the hip and knee joints increases passively, and dorsal flexion of the ankle is made active [17].

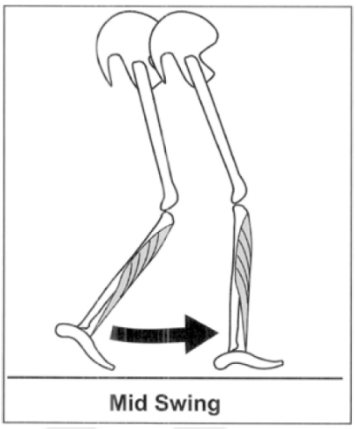

Figure 19. Mid-Swing phase [20]

2.8.2.3. Terminal Swing Phase (TSW)

It is between 87-100% of the gait cycle. The hip joint is flexed, and the knee joint is extended to increase the stride length (Figure 20). The ankle is in a neutral position in this phase. Hamstring group muscles work to control hip flexion and knee extension movements. The phase ends when the heel of the foot touches the ground. After this stage, the cycle starts again [17].

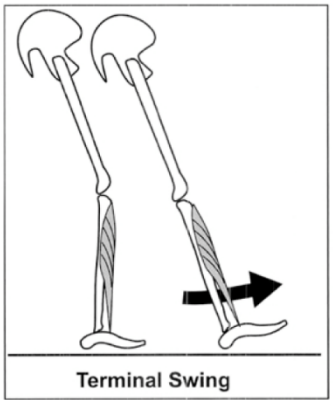

Figure 20. Terminal swing phase [20]

2.8.3. Basics of the Gait

The energy use during walking can be examined in three parts:

1. To walk, the muscles slow down and speed up. In this case, it consumes energy.
2. The energy expended due to increased cardiac and respiratory activity.
3. It is the energy expended by basal metabolism, which is constant at complete rest.

The aim is to keep this energy spent at a minimum during walking. The human body uses the center of gravity (COG) to keep its energy expenditure minimal. The change should be kept to a minimum. While moving forward, the center of gravity shifts approximately 5 cm (in the sagittal plane), about 4 cm from right to left (in the frontal plane), and by making rotational movements (4-8°) in the transverse plane. If this displacement is kept to a minimum, energy consumption is minimized [21].

2.8.3.1. Pelvic Rotation

In each gait cycle, the pelvis on the side of the swinging leg rotates forward approximately 4°. In this way, the lowering of the center of gravity is reduced, and at the same time, this mechanism increases the stride length.

2.8.3.2. Pelvic Drop

In the swing phase, the pelvis approaches the ground in the frontal plane, thereby reducing the weight.

2.8.3.3. Knee Flexion in the Stance Phase

The knee flexion movement in the loading phase prevents the center of gravity from rising too high.

2.8.3.4. Ankle Plantar Flexion

The PF movement from the IC phase until the foot touches the ground reduces the lowering of the center of gravity.

2.8.3.5. Foot and Ankle Rotation

The center of gravity from the middle of the stance phase shifts downward and forward. In this way, the balance of the foot is maintained. At the same time, the shortening of the leg length and, thus, the lowering of the center of gravity is also prevented.

2.8.3.6. Lateral Movements of the Pelvis

The pelvis shifts towards the leg in the stance phase, thus reducing the displacement of the center of gravity. (21)

2.8.4. Stride and Temporal Gait Parameters

Stride Length (meters): The linear distance between the IC of one foot and the following ipsilateral IC. In normal gait, it is equal to twice the step length.

Stride Width (meters): Drawn from the middle of the heel or ankle joint in the direction taken, a line is defined as a foot line. It is the distance between the lines of both feet.

Stride Time (seconds): The lapsed time related to the stride length.

Step Time (seconds): The lapsed time related to the step length.

Step Length (meters): The linear distance from IC of one foot to contralateral IC.

Double Limb Support (percentage of the overall gait cycle): The terminated gait cycle time when both feet touch the ground.

Single Limb Support (percentage of the overall gait cycle): The lapsed time of the gait cycle when one foot touches the ground.

Cadence (steps per minute): The value at which an individual walks.

Walking Speed (meters per second): Changes of the linear presumed direction of continuation per unit time [12, 24].

Stride and Temporal Gait Parameters have been shown in Figures 21 and 22.

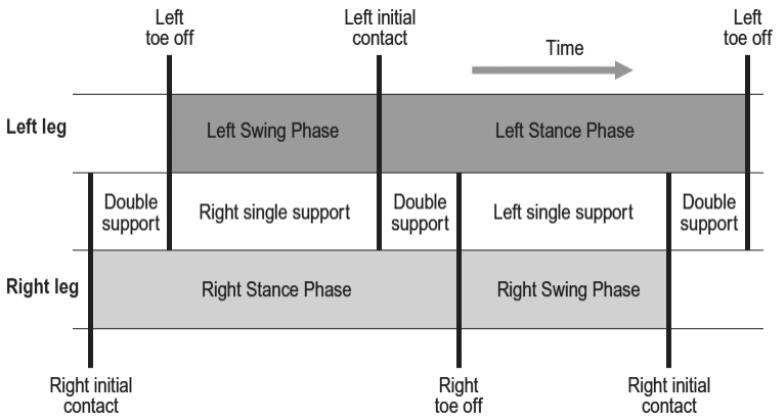

Figure 21. Single and double support during gait cycle (18)

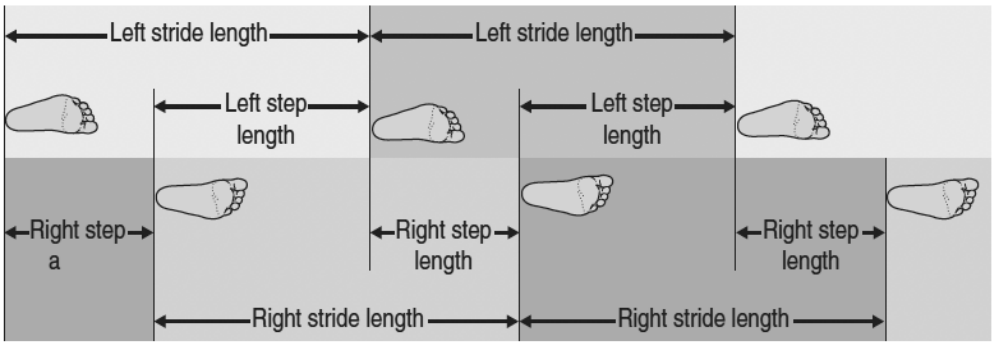

Figure 22. Static Parameters of step and stride during gait (23)

2.8.5. Physics and Biomechanical Terms Used in Gait

Mass: It is the amount of substance contained in an object (Kg).

Force: It is the effect that moves the objects (N, kg, m/s²).

Pressure: The amount of force per unit area (P) acting on a surface.

Movement: It is the displacement of the object.

Linear motion: If the force applied to an object is linear, its motion becomes linear (m).

Circular motion: The motion of rotating bodies (degrees (°)).

Speed: The distance traveled per unit time (m/s or degrees/s).

Acceleration: It is the change in velocity per unit time (m/s²).

Moment: Rotating effect of a force (M).

Energy: The ability to do work. (Joul (J) (Nm)).

Work: A force moves an object (Joul (J)).

Power: Work done per unit time (Watt (W) (J/s)).

Newton's first rule (inertia): Objects maintain their movement or immobility as long as they do not exert any force.

Newton's second rule: If a force is applied to an object, the object will move in the same direction as the force.

Newton's third rule: For every force opposite to itself, the same magnitude force is born.

Center of mass (COM): An anatomical point used to position the body mass in a three-dimensional reference coordinate system.

Center of gravity (COG): It represents the vertical projection of the COM on gravity. It is approximately 2 cm in front of the lumbosacral junction for the person.

Center of pressure (COP): It is the location of the vertical ground reaction force vector. COP acts on the plantar surface of the foot in contact with the ground. When both feet touch the ground, the COP is between the two feet.

Ground reaction force (GRF): It is the force vector of the same magnitude and opposite direction, formed by the ground versus the weight force vector created by the person on the ground while standing or walking.

Kinematics: The study of motion in terms of direction, velocity, angle, or acceleration.

Kinetics: The study of forces, moments and forces that cause motion.

Carried unit - carrier unit relationship: The head, trunk, and arms are carried in walking, pelvis, legs, and feet are the bearing unit [24-26]

2.8.6. Biomechanics of the Pelvis, Hip, Knee, and Ankle Joints

Pelvis transfers the weight of the head, neck, arms, and trunk to the lower extremities. It is also the attachment site of some trunk and lower extremity muscles involved during movement. Flexion movement occurs in the knee and ankle joints so that the swinging leg does not rub against the ground during the tilt or fall movement of the pelvis. During walking, rotational movements of the pelvis of approximately 4 degrees increase the stride length [12].

The hip joint is formed by the acetabulum and caput femoris. The hip joint can perform extension, flexion, adduction, abduction, external rotation, and internal rotation movements. Maximum hip flexion occurs when the leg touches the ground with heel strikes during walking. As the body moves forward, the flexion angle of the hip joint decreases, and the joint extends, reaching its maximum value before heel lift.

Abduction occurs when the toes are lifted off the ground, and hip joint abduction continues while the leg is advanced forward. When the heel touches the ground, the hip joint is in adduction, and this movement continues until the toes are lifted off the ground again. While internal rotation starts with the heel touching the ground and continues until the leg is lifted off the ground, external rotation occurs while the leg is moved forward. The knee joint has a very complex and easily affected structure anatomically. It carries about 86% of the whole-body weight. The ankle joint can carry heavy mechanical loads.

The heel, ankle, and forefoot, the three-foot rockers happening during the stance phase, help control the ahead drop of the body during the normal walk (Figure 23). Nevertheless, in pathological gait, one or more of these rockers may not be involved [22].

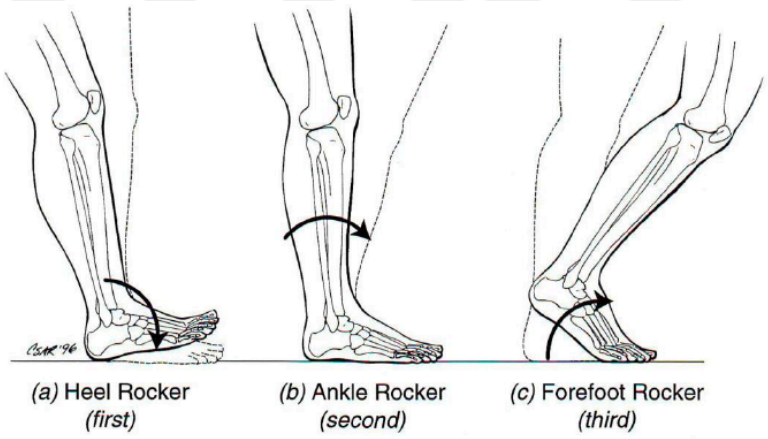

Figure 23. (a) the heel (first) rocker. (b) the ankle (second) rocker. (c) the forefoot (third) rocker [20].

The heel rocker happens when the heel touches the ground at IC and goes until the foot plantarflexes into full ground contact. At IC, foot contact is made at a single moment, causing the heel rocker to act as an unstable lever system. Throughout the heel rocker, the pretibial muscles (Peroneus tertius, Tibialis anterior, extensor digitorum longus, extensor hallucis longus) undergo controlled eccentric contraction

to resist the external moment created by gravity. This eccentric contraction causes the heel rocker to decelerate the foot at IC, which acts as a shock absorber.

The phase of MST starts when the contralateral foot clears the ground, beginning the opposite extremity swing phase, and terminates at the instant when the body COM is decelerating as it passes over the stance extremity forefoot. MST is the duration of the ankle rocker (second-foot rocker) when the ankle dorsiflexes. Momentum forces the tibia to rotate ahead over the plantigrade foot with the fulcrum at the ankle. The ankle rocker starts with the foot flat and terminates when muscle action controls further DF. This is caused by eccentric contraction of the plantar flexor muscles (Gastrocnemius and Soleus), especially the soleus.

The phase of TST is the duration of the forefoot rocker (third-foot rocker). This rocker starts at the end of MST and early TST, as the body center of pressure (COP) comes to the metatarsal heads, and the heel begins to rise. During this time, the metatarsophalangeal joints simulate a pivoted hinge, which functions as a rocker for the forward drop. This forward drop is started as the body COM leads the COP. During this period, the plantar flexors undergo concentric contraction. This causes the forefoot rocker (third rocker) to serve as an acceleration rocker to prepare for extremity progress in PSW. [12,20,27].

2.8.7. Gait Analysis Assessment Methods

Gait analysis involves the quantitative evaluation and interpretation of walking. During walking, the body's biodynamic systems work in coordination. Because walking involves complex movements, clinical analysis is difficult and may require advanced techniques. A comprehensive gait analysis requires physical examination, video recording, and devices that digitize muscle activity, strength, and lower extremity movements during walking (Table 9). Gait analysis is also used for clinical research purposes as well as being used to aid diagnosis and evaluate treatment progress. The evaluation consists of different types [40, 41].

One of the most important evaluation stages of the locomotor system is Gait Analysis. Evaluation of gait in surgical and medical branches is generally based on clinical and observational examination. However, it should not be forgotten that different pathologies may have similar gait patterns, and this may lead to inadequate treatment. In addition, evaluations based on observation alone were insufficient in revealing the complex structure of walking. Visually, the human eye cannot perceive events occurring in less than one 12th of a second (approximately 83 ms) nor distinguish simultaneous movements in different planes. In this case, the success of the evaluation of walking in this way depends on the experience and visual acuity of the person. Video recording of the patient's walking can be helpful in such cases, but the fact that only one plan can be evaluated makes this method insufficient.

Evaluation with computerized Three-Dimensional Gait Analysis technology provides objective data. The obtained Kinematic, Kinetic, numerical, and dynamic electromyographic data provide objective discrimination of gait adaptations and a more accurate understanding of the problem behind the complexity. Thus, it helps not only to evaluate the treatment result, but also to plan the interventions that can be applied by revealing the functional limitations [27].

Table 9. Gait analysis assessment methods [16]

Technique	Definition or Examples	Calculation Methods
Observational and clinical	- Gross Motor Function Measure (GMFM) - Functional Ambulation Profiles - Gross Motor Performance Measure (GMPM) - Range of Motion of hip, knee and ankle joints	- manually, by filling out checklists while patients engage in various activities - measuring the effect of purposely bending a joint on the adjacent tissue and joints (manually or with goniometers)
Time-distance measures	- Velocity - step length - cadence (steps per unit time)	- manually with stop watches - ink foot-print recordings - switches attached to feet or shoes - frame by frame video analysis - fibre optic sensors attached to computers
Foot contact patterns	- sequence in which various parts of the foot touch the ground	- ink footprint recordings - sensors on feet
2D and 3D kinematic features	- hip, knee and ankle joint angles angular and linear accelerations of limb segments	- goniometers and - electrogoniometers - frame by frame video analysis - computerized motion analysis systems
2D and 3D kinetic features	- ground reaction forces - hip, knee and ankle joint moments - location and linear and angular accelerations of whole body and specific joint centres of mass	- computerized analysis of data from forceplates - pressure sensors in shoes or on feet pedobarograph
Electromyography (EMG)	- electrical activity of muscles	- tethered vs. telemetry systems - surface vs. in-dwelling - electrodes - data output to paper charts, to oscilloscopes, or to computers for further processing
Energy/physiological cost	- estimated physiological cost of walking	- energy expenditure index (EEI), from algebraic manipulation of resting heart rate, walking heart rate, and walking velocity - oxygen consumption and/or carbon dioxide emission with special mechanical devices

2.8.7.1. Observation-Based Gait Analysis

It is the simplest form of gait analysis. The patient is observed first from the front and then from both sides. The walking distance is usually 8 m. Some researchers argue that it is more appropriate to prefer a distance of 12 m. This gives fast walkers time to take a few steps and catch up with the natural gait. Its width depends on the devices to be used for evaluation. While a 3 m width is sufficient for visual gait analysis, a distance of 5-6 m is required if a video camera is to be used.

Visual-only gait assessment is inexpensive, simple, and does not require equipment. However, it has some shortcomings. It does not give a permanent record. The disadvantages are that the eyes cannot perceive high-speed events, only movements can be observed, the force cannot be measured, and it depends on the observer's experience [42].

2.8.7.2. Video-Based Gait Analysis

Video recording can contribute to the assessment. Recordings can be slowed down and watched later to detect missed movements. It is a visual report about the progress of the patient's treatment. However, it does not provide numerical data, so it is not an objective method. Nowadays, new software is still developing, aiming to increase the validity of these types of analysis. Video cameras per second take 25-30 images, which is not fast enough to capture the details of movements [42].

2.8.7.3. Computerized Three-Dimensional Gait Analysis

With the development of technology, the evaluation and results of walking adaptations have become more objective. Thanks to the numerical, three-dimensional, and graphical data obtained, great convenience has been provided in the diagnosis, treatment, and follow-up of gait disorders (Picture 3). Gait problems have started to be

approached individually, that is, on a patient basis, and cooperation between different disciplines has increased. Thus, the ideal treatment schemes and possible risks can be determined objectively. The data obtained were used in scientific studies and contributed to the evaluation and treatment of gait disorders [20-25]

Picture 3. Evaluation procedure of the patient in the gait analysis laboratory

There are several components and specific applications of a computerized three-dimensional gait analysis system:

Markers: It can be of the type that receives, reflects, or directly transmits the signal. Reflective ones reflect the rays emitted from the infrared light source placed at the bottom of the camera. Transmitters, on the other hand, emit light for certain periods of time. These pointing devices are anatomically placed on prominent bony prominences close to the joints (Picture 4). However, due to the inability to detect bony prominences in overweight people and the mobility between skin and bone, problems may occur with the movement of markers during muscle contraction [12].

Optimal positioning of the markers on the anatomical landmarks relies on the overall accuracy of the system. Guidelines for marker placements depend on the biomechanical limb section model and the procedure for establishing joint centers. Inaccurate placement of the markers is a frequent error in collecting data. The most frequently used marker placement models are Newington-Gage and Helen Hayes-Kadaba [12].

Picture 4. Markers attached on the anatomical landmarks.

Recording Systems: Cameras capable of recording 25-30 frames per second or systems capable of recording 1000-2000 frames per second sensitive to infrared rays can be used (Picture 5). The data received with the recording devices are processed in a special operating system on the computer and provided graphically in three planes [43]. Gait analysis necessitates 8, 10, or more cameras to be utilized. The objective of the procedure is to achieve complete marker coverage and prevent the appearance of one or more markers during trial recording.

Picture 5. Infrared cameras and HD cameras of the gait analysis system

Calibration of the System: To diminish the potential sources of error, system and camera calibration is required. The main objective of the calibration is to achieve an image of the grid that covers the entire floor of view of the camera (Picture 6) [12].

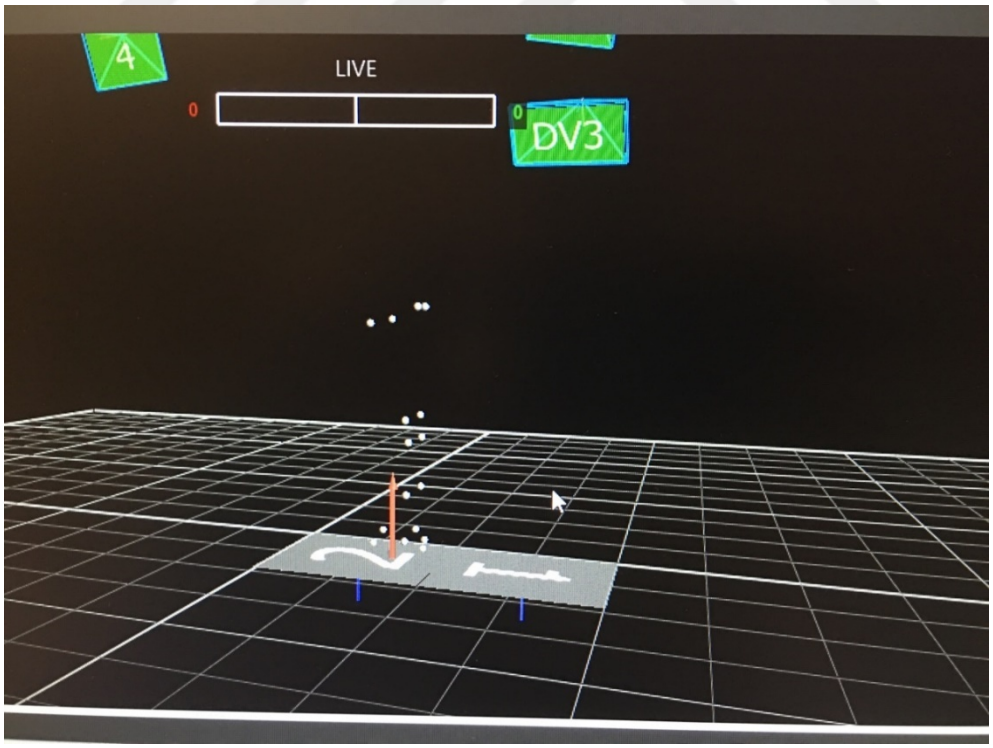

Picture 6. Gait analysis software demonstrating markers, force plates, infrared cameras, HD cameras and position of the patient during lower body protocol evaluation

Walking Path: The stride width, length, position of the foot on the ground, gait rhythm, and speed can be measured via the walking path.

Force Platform: Making the measurement is based on Newton's third law. If a force acts on an object, there is a reaction force of equal magnitude and opposite direction from the object to the force. It is routinely measured in gait analysis laboratories. The force platforms are 40x60 cm in size and 8-10 cm in height (Picture 7). It is placed on the walkway in such a way that the patient does not notice. A graph is created with this data in a computer environment. Applied torques and forces can be calculated by adding external moments (GRF). The force emerges in order to overcome this external moment to stay in balance while muscles around the joint contract and create the internal moment. The internal moment shows the total value of the agonist and antagonist muscles, not the moment of the individually contracted muscles [44].

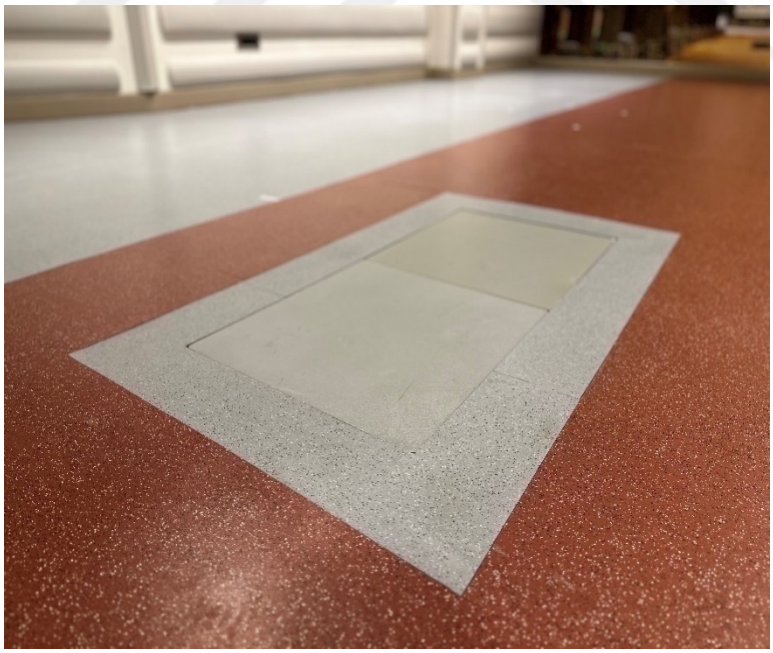

Picture 7. Force plates

Dynamic Pedobarography: It measures the pressure distribution under the sole. Depending on the size of the pressure, its distribution is determined according to the colors on the computer screen. Thus, it provides the opportunity to analyze the loading parameters and functional evaluation while walking [45].

Calculation Of Energy Consumption: Energy for acceleration, braking, and shock absorption during normal gait is necessary. In pathological gait, compensatory movements come into play, thus, the energy spent increases. Detection of oxygen (O2) consumption shows whether the patient is walking comfortably. Oxygen consumption can be calculated in different ways. The typical rate of oxygen consumption is 40%. However, this rate increases in those with walking difficulties [22].

Dynamic Electromyography: For dynamic EMG examination, surface and fine-wire electrodes are utilized in gait analysis. Surface electrodes are set on the skin over selected muscles. Two kinds of surface electrodes are often used in routine gait analysis: active electrodes with built-in amplifiers and silver–silver chloride (Ag–AgCl) disks. They have built-in filters and amplifiers to enhance the quality of the signal and to lower the effects of noise.

Both kinds of surface electrodes are effective because they are easily applied, can be used again, are noninvasive, and can reveal the activities of muscle groups. On the other hand, both types of surface electrodes have some drawbacks. They are not capable of recording the activities of specific muscles and crosstalk from neighboring muscles. It is essential to apply fine-wire EMG when the activity of specific and deep muscles needs to be monitored [46].

2.8.8. Biomechanical Modeling of Gait Data

In human gait analysis, the marker set is coupled with a biomechanical or mathematical model that defines the dynamics of various body segments (Figure 24) [47]. Standard gait analysis systems utilize inverse dynamics in order to compute joint moments and powers from limb motion kinematics and force platform ground reaction forces and moments [48]. Biomechanical models mainly originate from the assumption that body segments are rigid bodies. A minimum of three non-collinear markers must represent a rigid body in three-dimensional space [49].

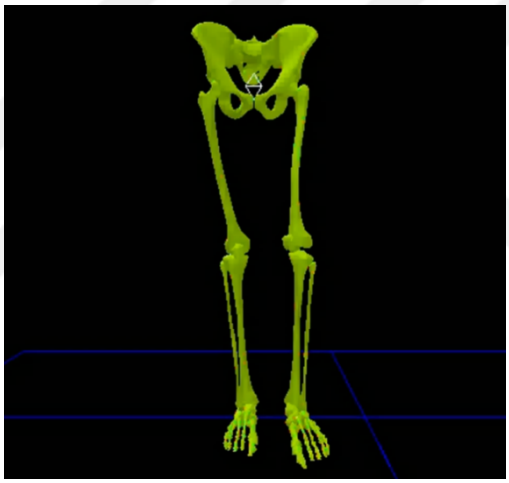

Figure 24. Three-dimensional image of the patient using lower body protocol

Various methods have been applied in the description of three-dimensional joint motion. These methods consist of Euler (Cardan) angles [50], direction cosines [51], and finite helical (screw) axes [52]. The reliability of the biomechanical link segment model employed in motion analysis is based on the accuracy of measurements and the reliability of several estimates. The model is synchronized with the marker set and is subject to specific underlying assumptions about anthropometric characteristics, such as segment masses, the center of mass, joint centers, mass moments of inertia, and segment length. This assumption is not accurate with femoral deformity or hip anteversion. There may be other sources of errors, like any kinematic errors and errors

in ground reaction force (GRF) measurement. Mathematical techniques employed in the biomechanical gait models may also differ between facilities; hence, the kinematic and kinetic data need to be studied rigorously. This emphasizes the fact that any gait analysis requires an accurate and meticulous clinical assessment [12].

2.8.8.1. Three-Dimensional Gait Analysis System Data Collection

Evaluation in the Gait Analysis laboratory first begins with a clinical examination. After the measurement of joint motion angles and different examination and evaluation tests, reflective markers adhere to certain anatomical regions of the patient in accordance with the protocol. Thanks to the infrared cameras, which are the most important parts of the system, the patient's walking and the movements of the markers are transferred to the computer system. In addition, two video cameras record the patient's gait.

The patient walks in a large area approximately 12-20 m long. Force platforms placed in the walking area measure the force and moment during walking. With the dynamic EMG integrated into the system, the muscles' initial contraction times and the interval of the contractions can be evaluated [20, 25].

Kinematic, kinetic, and temporal parameters are processed and expressed using computer software.

Kinematic data: Kinematics studies the relative movement between body segments. Data are represented in the sagittal, coronal, and transverse planes. In the sagittal plane, joint angular motions consist of pelvic tilt, hip flexion/extension, knee flexion/extension, and ankle PF/DF. In the coronal plane, joint angular motions include pelvic obliquity, hip abduction/adduction, knee valgum/varum and ankle

valgus/varus. Transverse plane joint angular motions involve pelvic rotation, hip rotation, tibial rotation, foot rotation, and foot progression angle. The data gathered from a patient are usually displayed together with standard control data for comparison purposes (Figure 25). Joint angle descriptions may alter in different systems and are significantly related to the arrangement of the markers and the applied biomechanical models [53].

For the analysis of gait disorders, kinematic data are crucial. On the other hand, they do not provide information on joint moments, ground reaction forces, joint powers, or biomechanical efficiency (oxygen consumption and cost). When an ambulatory individual shows stable kinematic patterns but presents noticeable variability in kinetic patterns, additional measurements become critical [54].

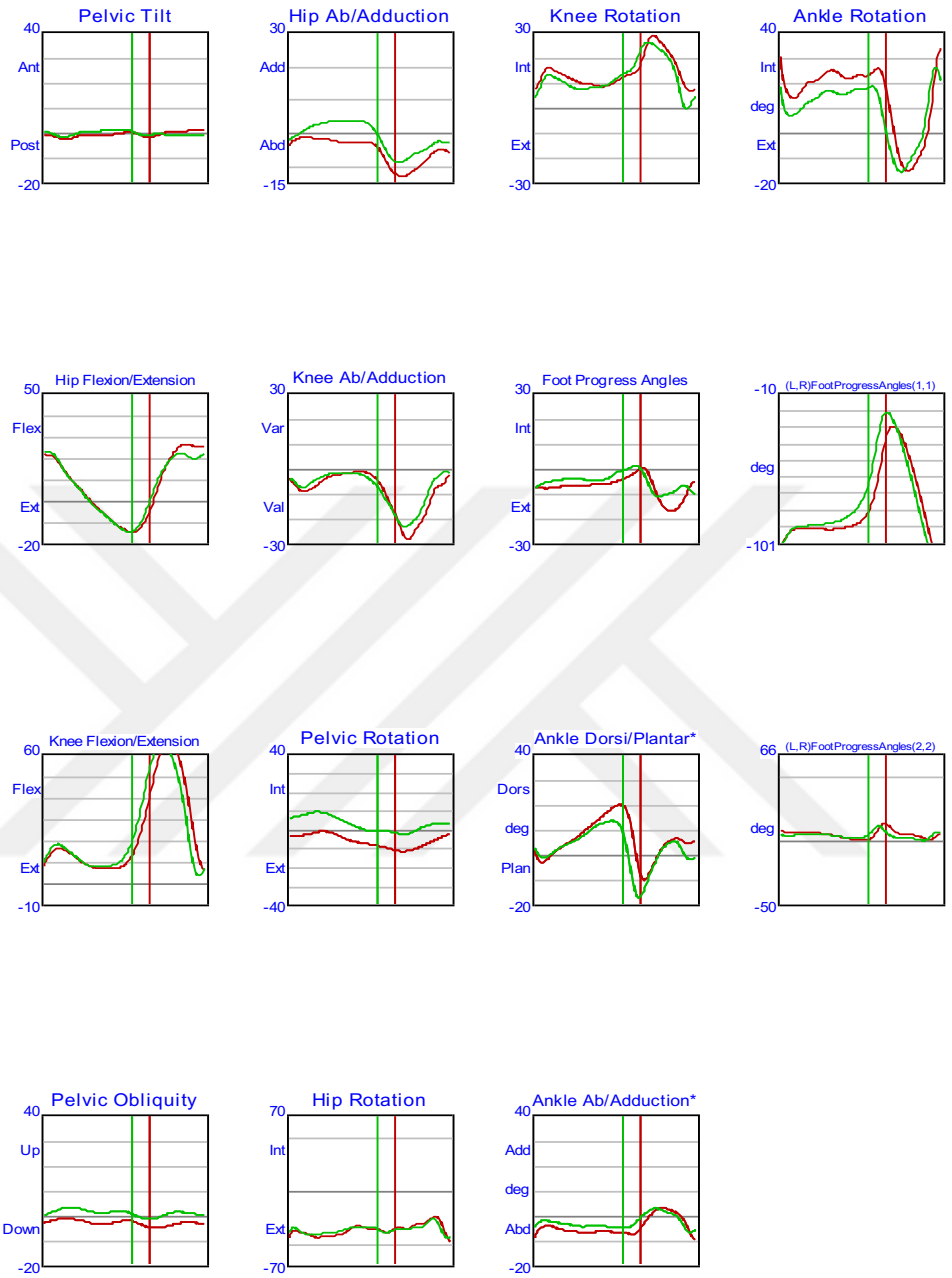

Figure 25. Kinematic graphics showing range of motion of the pelvis, hip joint, knee joint and ankle joint (red line presenting motion of the left side, green line presenting the motion of the right side)

Kinetic data: Kinetics is a field of engineering mechanics that studies motion in relation to the underlying forces that cause the movement. These forces consist of the external ground reaction forces and the internal joint, muscle, and ligamentous forces.

Human motion analysis is studied by the application of Newton's Second law and Euler's equations of motion. The three-dimensional joint reaction forces and moments are gained from both kinematic analysis and ground reaction forces (Figure 26). A state of equilibrium exists at each joint so that the internal joint reaction forces and moments balance the externally applied force. Moments are often normalized to body weight and leg length and are represented as a percentage of body weight multiplied by leg length. Joint powers are estimated once the moments, joint angles, and angular velocities are detected. The equations that describe joint reaction forces are represented in terms of Newton's Second Law as [47, 55]:

$$\Sigma \boldsymbol{F}x = m\ \boldsymbol{a}x$$

$$\Sigma \boldsymbol{F}y = m\ \boldsymbol{a}y$$

$$\Sigma \mathbf{F}z = \mathrm{m}\ \mathbf{a}z$$

At which,

ΣFx, ΣFy, ΣFz	= are the sums of external forces acting on a limb segment in the *x*, *y*, and *z* directions, respectively;
M	= the mass of the limb segment; and,
ax, ay, az	= are the linear accelerations of the center of mass of the limb segment in the *x*, *y*, and *z* directions, respectively. (46, 54)

Joint moments are calculated using Euler's equations of motion as

$$\Sigma \boldsymbol{M}\_x = Ixx\alpha x + (Izz - Iyy)\boldsymbol{\omega} y\ \boldsymbol{\omega} z$$

$$\Sigma \boldsymbol{M}\_y = Iyy\alpha y + (Ixx - Izz)\boldsymbol{\omega} z\ \boldsymbol{\omega} x$$

$$\Sigma \mathbf{M}\_z = \mathrm{Izz}\alpha z + (\mathrm{Iyy} - \mathrm{Ixx})\boldsymbol{\omega}\mathrm{x}\ \boldsymbol{\omega}\mathrm{y}$$

At which,

ΣMx, ΣMy, ΣMz	= are the sums of external moments applied to the limb segment in the *x*, *y*, and *z* directions, respectively;
Ixx, Iyy, Izz	= are the mass moments of inertia of the limb segment about the principal axes;
αx, αy, αz	= are the angular accelerations of the center of mass of the limb segment in the *x*, *y*, and *z* directions, respectively; and
ωx, ωy, ωz	= are the angular velocities of the center of mass of the limb segment in the x, y, and z directions, respectively. (46, 54)

Joint powers are calculated as

$$Px = \boldsymbol{Mx}\ \boldsymbol{\omega x}$$

$$Py = \boldsymbol{My}\ \boldsymbol{\omega y}$$

$$Pz = \boldsymbol{Mz}\ \boldsymbol{\omega z}$$

$$\Sigma P = Px + Py + Pz$$

At which,

Px, Py, Pz	= are the joint powers in the *x*, *y*, and *z* directions, respectively;
Mx, My, Mz	= are the external moments applied to the limb segment in the *x*, *y*, and *z* directions, respectively;
ωx, ωy, ωz	= are the angular velocities of the center of mass of the limb segment in the *x*, *y*, and *z* directions, respectively; and,
ΣP	= the total joint power. (46, 54)

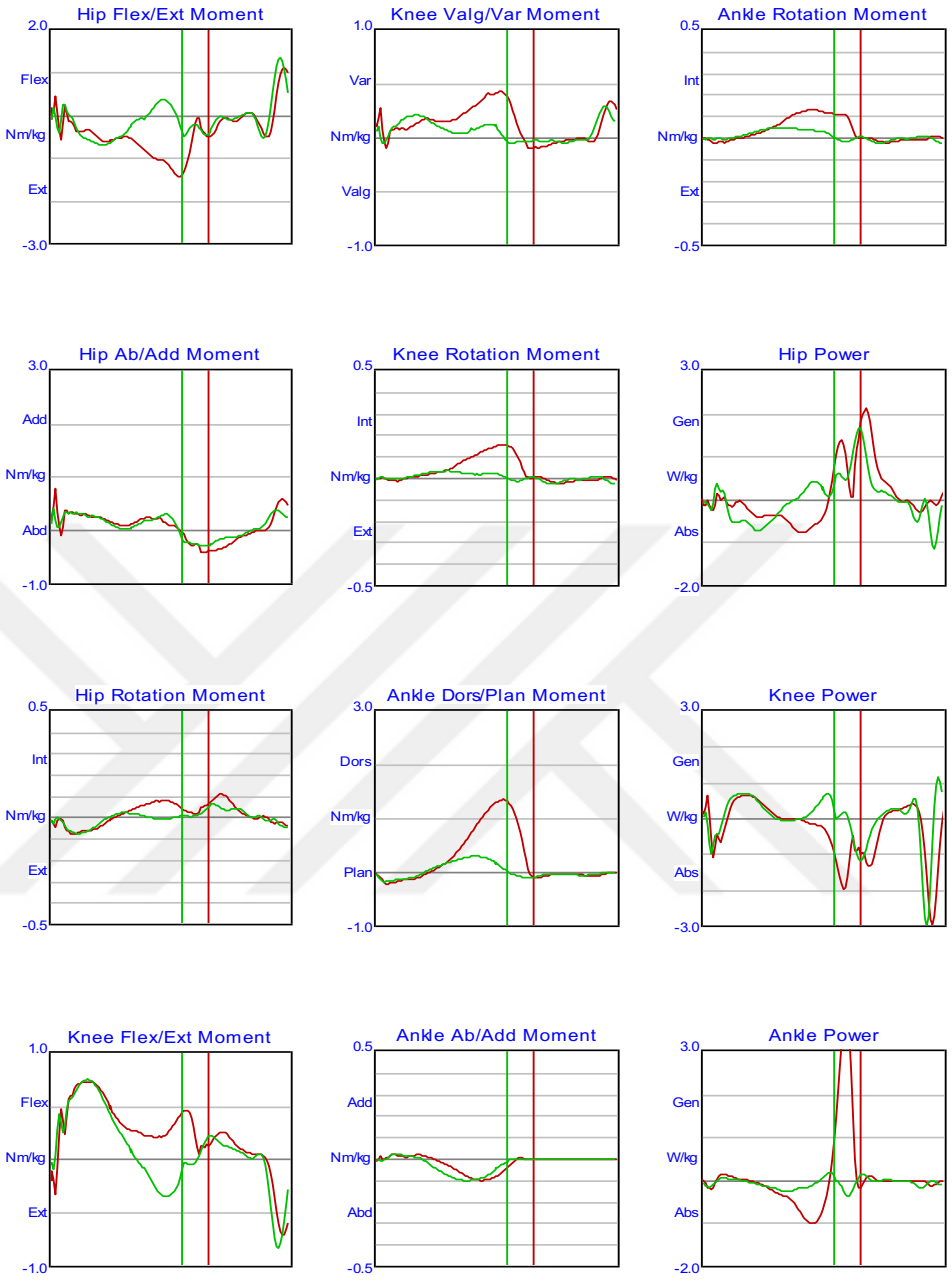

Figure 26. Kinetic graphics showing moment and power motion of the hip, knee and ankle joint (red line presenting motion of the left side, green line presenting the motion of the right side)

Temporal gait parameters: Parameters including length, time, and speed are expressed for both lower extremities (Table 10).

Table 10. Example of a temporal gait parameters of the gait cycle

	Left	Right	Normal
Cadence	129 s/m	131 s/m	114±6.43s/m
Double Support	0.15 s	0.13 s	0.23± 0.047 s
Foot Off	60.7 %	54.5 %	59.2± 2.57 %
Limb İndex	1.10	0.91	0.97±0.070
Opposite Foot On	54.5 %	44.5 %	49.8± 2.66 %
Opposite Foot Off	9.82 %	4.55 %	10.8± 1.67 %
Single Support	0.42 s	0.37 s	0.41± 0.042 s
Step Length	0.41 m	0.37 m	0.58± 0.052 m
Step Time	0.42 s	0.51 s	0.53± 0.032 s
Step Width	0.22 m	0.19 m	0.13± 0.020 m
Stride Lenght	0.77 m	0.77 m	1.18± 0.054 m
Walking speed	0.92 m/s	0.93 m/s	1.14±0.050

3. MATERIALS AND METHODS

3.1. Materials

3.1.1. Patients

Single center, retrospective, forty-one patients between 2 and 18 years of age (mean=7.8± 4.4) data who underwent surgery for SCM were included in the study. The study sample size satisfied a 0.80 power ratio and 0.8 effect size (10% standard deviation, 95% accuracy rate (z=1.96)) (GPower- Universität Düsseldorf, version 3.2.1). Thirty-two patients were Type I and nine were Type II SCM (Table 11). Exclusion criteria were permanent locomotor disorders and physical trauma due to any cause within the past one year. All surgical interventions were performed by the same licensed neurosurgeon. The mean age at diagnosis was 4.2±4.4 years (range, 0-16 years). L5-S1 was the most frequent site of involvement (29.3%), followed by L4-L5 (26.8%). Most patients had type 1 split cord malformation (78.1 %). The most common presenting symptom was hypertrichosis (28.5%), followed by extremity weakness (21.4%), gait disturbance (16.6%), hyperpigmentation (16.6%), scoliosis (7.1%), and urinary incontinence (4.7%). Tethered cord was the most common radiological sign (54.7%), followed by fatty filum (19%). Female and male patients had a similar distribution of these four radiological signs ($p>0.05$ for all) (Table 12). In addition, the distribution of these signs did not differ between type I SCM and type II SCM patients ($p>0.05$ for all). Fifteen SCM patients, randomly selected from 41 SCM patients, had follow-up data collection, on average 2.3 years after the initial data collection. The follow-up group sample size satisfied 0.8 power size with a 95% accuracy rate (z=1.96).

Table 11. Patient information

SCM Patients	**n=41**
Age at diagnosis, y, mean±SD	4.2±4.4
Male gender	22 (54%)
Side (right)	22 (54%)
Level	
T12-L1	5 (12.19%)
L1-L2	5 (12.19%)
L2-L3	4 (9.75%)
L3-L4	4 (9.75%)
L4-L5	11 (26.82%)
L5-S1	12 (29.26%)
Type	
SCM Type 1	32 (78.1%)
SCM Type 2	9 (21.9%)
Control Group	n=28
Age (year)	14.9 ± 5.5
Gender	21 Male, 7 Female

Twenty-eight age-matched typically developed children constituted the control group. Selection criteria for the control group included no prior history of cardiovascular, neurological, or musculoskeletal disorders. The participants had normal body mass index, ROM, and muscle strength and had no postural and motor deficits. The testing protocol was approved by the Institutional Review Board of Acibadem University Scientific Research Ethics Committee (approval number, 2016-7/8), and study consent was obtained from participants and their parents prior to the investigation.

Table 12. Patient Clinical and Demographic Information

Patient #	Date of Birth	Gender	Surgery Year	Age at First Gait Analysis	Age at Second Gait Analysis	Symptoms	Level	Diagnosis	Weak Side (R/L)	Radiological Information
1	2012	F	2012	4		Hyperpigmentation	L3-L4	SCM type 1	R	fatty filum
2	2011	M	2011	3		hypertrichosis	L4-L5	SCM type 1	R	Tethered cord
3	1997	M	2002	12	15	hypertrichosis	L5-S1	SCM type 1	R	Tethered cord
4	2001	F	2014	9		hypertrichosis	L3-L4	SCM type 1	L	Tethered cord, scoliosis
5	2010	M	2015	5	6	Gait disorder	L4-L5	SCM type 1	L	scoliosis
6	2001	F	2006	12		Gait disorder	T12-L1	SCM type 1	R	Tethered cord
7	2004	F	2016	12		Gait disorder	L5-S1	SCM type 2	R	Tethered cord
8	2012	F	2013	4		hypertrichosis	L2-L3	SCM type 2	L	dermal sinus
9	2003	M	2003	6		weakness in right limb	L5-S1	SCM type 1	R	Tethered cord
10	2004	M	2009	5	6	weakness in left limb	L5-S1	SCM type 1	L	Tethered cord
11	2003	F	2004	9		Hyperpigmentation	L4-L5	SCM type 1	L	Tethered cord
12	1998	F	2008	10		weakness in left limb	T12-L1	SCM type 2	L	Tethered cord
13	2006	M	2007	3	4	Hyperpigmentation	L5-S1	SCM type 1	R	fatty filum
14	2002	M	2003	14		Hyperpigmentation	L5-S1	SCM type 2	R	dermal sinus, Tethered cord
15	2002	M	2007	8	9	weakness in left limb	L5-S1	SCM type 2	L	Tethered cord
16	2002	M	2005	9		incontinence	L5-S1	SCM type 1	L	Tethered cord
17	1997	M	1997	12		scoliosis	L5-S1	SCM type 1	L	Tethered cord
18	2008	M	2009	4		Hyperpigmentation	T12-L1	SCM type 1	L	Tethered cord
19	2011	F	2014	5		hypertrichosis	L5-S1	SCM type 1	L	scoliosis
20	2004	M	2004	5		Gait disorder	L4-L5	SCM type 1	R	Tethered cord

Table 12. Continued

Patient #	Date of Birth	Gender	Surgery Year	Age at First Gait Analysis	Age at Second Gait Analysis	Symptoms	Level	Diagnosis	Weak Side (R/L)	Radiological Information
21	2010	F	2012	4	5	scoliosis	L1-L2	SCM type 2	R	fatty filum
22	2003	M	2009	6		weakness in left limb	L4-L5	SCM type 1	L	Tethered cord
23	2012	F	2013	2		scoliosis	T12-L1	SCM type 2	R	Tethered cord
24	2006	F	2009	2		hypertrichosis	L5-S1	SCM type 1	R	vertebral abnormality
25	2008	M	2012	4	5	weakness in right limb	L4-L5	SCM type 1	R	Tethered cord
26	1993	F	1993	16		Gait disorder	L4-L5	SCM type 1	R	Tethered cord
27	2001	M	2001	8	11	Hyperpigmentation	L2-L3	SCM type 1	R	dermal sinus
28	2007	M	2007	3		skin swelling	L1-L2	SCM type 1	L	vertebral abnormality
29	2009	M	2012	7	11	weakness in right limb	L5-S1	SCM type 1	R	Tethered cord
30	1994	M	2011	17		weakness in right limb	L3-L4	SCM type 1	R	fatty filum
31	2005	F	2015	11		hypertrichosis	L1-L2	SCM type 1	R	dermal sinus
32	1997	M	2013	12	14	incontinence	L4-L5	SCM type 1	R	Tethered cord
33	1996	M	1997	14		weakness in left limb	T12-L1	SCM type 1	L	fatty filum
34	2003	F	2010	7		Hyperpigmentation	L4-L5	SCM type 1	R	fatty filum
35	2007	F	2009	2	4	hypertrichosis	L4-L5	SCM type 1	L	bifid lamina
36	2004	F	2008	5	7	hypertrichosis	L3-L4	SCM type 2	L	Tethered cord
37	1994	F	2007	15		hypertrichosis	L2-L3	SCM type 1	L	fatty filum
38	2011	F	2017	5	7	Gait disorder	L4-L5	SCM type 1	L	Tethered cord
39	2001	M	2015	9		hypertrichosis	L1-L2	SCM type 1	L	scoliosis
40	2005	M	2007	2	4	Gait disorder	L2-L3	SCM type 2	R	fatty filum
41	2005	F	2005	6	7	hypertrichosis	L1-L2	SCM type 1	R	Tethered cord

3.2. Methods

3.2.1. Experiment Design and Procedure

Gait analysis was conducted using a motion capture system, including eight-cameras (Vicon Motion Systems Ltd, UK) and an AMTI force plate (AMTI Force and Motion, Watertown, MA). Each patient was set up with 16 retroreflective markers positioned at special points of reference directly on the patient's body. Based on the Halen-Hayes protocol, a total of 16 markers were attached to the following anatomical locations in both lower extremities using double-sided adhesive bands: anterior superior iliac spine, posterior superior iliac spine, lateral femoral condyle, the area between the head and lateral condyle of the femur, the area between the lateral malleolus and the lateral femoral condyle, lateral malleolus, heel and the point between the second and third metatarsal bones.

All patients walked barefoot in a fully equipped gait analysis laboratory under doctor and physical therapist supervision. Motion capture images were gathered at 100 Hz, and ground reaction forces (GRF) were gathered at 1200 Hz synchronously. The foot contact and GRF were used to detect the percentages of stride, which were normalized to 100%. Lengths of lower limb segments were manually calculated, using the landmark locations as references, along with patient height, weight, and foot length information. Data collection and analysis were done by Vicon and MATLAB (MathWorks, Natick, MA, USA).

A standard testing protocol was designed, and the same routine was carried out for each participant. Five acceptable trials of the foot squarely striking the force plate were gathered and averaged to show each collected parameter. If the patient correctly stepped on the force plate with the intended foot, the trial was considered successful. Self-selected speed was considered as the normal walking speed. Patients were instructed to walk on a 15-meter-long walking platform barefoot at self-selected speed.

3.2.2. Statistical analysis

Kinematic, kinetic and spatial/temporal parameters of the lower extremity joints were collected. To compare improvements between the initial and second data collection sessions, paired-samples t-tests and independent sample t-tests in a within-subject design were selected for statistical analysis.

All continuous variables were presented as mean ± SD. The Kolmogorov-Smirnov normality test was conducted to examine the distribution of the continuous variables. All tests were 2-tailed, and the significance level ($p < 0.05$) was considered statistically significant. The statistical analysis was performed using SPSS (version 12, Chicago, IL). The variations in the kinetic and kinematic data gathered during the initial and follow-up visits were evaluated for the bivariate analysis using the Pearson Correlation Coefficient and Root Mean Square Difference techniques. The error is calculated with the equation given below:

$$\text{Error}_{\text{(initial/follow up)}} = \sqrt{(X_{follow\ up} - X_{initial})^2 - (Y_{follow\ up} - Y_{initial})^2}$$

4. RESULTS

Forty-one patients and twenty- eight typically developed children completed the initial gait analysis, and follow-up data were collected from 15 SCM patients randomly selected from 41 SCM patients.

4.1. Subgroup Comparisons at Initial Data Collection

Initial data analysis included the kinetic and kinematic data comparisons of the following subgroups: 1) thicker-weaker hemi cord; 2) below- above L5 level; 3) below-above 7 years old; 4) tethered cord- no tethered cord; 5) Type I- Type II SCM. The subgroup comparisons did not show significant differences in kinetic and kinematic parameters. Pearson Correlation Coefficient (PCC) and Root Mean Square Error (RMSE) techniques were applied to evaluate the ROM and movement pattern similarities of lower extremity joint trajectories of the subgroups with Eq. Larger differences in RMSE showed a poor regression fit and a larger gap between the movement trajectories of conditions. On the contrary, smaller differences in RMSE displayed strong regression fit and similar movement trajectories. Larger differences in RMSE showed a poor regression fit and a larger gap between the movement trajectories of conditions. On the contrary, smaller differences in RMSE displayed strong regression fit and similar movement trajectories. (Table 13). Significantly high similarity and strong regression fit were obtained in most subgroup comparisons.

Table 13. Subgroups' Kinetic and Kinematic Parameters RMSE Comparisons

	Weak- Thick Hemi Cord	**Below L5- Above L5 Scm**	**Above 7- Below 7 Yrs Old**	**Tethered Cord- No Tethered Cord**	**Type I- Type Ii Scm**
Hip Moment	R^2: 0.8969 RMSE: 7.28	R^2:0.8365 RMSE:15.05	R^2:0.7906 RMSE:15.68	R^2:0.8060 RMSE: 19.08	R^2:0.7845 RMSE:15.05
Knee Moment	R^2:0.8338 RMSE:7.46	R^2:0.8952 RMSE:10.64	R^2:0.8853 RMSE:16.8	R^2:0.8965 RMSE: 12.03	R^2:0.7958 RMSE:10.64
Ankle Moment	R^2:0.8588 RMSE:6.52	R^2:0.7971 RMSE:12.77	R^2:0.8256 RMSE:23.04	R^2:0.7971 RMSE:12.77	R^2:0.8546 RMSE:22.77
Hip Force	R^2:0.8808 RMSE:13.77	R^2:0.8869 RMSE:17.56	R^2:0.8067 RMSE:11.44	R^2:0.8869 RMSE:17.56	R^2:0.8910 RMSE:17.56
Knee Force	R^2:0.8934 RMSE:16.05	R^2:0.7941 RMSE:12.94	R^2:0.8369 RMSE:15.62	R^2:0.8240 RMSE:12.94	R^2:0.7512 RMSE:18.04
Ankle Force	R^2:0.8355 RMSE: 21.5	R^2:0.8520 RMSE:17.51	R^2:0.9055 RMSE:13.85	R^2:0.7515 RMSE:17.51	R^2:0.9021 RMSE:17.51
Hip Angle	R^2:0.7836 RMSE:11.84	R^2:0.8096 RMSE:19.72	R^2:0.7849 RMSE:19.3	R^2:0.8654 RMSE:23.72	R^2:0.8012 RMSE:13.72
Knee Angle	R^2:0.8880 RMSE:21.50	R^2:0.9298 RMSE:17.51	R^2:0.8978 RMSE:19.63	R^2:0.8623 RMSE:17.51	R^2:0.8215 RMSE:17.51
Ankle Angle	R^2:0.7315 RMSE:15.74	R^2:0.8170 RMSE: 16.93	R^2:0.9113 RMSE:19.85	R^2:0.8421 RMSE: 16.93	R^2:0.8745 RMSE: 16.93
Foot Progress Angle	R^2:0.8979 RMSE:16.15	R^2:0.7952 RMSE: 21.41	R^2:0.9267 RMSE:19.15	R^2:0.8326 RMSE: 16.41	R^2:0.7894 RMSE: 26.56
Pelvis Tilt	R^2:0.8469 RMSE:17.95	R^2:0.8299 RMSE: 24.49	R^2:0.9031 RMSE:11.93	R^2:0.8454 RMSE: 14.49	R^2:0.8965 RMSE: 24.19
Pelvis Obliquity	R^2:0.8907 RMSE:10.49	R^2:0.8361 RMSE:18.65	R^2:0.8704 RMSE:12.85	R^2:0.8612 RMSE:18.65	R^2:0.7895 RMSE:16.05
Pelvis Rotation	R^2:0.8207 RMSE:11.49	R^2:0.8216 RMSE:18.34	R^2:0.8207 RMSE:13.56	R^2:0.8207 RMSE:11.49	R^2:0.7854 RMSE:16.40

4.2. Long-term Assessment of Gait Parameters: Initial vs. Follow-Up Data Analyses

The follow-up data analysis included the kinetic and kinematic data comparisons of the initial data collected from 41 SCM patients- follow-up data collected from 15 SCM patients and control data collected from 28 typically developed children. The

spatial temporal parameters comparisons of initial vs. follow-up groups and follow-up vs. control groups are shown in Table 14.

Table 14. Mean spatiotemporal parameters of SCM patients' compared to healthy control group subjects.

Spatiotemporal Parameters	Initial	Follow Up	p- value	Follow Up	Control Group	p- value
Cadence (steps/min)	128.47±12.1	127.61±10.7	0.189	127.61±10.7	114.74±11.6	< 0.05
Stride Time (s)	0.95±1.2	0.96±0.9	0.478	0.96±0.9	1.06±0.4	0.062
Opposite Foot Off (%)	10.05±5.6	10.65±9.2	0.816	10.65±9.2	8.54±5.4	< 0.05
Opposite Foot Contact (%)	48.65±15.9	51.78±14.1	0.063	51.78±14.1	48.78±7.6	0.179
Step Time (s)	0.49±0.21	0.46±0.32	0.455	0.46±0.32	0.53±0.21	< 0.05
Single Support (s)	0.36±0.23	0.37±0.2	0.546	0.37±0.2	0.33±0.1	0.525
Double Support (s)	0.20±0.14	0.20±0.25	0.179	0.20±0.25	0.11±0.2	< 0.005
Foot Off (%)	60.08±12.1	61.88±15.2	0.927	61.88±15.2	53.66±7.3	< 0.05
Stride Length (m)	0.88±0.2	0.90±0.31	0.927	0.90±0.31	1.10±0.15	< 0.05
Step Length (m)	0.44±0.28	0.45±0.36	0.214	0.45±0.36	0.54±0.2	< 0.05
Walking Speed (m/s)	0.93±0.1	0.95±0.16	0.807	0.95±0.16	1.04±0.2	0.165

*Significant difference between initial and final - final and control groups $p<0.05$

In Table 14, the mean values of spatial-temporal parameters of SCM patients and healthy control group participants were reported. The SCM group was characterized by higher cadence, shorter stride time, higher opposite foot off percentage, lower step time, significantly higher double support percentage, shorter step length and slightly lower walking speed compared to the control group. The differences in these parameters for thicker and weaker sides were not statistically significant.

In Figure 27-41, kinetic and kinematic parameters of the lower extremity joints were represented for initial and follow up data collection from SCM patients. The control group data were also included in the graphs for comparison.

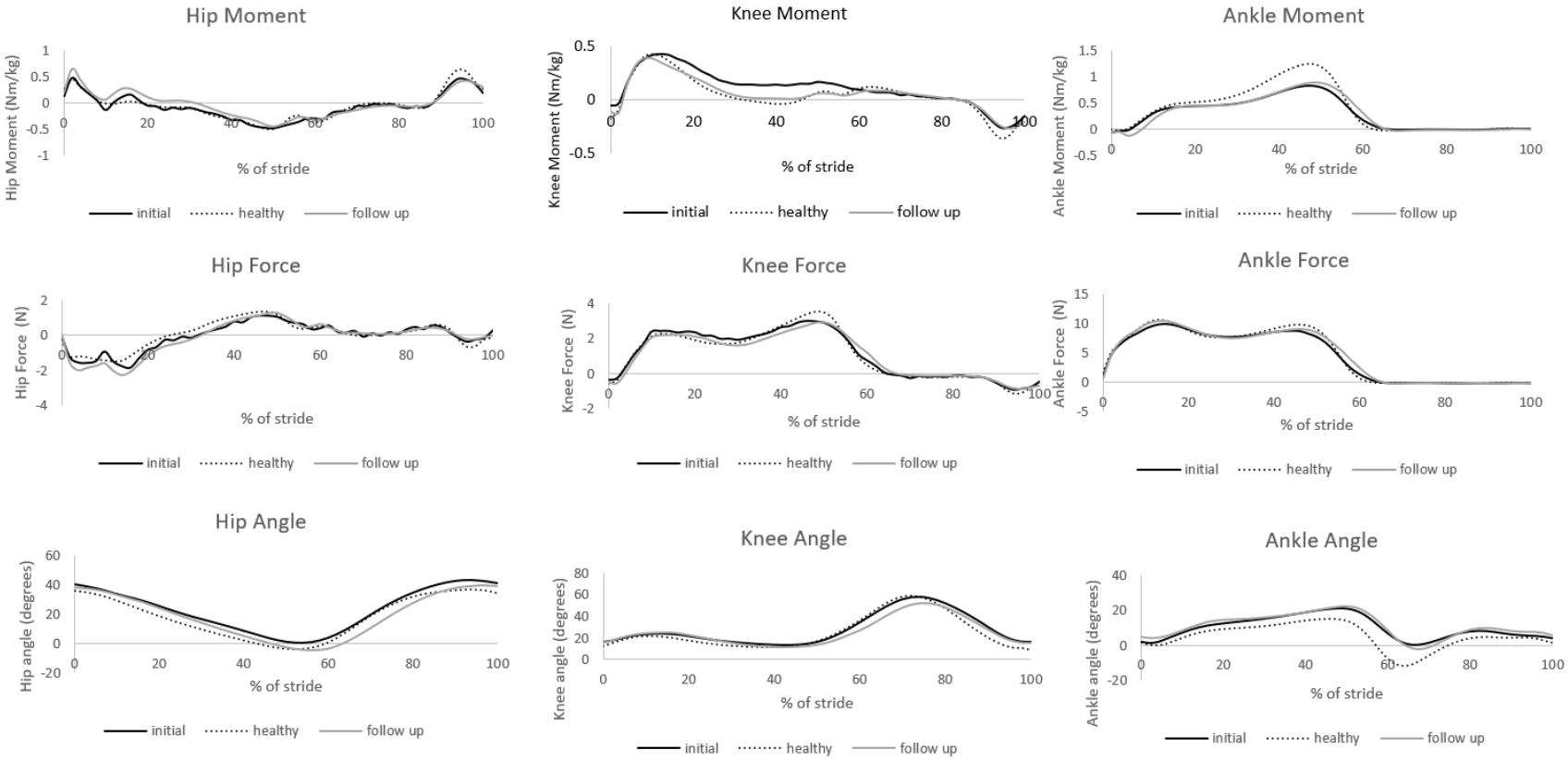

Figure 27. Long-term assessment of gait parameters: comparison of the hip, knee and ankle joint moment, force and angle

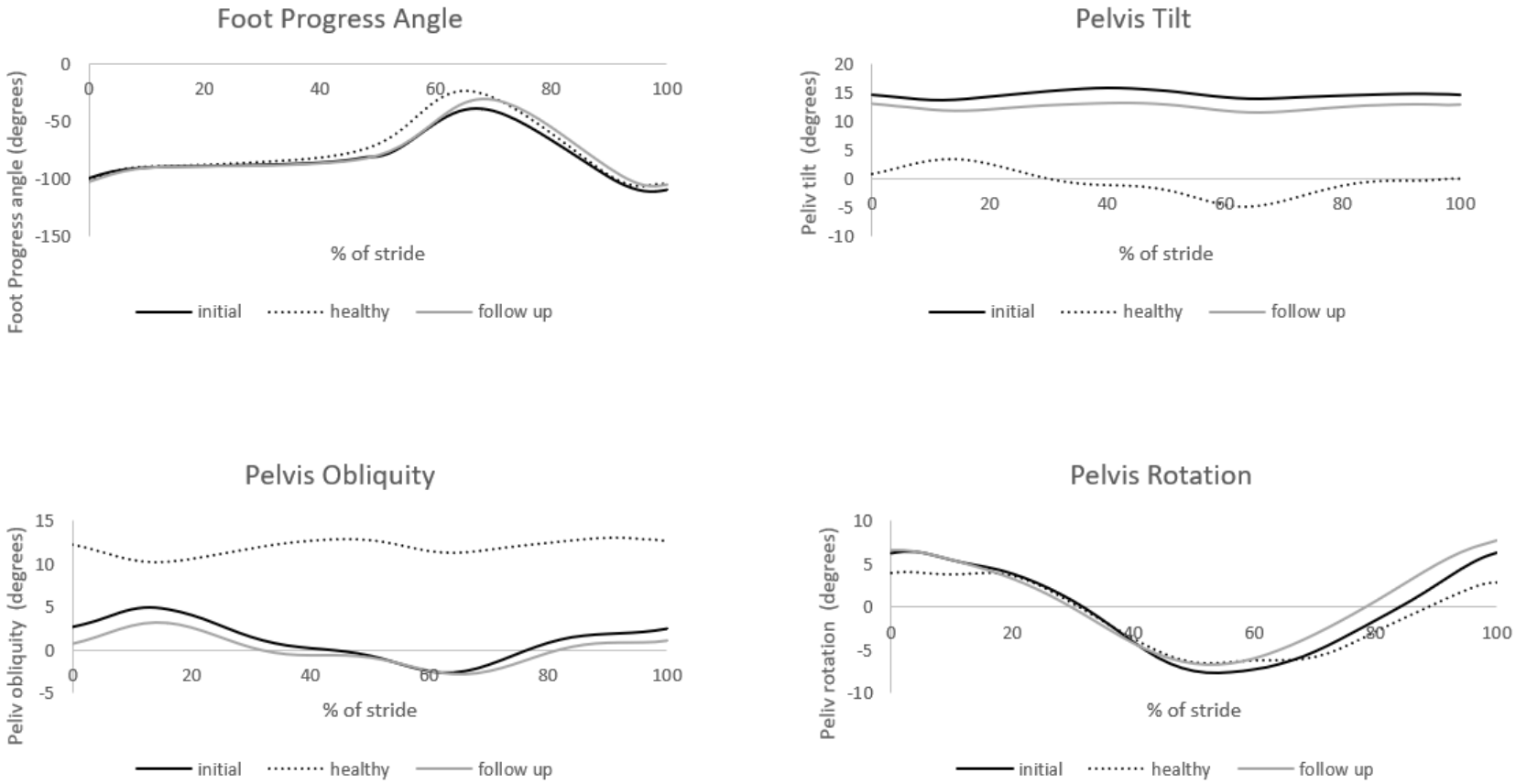

Figure 28. Long-term assessment of gait parameters: kinematic parameters comparisons of pelvis and foot

HIP MOMENT

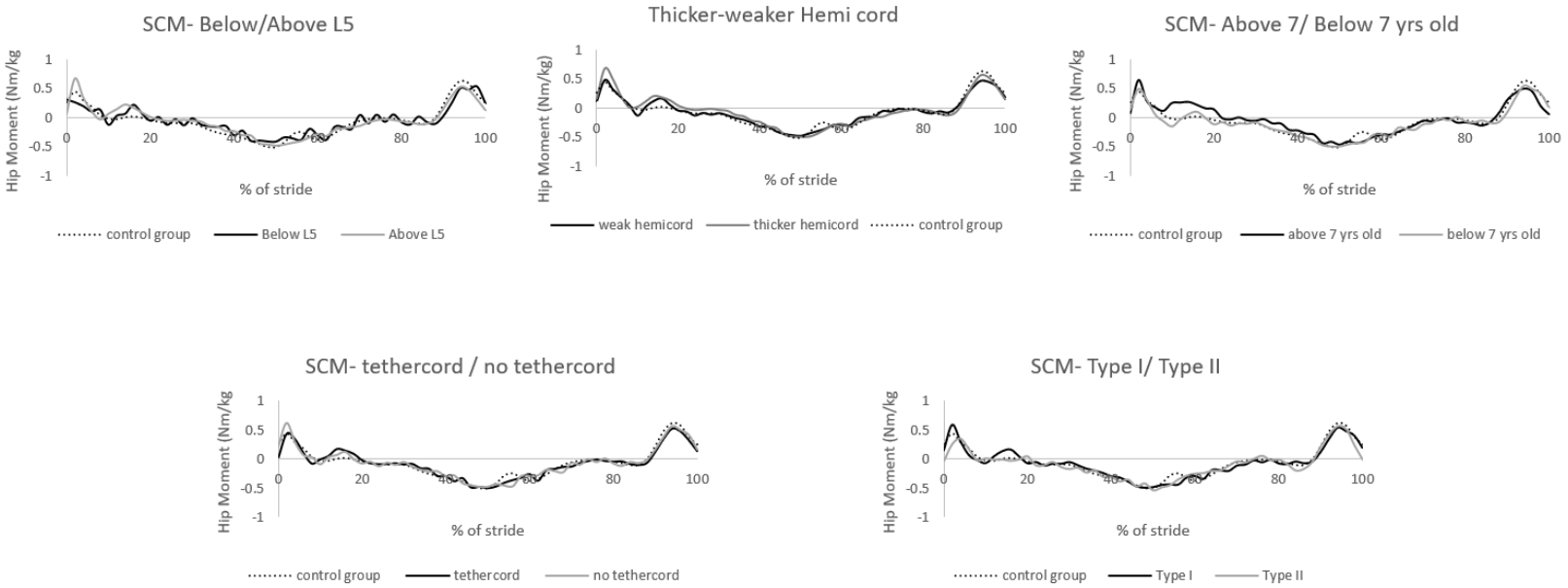

Figure 29. Long-term assessment of gait parameters: hip moment

KNEE MOMENT

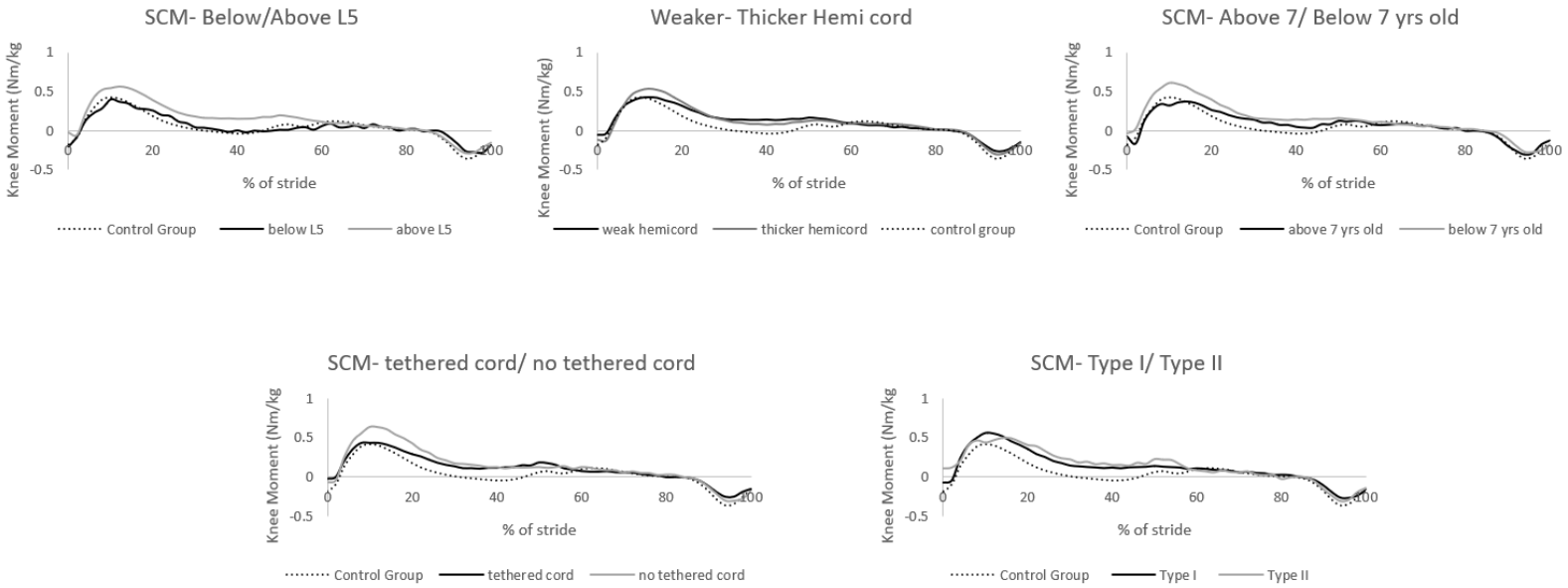

Figure 30. Long-term assessment of gait parameters: knee moment

ANKLE MOMENT

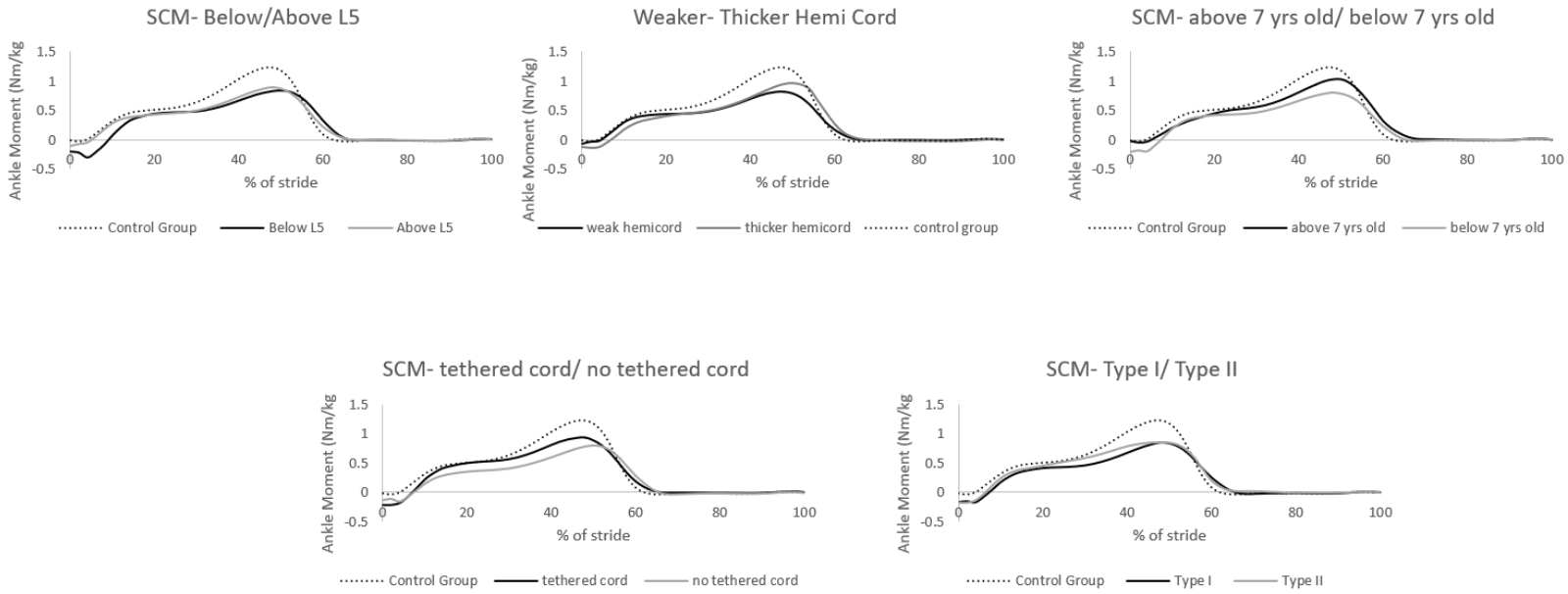

Figure 31. Long-term assessment of gait parameters: ankle moment

HIP FORCE

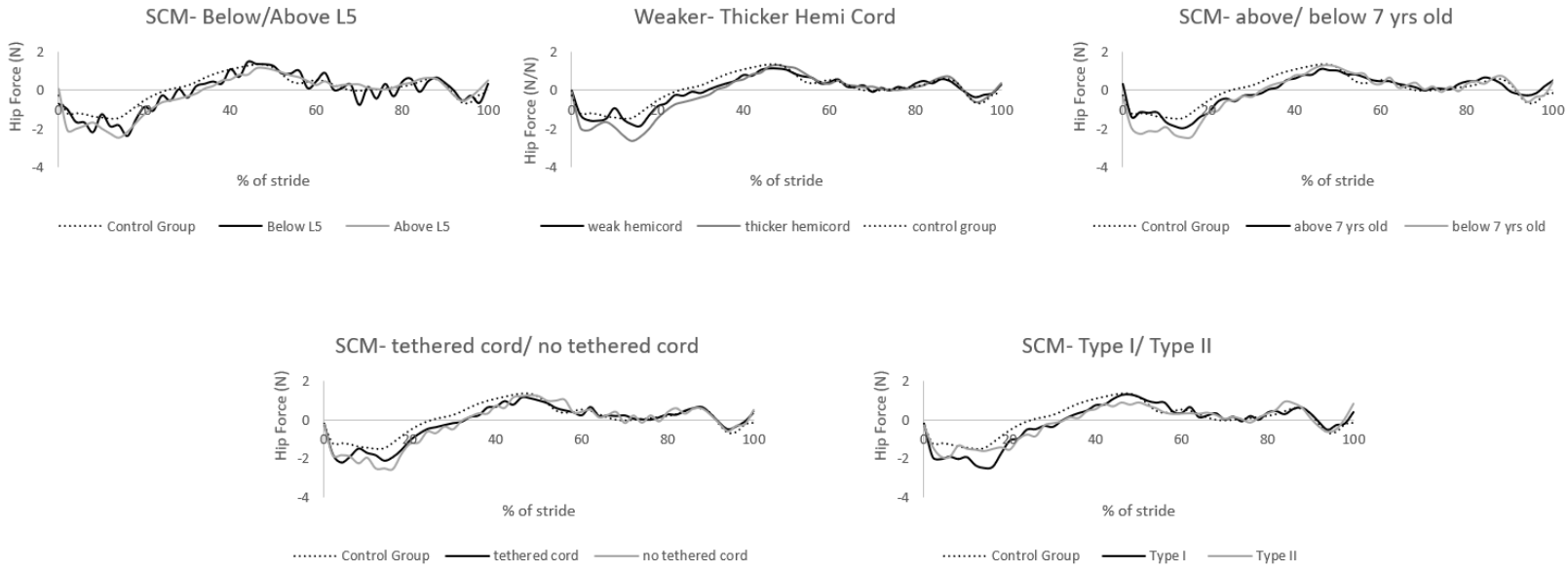

Figure 32. Long-term assessment of gait parameters: hip force

KNEE FORCE

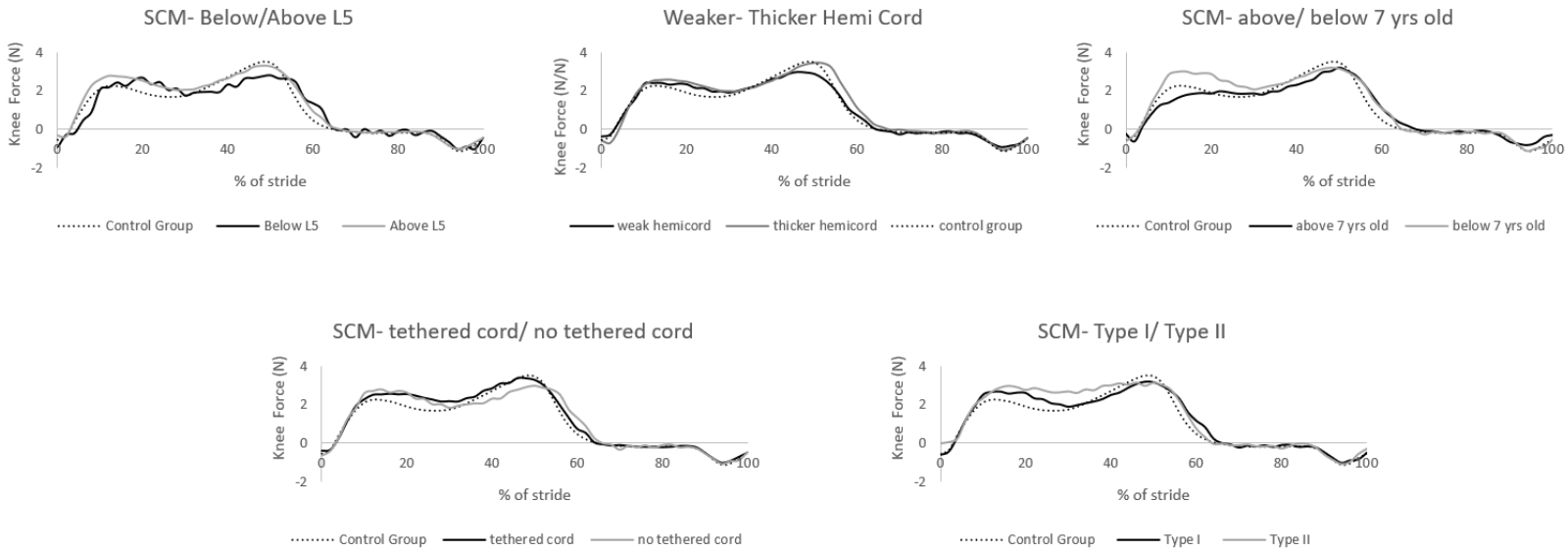

Figure 33. Long-term assessment of gait parameters: knee force

ANKLE FORCE

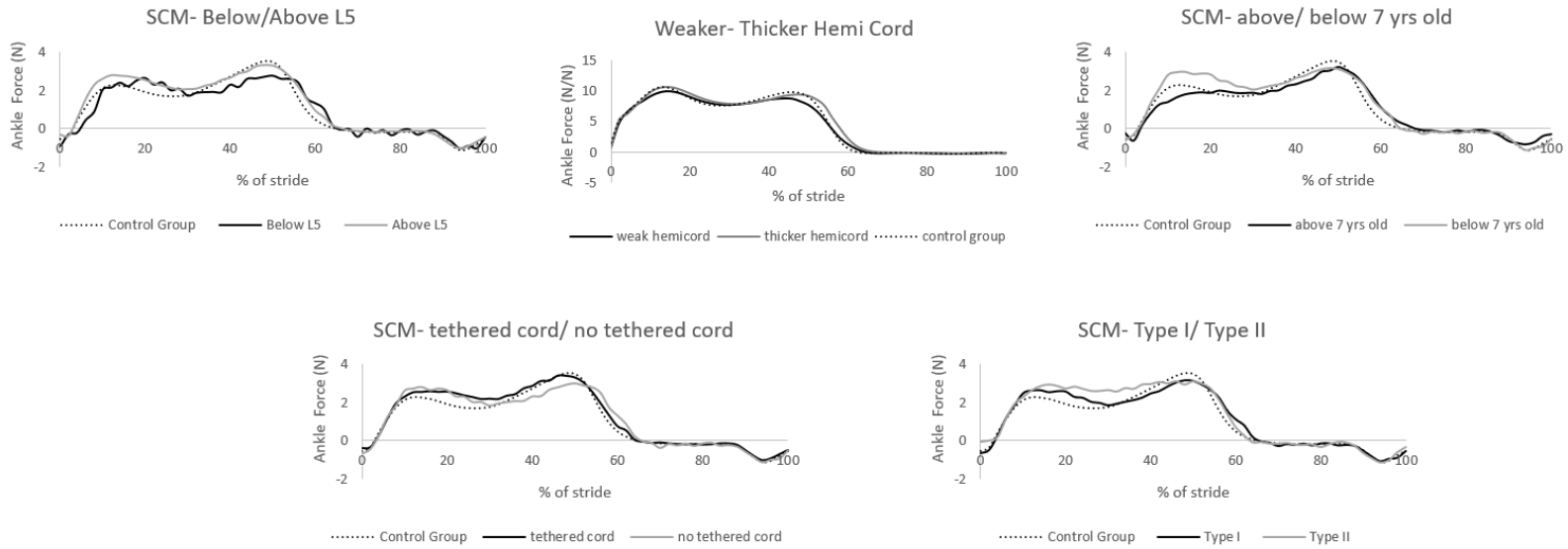

Figure 34. Long-term assessment of gait parameters: ankle force

HIP ANGLE

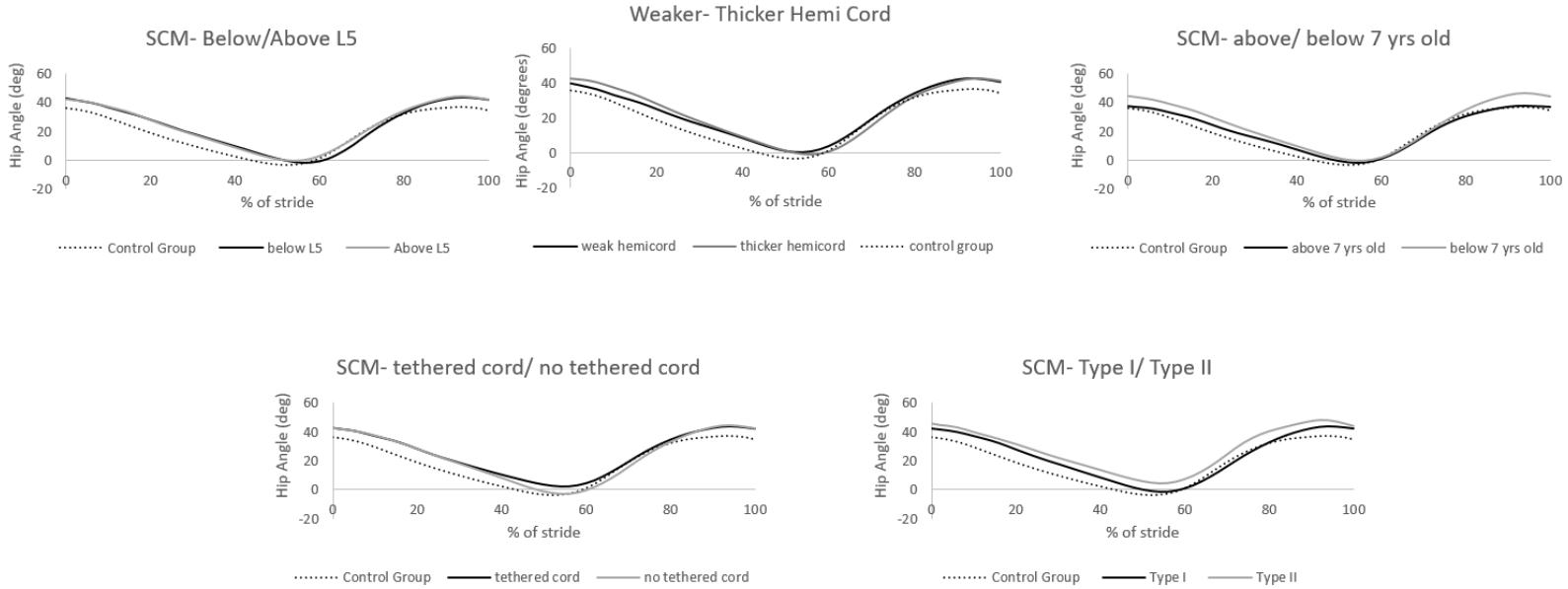

Figure 35. Assessment of gait parameters: hip range of motion

KNEE ANGLE

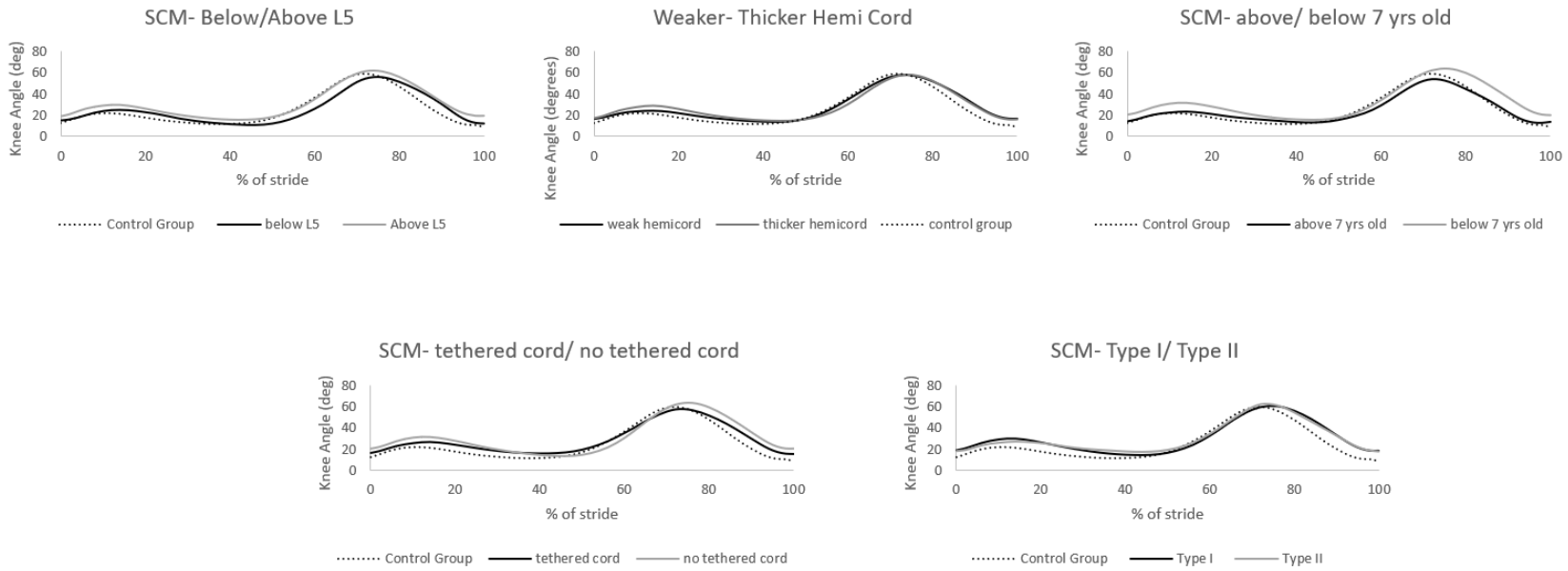

Figure 36. Assessment of gait parameters: knee range of motion

ANKLE ANGLE

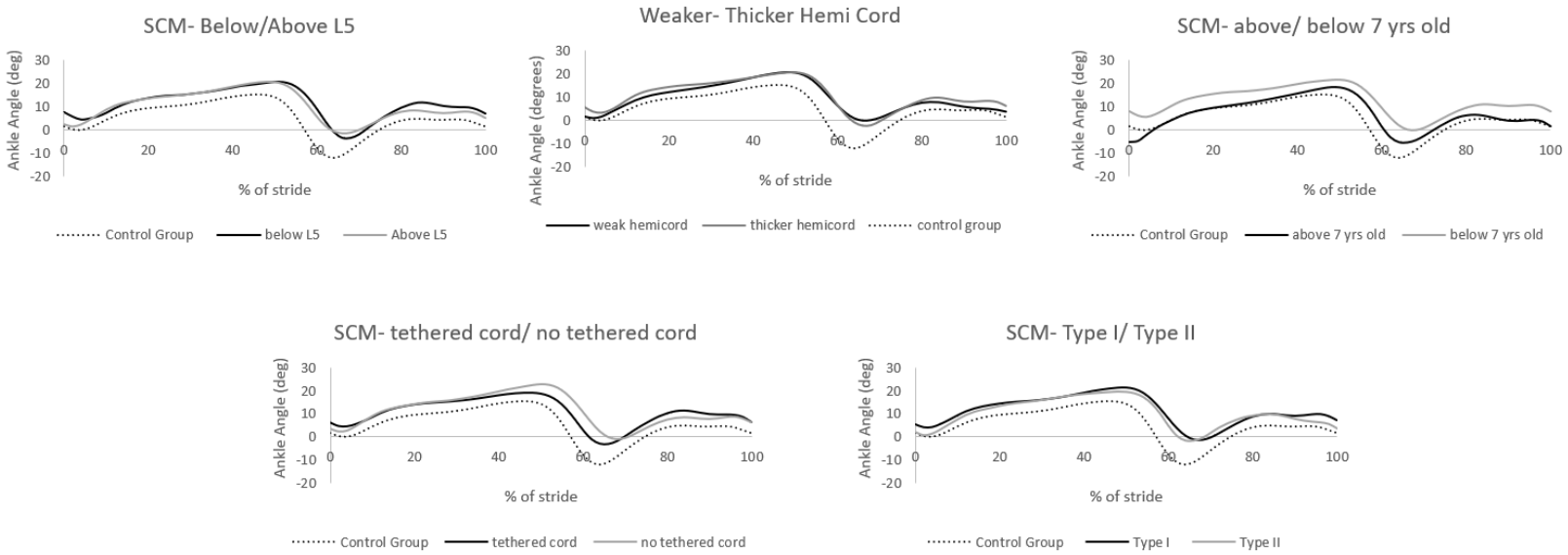

Figure 37. Assessment of gait parameters: ankle range of motion

FOOT PROGRESS ANGLE

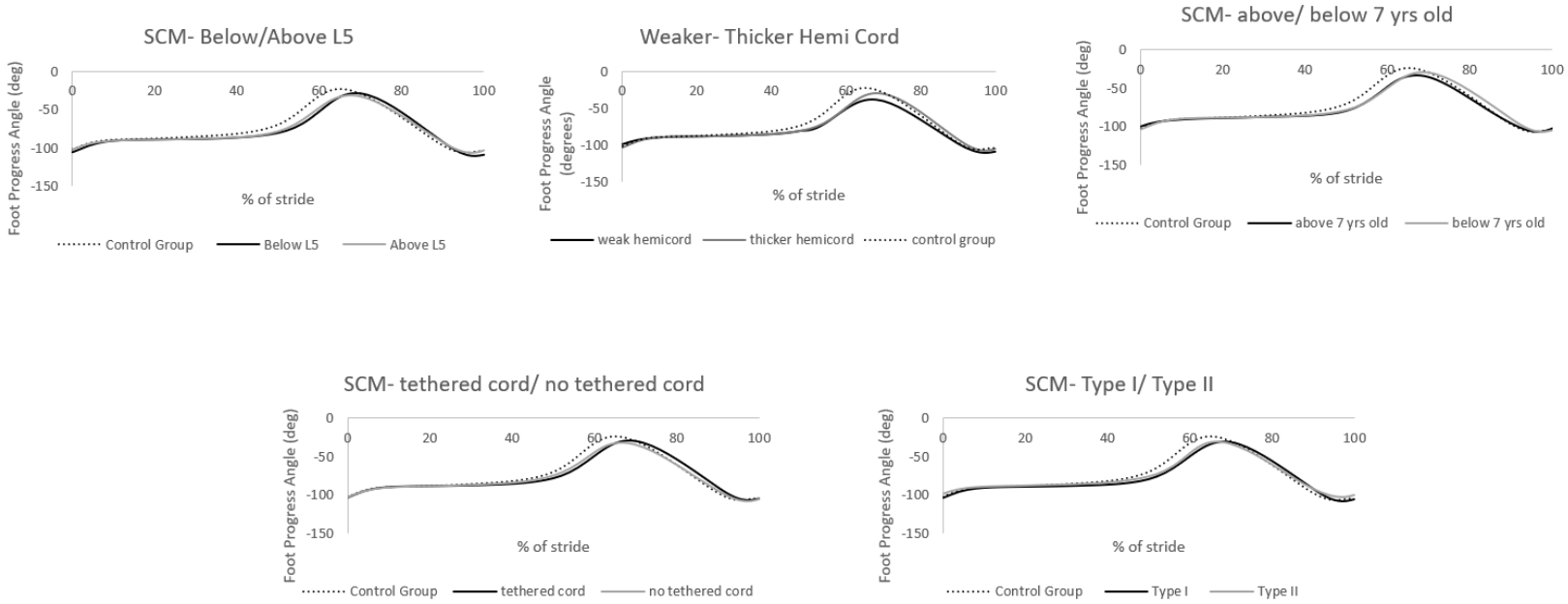

Figure 38. Assessment of gait parameters: foot progression angle

PELVIC TILT

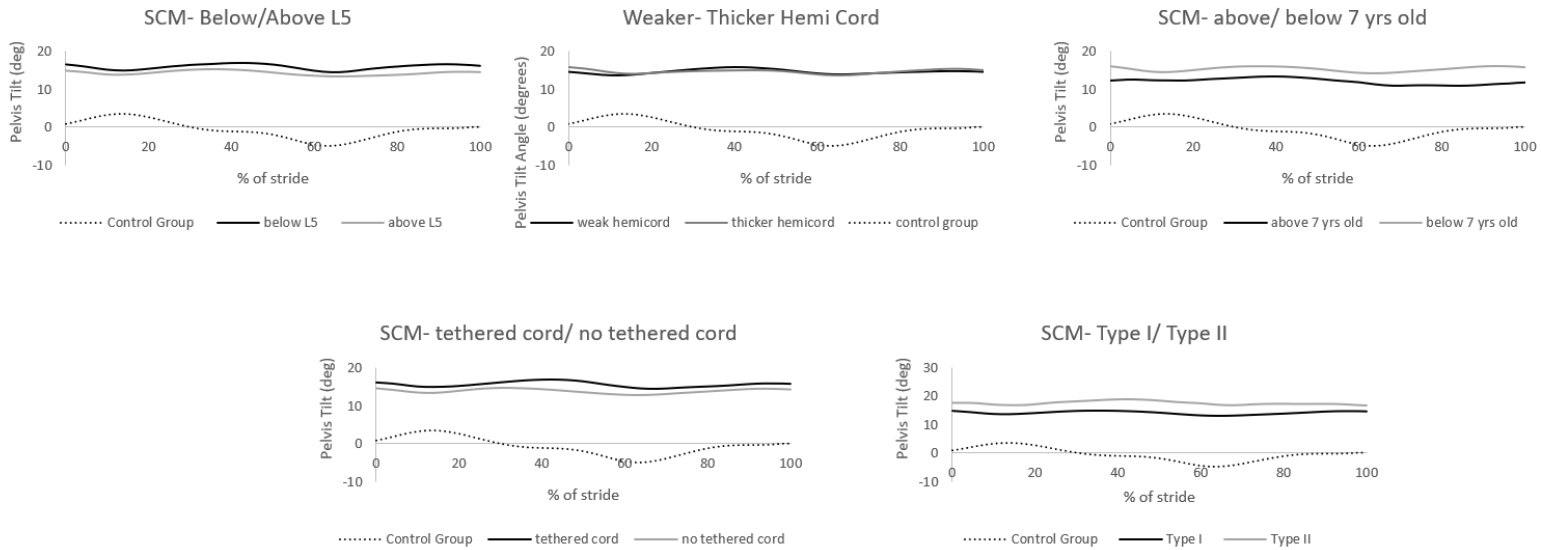

Figure 39. Assessment of gait parameters: comparison of pelvic tilt range of motion

PELVIC OBLIGUITY

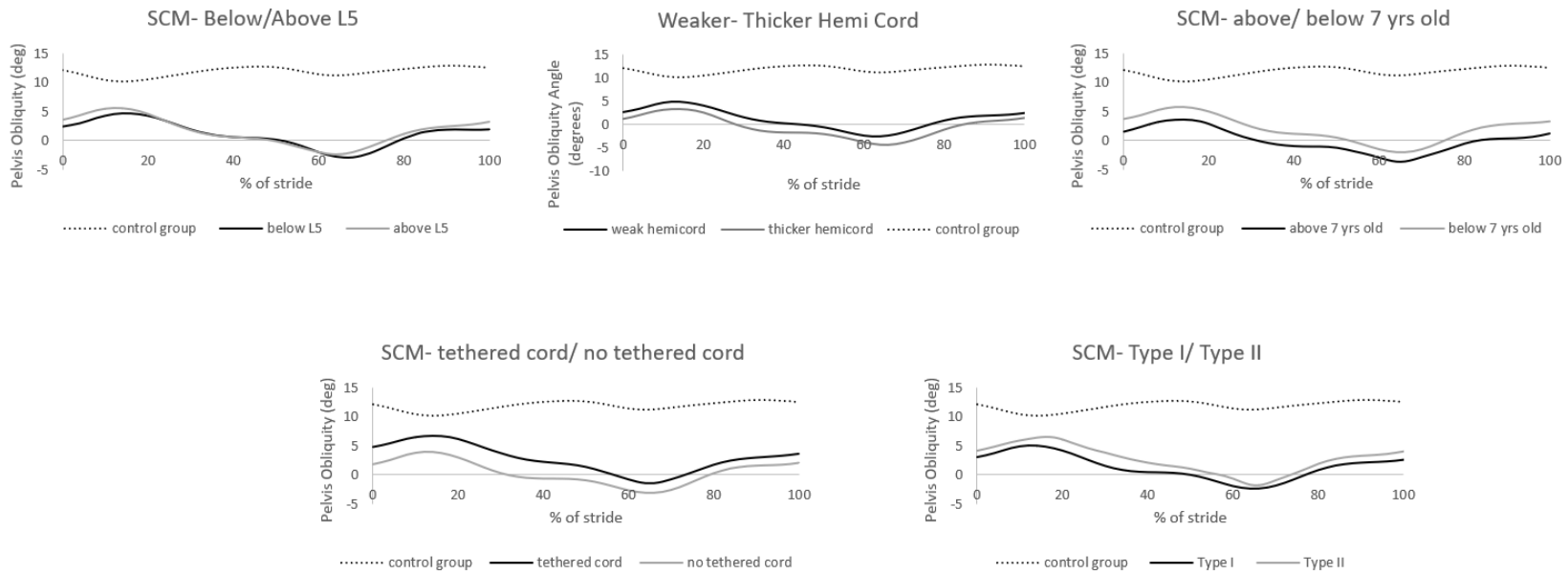

Figure 40. Assessment of gait parameters: comparison of pelvic obligity range of motion

PELVIC ROTATION

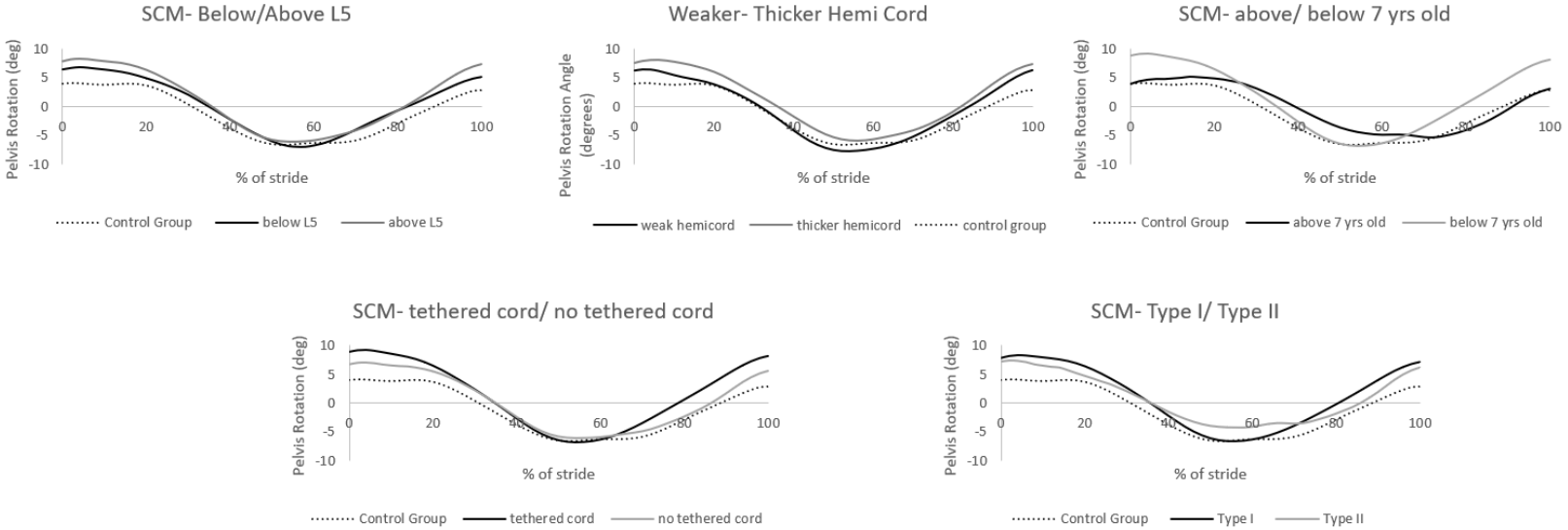

Figure 41. Assessment of gait parameters: comparison of pelvic rotation range of motion

One-way repeated measures ANOVA was performed to evaluate the significant difference among initial and follow-up groups (Table 16). The results indicated statistically significant differences of initial and follow-up groups' kinetic and kinematic parameters at $p < 0.05$.

Table 15. One-way repeated ANOVA comparisons of initial and follow up group participants

Kinetic and Kinematic Parameter	Sum of Squares	Mean Square	F	df	Sig.
Hip Moment	1825.5	912.8	9.005	24	0.023
Knee Moment	1381.9	690.9	4.515	26	0.014
Ankle Moment	313.4	156.7	2.483	18	0.090
Hip Force	2497.1	1248.6	9.355	27	<0.05
Knee Force	2478.1	1239.1	8.341	18	<0.05
Ankle Force	4641.6	2320.8	3.919	20	0.057
Hip Angle	82347.8	41173.9	66.226	22	<0.05
Knee Angle	2317.5	1158.8	7.547	19	<0.05
Ankle Angle	4492.6	2246.3	14.983	21	<0.05
Foot Progress Angle	3424.5	1712.2	14.708	17	<0.05
Pelvis Tilt	2607.2	1303.6	19.593	19	<0.05
Pelvic Obliquity	11226.6	563.3	2.598	24	0.081
Pelvic Rotation	3.450	3.450	0.021	21	0.083

Post-hoc pairwise comparisons of the initial and follow up data were performed after one-way repeated ANOVA. Results are shown in Table 16.

Table 16. Pairwise comparisons of Initial and Follow Up Kinetic and Kinematic Parameters

	Groups	N	Mean	Std. Dev.	Std. Error	95% Confidence Interval for Mean	
						Lower Bound	Upper Bound
Hip Moment	Peak Hip Extension Moment Initial vs. Follow Up	14	1.10	1.1	1.7	0.98	1.54
	Peak Hip Flexion Moment Initial vs. Follow Up	14	-0.75	0.8	1.3	-0.72	-1.02
Knee Moment	Peak Knee Extension Moment Initial vs. Follow Up	14	-0.71	1.2	1.3	-0.65	-.0.85
	Peak Knee Flexion Moment Initial vs. Follow Up	14	0.68	0.56	0.9	0.58	0.72
Ankle Moment	Peak Ankle PF Moment Initial vs. Follow Up	14	1.46	1.2	1.4	1.07	2.40
	Peak Ankle DF Moment Initial vs. Follow Up	14	-0.41	0.23	0.9	-0.21	-0.57
Hip Force	Peak Hip Flexion Force Initial vs. Follow Up (N/N)	14	0.045	1.2	1.9	0.062	-0.015
Knee Force	Peak Knee Flexion Force Initial vs. Follow Up (N/N)	14	0.052	0.02	2.4	-0.053	0.093
Ankle Force	Peak Ankle Flexion Force Initial vs. Follow Up (N/N)	14	0.11	0.03	1.6	0.28	-0.015
Hip Angle	Peak Hip Angle Initial vs. Follow Up	14	12.56	19.9	4.3	24.26	-22.65
Knee Angle	Peak Knee Angle Initial vs. Follow Up	14	59.1	6.2	1.1	72.85	-4.26
Ankle Angle	Peak Ankle Angle Initial vs. Follow Up	14	16.2	14.4	2.6	24.37	-3.75
Pelvic Tilt	Peak Pelvic Tilt Initial vs. Follow Up	14	14.01	8.0	1.6	12.01	16.4
Pelvis Obliquity	Peak Pelvis Obliquity Initial vs. Follow Up	14	11.45	4.4	2.9	12.3	-3.45
Pelvis Rotation	Peak Pelvis Rotation Initial vs. Follow Up	14	60.2	14.4	2.9	62.01	-11.26

5. DISCUSSION

Prior statements about gait characteristics in individuals with Spina Bifida characterize gait in children [56], and few studies on gait in adults have concentrated on ambulation concerning neurologic impairment [57]. Spina bifida children usually have multiple gait anomalies that are complicated and interrelated, making it challenging to decide prior pathologies using visual assessments alone. Gait pathologies must be accurately specified for treatments to be prescribed properly. Gait analysis provides clinicians with extra knowledge to be able to more accurately and objectively define prior pathologies based on quantitative data regarding the function of joint kinematics and kinetics [58].

Visual evaluation of hip flexion can be difficult due to the hardship of appreciating pelvic sagittal plane motion, which may vary throughout the gait cycle in some patients. Evaluating children with neuromuscular disorders in a gait laboratory and identifying femoral rotation from visual observation alone are challenging for even experienced specialists. One of the main reasons behind this is the fact that these patients display complicated simultaneous rotational profiles during gait, which may include large transverse plane rotations of the pelvis [59].

This thesis examined the long-term gait adaptation of SCM patients following surgery. The primary aim of surgical treatment in SCM is to prevent irreversible neurological deficits [60], which may include urinary or fecal incontinence or sexual dysfunction [61]. Also, neurological follow-up of the patient's mobility as well as early initiation of physical therapy are other important considerations for the management of SCM.

In the Mahapatra and Gupta series, [62] the follow-up period ranged from 3 months to 12 years. Of their patients, 68 (39%) revealed progress in their motor

function, 33 of 57 (60%) enhanced their sensation, and 20 of 73 (27%) regained continence. Different series, including 51 patients who had removed a bony spur, was examined by Hood et al [63]. No difference in the neurological condition was found in 61% of the patients, and 39% showed only a relatively fair progress, e.g., the return of a stretch reflex or a gain of one point on the motor scale. Lapras documented that patients suffering from orthopedic syndrome can be stabilized but not made better. The only exception to this statement is the partial regression of clubfoot deformity in patients operated on in the early stages of the disease [64]. Beuriat et al. marked motor deficit progress after the first six postoperative months, and it continued during the first two years after the operation.

In addition, due to the high number of homogeneous patient participants, we were able to analyze subgroups. The kinetic and kinematic data of patients who had undergone surgery with different symptoms and radiological findings were compared based on groups, and limitations were revealed. The subgroup comparison results showed that the kinetic and kinematic parameters were not significantly different among different groups of SCM patients. The detailed comparison included age, spinal level of SCM, presence of tethered cord, SCM type, and hemi cord thickness. Each category contained a statistically significant number of patients, and no statistical difference was discovered between these groups. This demonstrated that the gait pattern attained after the surgery was not altered by the patient falling into any of the analyzed groups. All subgroups of SCM patients displayed similar lower extremity kinetics and kinematics. On the other hand, unlike the other joints, the pelvis showed adaptation following surgery in all SCM patients from the control group. The cause of this adaptation can be attributed to the hip joint receiving weight to address the balance impairment that arises during the loading phase of the body weight. The hip joint is particularly vulnerable, as it has a major role in carrying the body weight and is connected to the muscles of the trunk. In this respect, the timing of the surgery and consistent physical therapy program may aid in limiting these adaptations and enhancing balance control in SCM patients.

Several studies demonstrate gait deviations, such as crouch gait and increased pelvic anterior tilt, obliquity, and rotation [65]. Although several studies have investigated the gait kinematics in Spina Bifida, only a few studies have explored the spatiotemporal gait parameters in children with MM. Gait velocity at self-selected walking speed and stride length is the most frequently reported spatiotemporal gait parameters [66]. Gutierrez et al. [67] illustrated that hip extensor strength strongly influences gait velocity in ambulatory children with lumbosacral MM. Despite that, as far as we know, no studies have examined the influence of postural control on spatiotemporal gait parameters in this population.

As for the spatial-temporal parameters of SCM patients and healthy control group participants, we found that the SCM group was characterized by higher cadence, shorter stride time, higher opposite foot-off percentage, lower step time, significantly higher double support percentage, shorter step length, and slightly lower walking speed compared to the control group. The differences in these parameters for thicker and weaker sides were not statistically significant.

When the kinetic and kinematic parameters of the weak and thicker hemi cord sides were examined, we found that the asymmetrical cord did not cause any change in the gait parameters of SCM patients. Therefore, we concluded that physical treatment should be administered with an equal emphasis on both extremities rather than just the weaker hemi cord. The comparison of the alterations in the ankle and pelvic movements did not reveal significant differences between the initial and follow-up group participants. On the other hand, Galli et al. [68] examined the changes in gait patterns in patients with myelomeningocele using gait analysis technology. They found increased anterior pelvic tilt, hip flexion, knee flexion, and ankle DF angle that closely coincided with the findings of our study. The gait analysis performed after an

average of 1 year and again after an average of 2.5 years did not reveal any deterioration or improvement in the alterations of the hip and pelvic joints' biomechanics. This indicated the initiation of physical therapy following the surgery and being closely monitored.

Our clinical experience indicates that muscle weakness on the pathological side could be prevented by some factors. The most prominent factor is providing a timely surgical procedure and post-op physiotherapy program. Another significant factor is that the patients were operated in the same university hospital by the same experienced neurosurgeon. Moreover, in the post-op follow-up period of the patients, clinical examination of ROM and muscle strength demonstrate improvement. However, it is interesting that parents frequently relate leg thickness and foot discrepancy in SCM to muscle weakness on the pathological side. Therefore, we also employ 3D gait analysis on these patients to examine the validity of this observational claim of the parents.

Detailed analysis of kinetic and kinematic parameters of SCM subgroup patients has not been investigated in a previous study. To our knowledge, this study is the first study in the literature in which the gait patterns of patients with SCM who had undergone surgery were examined in the long term and their limitations and adaptations were quantitatively determined.

5.1. Limitations

The primary limitation of this study was the absence of the preoperative gait analysis of the SCM patients. This was mainly due to the inclusion of very young patients (< 3 years of age) at the time of diagnosis and surgery. A gait analysis prior to 3 years of age has been reported to present significant challenges due to cooperation difficulties, as well as due to the inability to follow instructions properly and age-related development of the gait pattern in children [69].

Another limitation of the study is the lack of dynamic EMG data during gait analysis. Dynamic EMG can provide valuable information about the functional status of individual muscle or muscle groups.

6. CONCLUSION

This study investigated the long-term gait adaptation of patients with SCM. The results showed that the alterations in ankle and hip joints' biomechanics resulted in compulsory adaptation in the pelvic joint. The findings imply that balance control, loading, and muscular strengthening of the hip and pelvic joint muscles should be included in the physical therapy program, and the importance of adherence to postoperative follow-up examinations should be clearly communicated to the patient. Timing of the surgical procedure and post-op physiotherapy program are significant factors in preventing the weakness of the muscles. Postop treatment and follow-up plans should be tailored to each person's unique 3D gait analysis results and may involve ongoing rehabilitation to optimize functional outcomes.

7. FUTURE WORK

Further aims are to collect kinetic, kinematic and dynamic EMG data from pediatric patients with SCM prior to surgery so that the effect of the surgery on the gait parameters will be determined. Furthermore, patients with different levels of lesions from the lumbar to the sacral were examined concurrently. It is almost obvious that a higher level of lesion that would have more significant gait complexness would show even more differences in the identification of gait pathology.

8. REFERENCES

1. Pang D, Dias MS, Ahab-Barmada M. Split cord malformation: Part I: A unified theory of embryogenesis for double spinal cord malformations. Neurosurgery. 1992;31(3):451-80.
2. Pang D. Split cord malformation: Part II: Clinical syndrome. Neurosurgery. 1992;31(3):481-500.
3. Raskin J, Litvack Z, Selden N. Youmans and Winn Neurological Surgery. Elsevier Amsterdam, The Netherlands:; 2022.
4. Schropp C, Sörensen N, Collmann H, Krauss J. Cutaneous lesions in occult spinal dysraphism—correlation with intraspinal findings. Child's Nervous System. 2006;22:125-31.
5. James CM, Lassman L. Diastematomyelia: a critical survey of 24 cases submitted to laminectomy. Archives of disease in childhood. 1964;39(204):125.
6. Miller A, Guille JT, Bowen JR. Evaluation and treatment of diastematomyelia. JBJS. 1993;75(9):1308-17.
7. Bartonek Å, Saraste H, Knutson LM. Comparison of different systems to classify the neurological level of lesion in patients with myelomeningocele. Developmental medicine and child neurology. 1999;41(12):796-805.
8. Matson DD, Woods RP, Campbell JB, Ingraham FD. Diastematomyelia (congenital clefts of the spinal cord) Diagnosis and surgical treatment. Pediatrics. 1950;6(1):98-112.
9. Duffy C, Hill A, Cosgrove A, Corry I, Mollan R, Graham H. Three-dimensional gait analysis in spina bifida. Journal of Pediatric Orthopaedics. 1996;16(6):786-91.
10. Özek MM, Cinalli G, Maixner WJ, Maixner W. Spina bifida: management and outcome: Springer; 2008.
11. Pierre-Aurelien B, Federico DR, Alexandru S, Carmine M. Management of split cord malformation in children: the Lyon experience. Child's Nervous System. 2018;34:883-91.

12. Abu-Faraj ZO, Harris GF, Smith PA, Hassani S. Human gait and clinical movement analysis. Wiley Encyclopedia of Electrical and Electronics Engineering. 2015:1-34.
13. Netter FH. Netter Atlas of Human Anatomy: Classic Regional Approach-Ebook: Elsevier Health Sciences; 2022.
14. Moore KL, Dalley AF. Clinically oriented anatomy: Wolters kluwer india Pvt Ltd; 2018.
15. Snell RS. Clinical anatomy by regions: Lippincott Williams & Wilkins; 2011.
16. Tomie J-A, Hailey D. Computerized gait analysis in the rehabilitation of children with cerebral palsy and spina bifida: Alberta Heritage Foundation for Medical Research; 1997.
17. Levine D, Richards J, Whittle M. Whittle's Gait Analysis: Churchill Livingstone/Elsevier; 2012.
18. Whittle MW. Gait analysis: an introduction: Butterworth-Heinemann; 2014.
19. Malanga G, Delisa J. Clinical observation. Monograph 002: Gait analysis in the science of rehabilitation. J Delisa Washington, DC, Department of veterans Affairs. 1998.
20. Perry J, Burnfield JM. Gait analysis. Normal and pathological function 2nd ed. California: Slack. 2010.
21. Della Croce U, Riley PO, Lelas JL, Kerrigan DC. A refined view of the determinants of gait. Gait & posture. 2001;14(2):79-84.
22. Vaughan CL, Davis BL, O'connor JC. Dynamics of human gait: Human Kinetics Publishers; 1992.
23. Kirtley C. Clinical Gait Analysis: Theory and Practice: Elsevier; 2006.
24. Winter DA. ABC (anatomy, biomechanics and control) of balance during standing and walking. (No Title). 1995.
25. Özaras N, Yalçın S, Yavuzer G, Gök H. Yürüme analizi. İstanbul Avrupa Tıp Kitapçılık. 2001:5-20.
26. Frankel VH, Nordin M. Basic biomechanics of the skeletal system: Lea & Febiger; 1980.
27. Gage JR. Gait analysis in cerebral palsy. Clinics in developmental medicine. 1991;121.

28. Peck AL, Forster ES. Parts of Animals: Harvard University Press; 1968.
29. Borelli GA, Maquet P. On the Movement of Animals: Springer Berlin Heidelberg; 1989.
30. Boerhaave H, Kegel-Brinkgreve E, Luyendijk-Elshout A. De usu ratiocinii mechanici in medicina [Oration on the Usefulness of the Mechanical Method in Medicine]. E. Kegel-Brinkgreve and AM Luyendijk-Elshout (trans. and eds.) Boerhaave's …; 1983.
31. Maquet P, Furlong R. Mechanics of the human walking apparatus [Transl. of W. Weber and E. Weber]. Berlin, Germany: Springer; 1991.
32. Braun M. Picturing time: the work of Etienne-Jules Marey (1830-1904): University of Chicago Press; 1992.
33. Braune W, Fischer O. On the centre of gravity of the human body. Translated by Maquet P, Furlong R. Berlin: Springer-Verlag; 1984.
34. Marey E-J. Animal mechanism: a treatise on terrestrial and aerial locomotion: Henry S. King & Company; 1874.
35. Amar J. Trottoir dynamographique. Comptes rendus hebdomadaires des seances de l, Academie des Sciences. 1916;163:130-3.
36. Amar J, Butterworth EP, Wright GE. The Human Motor: Or, The Scientific Foundations of Labour and Industry: Routledge; 1920.
37. Inman VT, Eberhart HD. The major determinants in normal and pathological gait. JBJS. 1953;35(3):543-58.
38. Sutherland DH, Hagy JL. Measurement of gait movements from motion picture film. JBJS. 1972;54(4):787-97.
39. Erdoğmuş B, Tüzün Ş. Yaşlılarda yürüme kinematiği. Turkish Journal of Geriatrics. 2001;4(1):33-9.
40. Akalan NE, Temelli Y. Serebral Parezide Gözlemsel Yürüme Analizinin Yeri ve Kullanılabilirliği. Sağlık Bilimleri ve Meslekleri Dergisi. 2014;1(1):28-45.
41. Wren TA, Elihu KJ, Mansour S, Rethlefsen SA, Ryan DD, Smith ML, et al. Differences in implementation of gait analysis recommendations based on affiliation with a gait laboratory. Gait & posture. 2013;37(2):206-9.
42. Bella GP, Rodrigues NB, Valenciano PJ, Silva LM, Souza RC. Correlation among the visual gait assessment scale, Edinburgh visual gait scale and observational

gait scale in children with spastic diplegic cerebral palsy. Brazilian Journal of Physical Therapy. 2012;16:134-40.

43. Muro-De-La-Herran A, Garcia-Zapirain B, Mendez-Zorrilla A. Gait analysis methods: An overview of wearable and non-wearable systems, highlighting clinical applications. Sensors. 2014;14(2):3362-94.

44. Criswell E. Cram's Introduction to Surface Electromyography: Jones & Bartlett Learning; 2011.

45. Riad J, Henley J, Miller F. Does footprint and foot progression matter for ankle power generation in spastic hemiplegic cerebral palsy? Acta Orthop Traumatol Turc. 2009;43(2):128-34.

46. Perry J, Easterday CS, Antonelli DJ. Surface versus intramuscular electrodes for electromyography of superficial and deep muscles. Physical therapy. 1981;61(1):7-15.

47. Winter D. Biomechanics and motor control of human movement, 2nd edn John Wiley and Sons. New York. 1990.

48. Nunes JF. Novel computational methodologies for detailed analysis and simulation of human motion from image sequences: Ph. D. Dissertation, University of Porto, Porto, Portugal; 2013.

49. Antonsson EK. A three-dimensional kinematic acquisition and intersegmental dynamic analysis system for human motion: Massachusetts Institute of Technology; 1982.

50. Chao EY. Justification of triaxial goniometer for the measurement of joint rotation. Journal of Biomechanics. 1980;13(12):989-1006.

51. Shames IH. Solutions manual, Engineering Mechanics : dynamics. 2nd ed. Englewood Cliffs, N.J.: Prentice-Hall; 1967.

52. Woltring H, Huiskes R, De Lange A, Veldpaus F. Finite centroid and helical axis estimation from noisy landmark measurements in the study of human joint kinematics. Journal of biomechanics. 1985;18(5):379-89.

53. Õunpuu S. Terminology for clinical gait analysis. American Academy of Cerebral Palsy Developmental Medicine Gait Lab Committee. 1994:41-5.

54. Winter DA. Kinematic and kinetic patterns in human gait: variability and compensating effects. Human movement science. 1984;3(1-2):51-76.

55. Seireg A, Arvikar R. The prediction of muscular load sharing and joint forces in the lower extremities during walking. Journal of biomechanics. 1975;8(2):89-102.
56. Gutierrez EM, Bartonek Å, Haglund-Åkerlind Y, Saraste H. Kinetics of compensatory gait in persons with myelomeningocele. Gait & posture. 2005;21(1):12-23
57. Bendt M, Seiger Å, Hagman G, Hultling C, Franzén E, Forslund EB. Adults with spina bifida: ambulatory performance and cognitive capacity in relation to muscle function. Spinal Cord. 2022;60(2):122-8.
58. Gabrieli APT, Vankoski SJ, Dias LS, Milani C, Lourenco A, Laredo Filho J, et al. Gait analysis in low lumbar myelomeningocele patients with unilateral hip dislocation or subluxation. Journal of Pediatric Orthopaedics. 2003;23(3):330-4.
59. Gutierrez EM, Bartonek Å, Haglund-Åkerlind Y, Saraste H. Characteristic gait kinematics in persons with lumbosacral myelomeningocele. Gait & posture. 2003;18(3):170-7.
60. Gan Y, Sgouros S, Walsh A, Hockley A. Diastematomyelia in children: treatment outcome and natural history of associated syringomyelia. Child's Nervous System. 2007;23:515-9.
61. Mathieu J, Decarie M, Dube J, Marton D. Diastematomyelia. Study of 69 cases (author's transl). Chirurgie Pediatrique. 1982;23(1):29-35.
62. Mahapatra AK, Gupta DK. Split cord malformations: a clinical study of 254 patients and a proposal for a new clinical—imaging classification. Journal of Neurosurgery: Pediatrics. 2005;103(6):531-6.
63. Hood RW, Riseborough E, Nehme A, Micheli L, Strand R, Neuhauser E. Diastematomyelia and structural spinal deformities. JBJS. 1980;62(4):520-8.
64. Dawson CW, Dreisbach JH. Diastematomyelia and Acquired Clubfoot Deformity: Reports of Two Cases Indicate That Early Surgical Procedures Offer Children the Possibilities of Normal Gait and Stance. JAMA. 1961;175(7):569-72.
65. Kane, K., & Barden, J. (2010). Comparison of ground reaction and articulated ankle-foot orthoses in a child with lumbosacral myelomeningocele and tibial torsion. JPO: Journal of Prosthetics and Orthotics, 22(4), 222-229.
66. Ivanyi, B., Schoenmakers, M., van Veen, N., Maathuis, K., Nollet, K., & Nederhand, M. (2015). The effects of orthoses, footwear, and walking aids on the

walking ability of children and adolescents with spina bifida; A systematic review using International Classification of Functioning, Disability and Health for Children and Youth (ICF-CY) as a reference framework. Prosthetics and Orthotics International, 39(6), 437–443.

67. Gutierrez, E. M., Bartonek, A., Haglund-Akerlind, Y., & Saraste, H. (2003). Characteristic gait kinematics in persons with lumbosacral myelomeningocele. Gait & Posture, 18(3), 170–171.

68. Galli M, Crivellini M, Fazzi E, Motta F. Energy consumption and gait analysis in children with myelomeningocele. Funct Neurol. 2000;15(3):171-5.

69. Cigali BS, Uluçam E, Bozer C. 3D motion analysis of hip, knee and ankle joints of children aged between 7-11 years during gait. Balkan Medical Journal. 2011;2011(2):197-201.

70. Özek MM. Diastematomyelia. Neurocirurgia Pediatrica : Da Simulacao a Pratica .GEN, 2020